CYANO COMPLEXES WITH HIGH COORDINATION NUMBERS AND RELATED SPECIES.

A thesis submitted by

ANA MARIA SOARES

for the

DIPLOMA OF MEMBERSHIP

OF

IMPERIAL COLLEGE

Department of Chemistry,
Imperial College,
London, SW7 2AY.

JANUARY, 1981.

CONTENTS

	PAGE:
ACKNOWLEDGEMENTS	v
LIST OF TABLES	vii
LIST OF FIGURES	ix
ABBREVIATIONS	xi
ABSTRACT	xii

CHAPTER I

GENERAL INTRODUCTION	1
1. Cyanide ion, CN^-.	4
2. Coordination Number.	5
3. Stereochemistry of Octacyano Complexes.	6
4. Stereochemistry of Heptacyano Complexes.	13
5. Physical Methods.	20
(a) X-ray Diffraction	20
(b) Magnetic Measurements	20
(c) ^1H Nuclear Magnetic Resonance (NMR)	23
(d) ^{13}C Nuclear Magnetic Resonance (^{13}C NMR)	24
(e) Electronic Pramagnetic Resonance (EPR)	25
(f) Vibrational Spectra	27
(g) Electronic Spectra	30

CHAPTER II - GROUP V	31
NIOBIUM AND VANADIUM	31
A. Niobium	31
A.1. $K_5[Nb(CN)_8]$	31

I. LITERATURE INTRODUCTION 31

II RESULTS AND DISCUSSION 31

(a) X-Ray Crystal Structure of $K_5[Nb(CN)_8]$ 32

(b) Vibrational Spectra 35

(c) ^{13}C NMR 38

(d) Conclusions 43

A.2. $K_4[Nb(CN)_8].2H_2O$, $K_4[Mo(CN)_8].2HO_2$ and $K_4[W(CN)_8].2H_2O$ 44

(a) Raman Spectra 44

(b) Conclusions. 48

B. Vanadium 49

B.1. $K_4[V(CN)_7].2H_2O$.

I LITERATURE INTRODUCTION 49

II RESULTS AND DISCUSSION 50

(a) Vibrational Spectra 50

(b) EPR Spectra 52

(c) Conclusions 53

III MISCELLANEOUS 54

EXPERIMENTAL 54

CHAPTER III - GROUP VI 57

TUNGSTEN AND MOLYBDENUM 57

I LITERATURE INTRODUCTION 57

II AIM 58

III RESULTS AND DISCUSSION 58

A. Tungsten 58

A.1. $K_4[W(CN)_7H].2H_2O$ and $K_5[W(CN)_7].H_2O$ 58

(a) Preparation of the complexes 59

(b) X-ray Studies 61

(c) Magnetic Data 61

(d) ^1H NMR Spectra of $K_4[W(CN)_7H].2H_2O$ 64

(e) ^{13}C NMR of $[W(CN)_7H]^{4-}$ and $[W(CN)_7]^{5-}$ 68

(f) Vibrational Spectra 72

(g) The EPR Spectra of $K_4[W(CN)_7].2H_2O$ 80

(h) Electronic Spectra 83

(i) Polarography 83

(j) Properties 84

(k) Chemical Reactions of $K_4[W(CN)_7H].2H_2O$ 85

(ℓ) Conclusions 87

EXPERIMENTAL

B. Molybdenum

I AIM 95

II LITERATURE INTRODUCTION 95

III RESULTS AND DISCUSSION 95

B.1. $NaK_3[Mo(CN)_7].2H_2O$ 95

(a) Single Crystal X-ray Structure 96

(b) Magnetic Properties 96

(c) EPR Spectra 96

(d) Vibrational Spectra 101

(e) Properties 101

(f) Conclusions 104

B.2. $K_4[Mo(CN)_7].2H_2O$

(a) X-ray Studies 104

(b) Magnetic Properties 104

(c) EPR Spectra 104

(d) Vibrational Spectra 106

(e) Reactions 108

(f) Conclusions 110

B.3. $K_5[Mo(CN)_7].H_2O$ and $Na_4[Mo(CN)_7H].2H_2O$ 110

(a) Synthetic Methods 110

(b) X-ray of $K_5[Mo(CN)_7].H_2O$ 111

(c) Magnetic Properties of $K_5[Mo(CN)_7].H_2O$ 111

(d) ^1H NMR of $[Mo(CN)_7H]^{4-}$ 111

(e) ^{13}C NMR of $[Mo(CN)_7]^{5-}$ and $[Mo(CN)_7H]^{4-}$ 111

(f) Vibrational Spectra 114

(g) Properties 118

(h) Reactions 118

(i) Conclusions 119

EXPERIMENTAL 120

GENERAL TECHNIQUES AND INSTRUMENTATION 123

ACKNOWLEDGEMENTS

I am indebted to my supervisor, Dr. W.P. Griffith, for his friendly advice, encouragement and helpfulness throughout the duration of this research project and also to his wife Anne, and their daughters Helen and Miranda, for their amity.

I am very obliged to Professor Sir Geoffrey Wilkinson for accepting me in this Department.

My thanks to Dr. J.F. Gibson for the assistance with the EPR work and many helpful discussions, and to Mr. P. Beardwood for his friendship when I arrived here and for his subsequent help with the Raman spectra.

I wish to thank all my colleagues, past and present, for helpful discussions and the staff of Imperial College for their assistance, particularly Dr. D.F. Evans, Mr. Dick Sheppard and Miss Sue Johnson.

I also thank the staff at the Imperial College Day Nursery for taking so much care of Jonas while I was working on this project.

I also thank Moira for typing this thesis.

I am deeply grateful to my colleagues at Departamento de Quimica of ICex-UFMG (Brazil) for the extra work they have done since I have been doing my research here, particularly Mr. Sidney Augusto Vieira Filho

All my thanks to Conselho Nacional de Desenvolvimento Cientifico e Tecnologico (CNPq-Brazil) for financial support.

To Jaçanã my thankfulness for her solidariety.

To Zé Carlos, who shared all my worries throughout the hard and the good times with love, my very special gratitude.

To

Telma

Jonas and Gabriel

LIST OF TABLES

		PAGE:
Table I.	Known Octacyano Complexes and their Crystallographic Data.	7
Table II.	Known Heptacyano Complexes and their Crystallographic Data.	9
Table III.	Possible Geometries for $[ML_7]^{n-}$ Complexes.	14
Table IV.	Paramagnetic Hepta- and Octacyano Complexes.	22
Table V.	Chemical Shifts for Transition Metal Hydrides.	23
Table VI.	Selection Rules for Octacyano Complexes $[M(CN)_8]^{n-}$.	28
Table VII.	Selection Rules for Heptacyano Complexes $[M(CN)_7]^{n-}$.	29
Table 2.1	Vibrational Spectra Data for $K_5[Nb(CN)_8]$.	37
Table 2.2	Chemical Shifts for Diamagnetic Cyano Complexes in ^2H_2O.	41
Table 2.3	Raman Data for $K_4[M(CN)_8].2H_2O$ in Aqueous Solution (ν_{CN} region).	44
Table 2.4	C≡N and M-C Stretches (A_1' modes) in the Raman Spectra of $[M(CN)_8]^{n-}$ in Aqueous Solution.	47
Table 2.5	Vibrational Data for $K_4[V(CN)_7].2H_2O$.	50
Table 2.6	C≡N and M-C Stretches (A_1' modes) in the Raman Spectra of $[M(CN)_7]^{n-}$ in Aqueous Solution.	52
Table 3.1	X-Ray Powder Pattern Data for $K_5[W(CN)_7].H_2O$ and $K_5[Mo(CN)_7].H_2O$.	62
Table 3.2	X-Ray Powder Pattern Data for $K_4[W(CN)_7H].2H_2O$.	63
Table 3.3	Vibrational Spectra Data for $K_5[W(CN)_7].H_2O$.	74

Table 3.4	Vibrational Spectra Data for Tungstate(IV).	76
Table 3.5	Experimental Data for the Equilibrium Constant Calculations.	81
Table 3.6	Chemical Reactions of $K_4[W(CN)_7H].2H_2O$ in 0.1 M CN^-.	93
Table 3.7	X-Ray Powder Pattern Data for $NaK_3[Mo(CN)_7].2H_2O$.	98
Table 3.8	EPR Data for $NaK_3[Mo(CN)_7].2H_2O$ in the Solid State and in 0.1 M CN^- aqueous solution.	99
Table 3.9	Vibrational Spectra data for $NaK_3[Mo(CN)_7].2H_2O$.	103
Table 3.10	X-ray Powder Pattern Data for $K_4[Mo(CN)_7].2H_2O$.	105
Table 3.11	EPR Data for $K_4[Mo(CN)_7].2H_2O$ in the Solid State.	106
Table 3.12	Vibrational Data for $K_4[Mo(CN)_7].2H_2O$.	109
Table 3.13	Vibrational Data for $K_5[Mo(CN)_7].H_2O$.	115
Table 3.14	Vibrational Data for $Na_4[Mo(CN)_7H].2H_2O$.	116

LIST OF FIGURES

		PAGE:
Figure 1	The Square Antiprism (D_{4d}).	11
Figure 2	The Dodecahedron (D_{2d}).	12
Figure 2a	The 4,4-Bicapped Trigonal Prism (C_{2v}).	13
Figure 3	The Relation Between the Polyhedra.	12
Figure 4	The Pentagonal Bipyramid (D_{5h}).	16
Figure 5	The Capped Trigonal Prism (C_{2v}).	17
Figure 6	The Capped Octahedron.	17
Figure 7	Pathway of Interconversion from PB to CTP.	18
Figure 8	Pathway of Interconversion from PB to COct.	18
Figure 9	Pathway of Interconversion from CTP to COct.	19
Figure 10	Ligand Field Energy Level Diagrams and Ground State Electronic Configurations for Mono-capped Trigonal Prismatic (C_{2v}) and Pentagonal Bipyramidal (D_{5h}) Isomers of $[Mo(CN)_7]^{4-}$.	21
Figure 2.1	X-Ray Crystal Structure of $[Nb(CN)_8]^{5-}$ in $K_5[Nb(CN)_8]$.	34
Figure 2.2	Raman Spectra in the ν_{CN} Region of $[Nb(CN)_8]^{5-}$ in Solid $K_5[Nb(CN)_8]$ and of the Sodium Salt in Aqueous 0.1 M CN^-.	36
Figure 2.3	The ^{13}C NMR Spectra of $K_5[Nb(CN)_8]$ and $K_4[M(CN)_8].2H_2O$ (M = W, Mo) in ^2H_2O Solutions in Excess Cyanide.	39
Figure 2.4	Raman Spectra in the ν_{CN} Region of $[M(CN)_8]^{4-}$ (M = W, Mo, Nb) in Aqueous Solution (0.1 M CN^-).	45

Figure 3.1	^1H NMR Spectra of $[W(CN)_7H]^{4-}$ in Excess Cyanide Aqueous Solution at Various Spinning Speeds.	65
Figure 3.2	^1H NMR Spectra of $[W(CN)_7H]^{4-}$ in Excess CN^- Aqueous Solution on Addition of KOH 5.0 M.	67
Figure 3.3	The Decoupled ^{13}C NMR Spectrum of (a) $[W(CN)_7H]^{4-}$ and (b) $[W(CN)_7]^{5-}$ in Aqueous Excess CN^- (c)	69
Figure 3.4	The Undecoupled ^{13}C NMR Spectrum of $[W(CN)_7H]^{4-}$ and $[W(CN)_7]^{4-}$.	70
Figure 3.5	The Undecoupled ^{13}C NMR Spectrum of $[W(CN)_7H]^{4-}$ and $[W(CN)_7]^{5-}$ in Aqueous Excess CN^- on Addition of 1.0 M OH^-.	71
Figure 3.6	Vibrational Spectra of $K_4[W(CN)_7H].2H_2O$ and $K_5[W(CN)_7].H_2O$ in the Solid State.	73
Figure 3.7	Raman Spectra of the Titration with NaOH of $[W(CN)_7H]^{4-}$ in 0.1 M CN^- Aqueous Solution at a Total Ionic Strength of 5.5 M.	79
Figure 3.8	EPR Spectrum of $K_4[W(CN)_7].2H_2O$ in the Solid State at 27 K.	82
Figure 3.9	X-Ray Crystal Structure of $[Mo(CN)_7]^{4-}$ in $NaK_3[Mo(CN)_7].2H_2O$.	97
Figure 3.10	EPR Spectrum of Solid $NaK_3[Mo(CN)_7].2H_2O$.	100
Figure 3.11	Vibrational Spectra of Solid $NaK_3[Mo(CN)_7].2H_2O$.	102
Figure 3.12	EPR Spectra of $K_4[Mo(CN)_7].2H_2O$ in the Solid State at Various Temperatures.	107
Figure 3.13	The Undecoupled ^{13}C NMR Spectrum of (a) $[Mo(CN)_7]^{5-}$, (c) $[Mo(CN)_7H]^{4-}$ and (d) $[Mo(CN)_8]^{4-}$ (b) CN^- in Aqueous Solution.	112
Figure 3.14	Vibrational Spectra of Solid $Na_4[Mo(CN)_7H].nH_2O$.	117

ABBREVIATIONS

Me	Methyl
Et	Ethyl
Pr	Propyl
Bu	Butyl
Ph, Ø	Phenyl
en	1,2-diaminoethane
DSS	2,2-dimethyl-2-silapentane-5-sulphonate
mhp	2-hydroxy -6-methyl-pyridine
OAc	CH_3COO^- (acetate)
PB	Pentagonal Bipyramid
CTP	Capped Trigonal Prism
COct	Capped Octahedron

ABSTRACT

CYANO COMPLEXES WITH HIGH COORDINATION NUMBERS AND RELATED SPECIES.

The work presented here is concerned with octa- and hepta-cyano complexes of transition metals from Groups Va-VIIa.

Eight coordinate complexes of the form $[M(CN)_8]^{n-}$ have been studied by vibrational and ^{13}C NMR spectroscopy ($M = Nb^{IV}$, Nb^{III}, Mo^{IV}, W^{IV}) and it is concluded that they have an antiprismatic structure in aqueous solution. An X-ray crystal structure study on $K_5[Nb(CN)_8]$ shows that its anion has dodecahedral symmetry in the solid state.

Seven coordinate species of the form $[M(CN)_7]^{n-}$ ($M = V^{III}$, Mo^{III}, Mo^{II}, W^{II}, Re^{III}) were similarly studied and these all have pentagonal bipyramidal structures in aqueous solution, a structure also established by X-ray studies for the anion in solid $NaK_3[Mo(CN)_7].2H_2O$. The new salts $K_5[W(CN)_7].2H_2O$ and $NaK_3[Mo(CN)_7].2H_2O$ were made. Further studies on $K_4[Mo(CN)_7].2H_2O$ support earlier suggestions that it may have a capped trigonal prismatic structure in the solid state.

The new eight coordinate $[M(CN)_7H]^{4-}$ ($M = Mo, W$) species have been made, the first eight coordinate cyanide hydrides. Spectroscopic evidence (Raman, infrared, ^1H and ^{13}C NMR) were used to demonstrate the existence of the equilibrium

$$[W(CN)_7H]^{4-} + OH^- \rightleftharpoons [W(CN)_7]^{5-} + H_2O$$

Chemical reactions of $[W(CN)_7H]^{4-}$ with organic and inorganic substrates are described. A bi-capped trigonal prismatic structure for the anion in $K_4[W(CN)_7H].2H_2O$ is suggested.

CHAPTER I

GENERAL INTRODUCTION

This thesis is principally concerned with the preparation and structural characterisation in solution and the solid state of a number of hepta- and octa-cyano complexes, and with the investigation of cyano hydride complexes of molybdenum and tungsten. The early transition metals (particularly niobium, vanadium, tungsten and molybdenum) have been chosen for study since they have suitably accessible high oxidation states for formation of complexes of high coordination number.

Few examples of seven- and eight-coordinate complexes ($[ML_7]^{x-}$ and $[ML_8]^{x-}$) containing equivalent unidentate ligands are known.[1,2] Apart from the hepta- and octa-fluorides, $M'_x[MF_7]$ and $M'_x[MF_8]$, (e.g., $(NH_4)_3[ZrF_7]$, PB geometry ; $K_2[NbF_7]$, CTP geometry; $Li_6(BeF_4)[ZrF_8]$, $[Cu(H_2O)_6]_2[ZrF_8]$, $Na_3[TaF_8]$, all having square antimprismatic geometry),[1,2] only a small number have been characterised by X-ray diffraction. These are (with idealised structures of complex anions or cations in parentheses):

- $[ML_7]^{x-}$:

$[Mo(CNBu^t)_7].(PF_6)_2$ (a regular CTP)[3]

$K_4[V(CN)_7].2H_2O$ (a regular PB)[4]

$[Er(dmp)_7].(ClO_4)_3$ (a distored PB)[5]

$K_4[Re(CN)_7].2H_2O$ (a regular PB)[6]

$[Mo(CN)_7]^{5-}$ (a regular PB in the sodium salt and distorted PB in the potassium salt)[7]

$NaK_3[Mo(CN)_7].2H_2O$ (a regular PB) this work

$[Mo(CNMe)_7].(BF_4)_2$ (a regular COct)[8]

and

$[W(CNBu^t)_7]W_6O_{19}$ (distorted CTP)[9]

- $[ML_8]^{x-}$:

$K_4[Mo(CN)_8].2H_2O$ (dodecahedron)[10]

$(nBu_4N)_3[Mo(CN)_8]$ (dodecahedron)[11]

$K_4[Nb(CN)_8].2H_2O$ (dodecahedron)[12]

$K_5[Nb(CN)_8]$ (dodecahedron) this work

$H_4[W(CN)_8].6H_2O$ (square antiprismatic)[13]

$Na_3[W(CN)_8].4H_2O$ (square antiprismatic)[14]

$H_4[W(CN)_8].4HCl.12H_2O$ (square antiprismatic)[15]

$Cd_2[Mo(CN)_8].2N_2H_4.4H_2O$ (square antiprismatic)[16]

$Cs_4[U(NCS)_8]$ (square antiprismatic)[17]

$Cs_3[Mo(CN)_8].2H_2O$ (4,4-bicapped trigonal prism)[17a]

$[H\text{-}N(C_2H_5)_3]_2[H_3O]_2[Mo(CN)_8]$ (between dodecahedron and square antiprismatic)[17b]

and

$\{La[OC(CHMe)_2O]_8\}.(ClO_4)_3$ (square antiprismatic)[18]

The existence of octa- and hepta-cyano complexes of the early transition metals can be semi-empirically rationalised by the "nine-orbital" rule. This proposes that transition metals having few d electrons will tend to use all five n d orbitals, as well as one (n + 1) s and three (n + 1) p orbitals (nine in all) in their complexes.[19,20]

Then, among the cyanide complexes this general feature can be observed. For heptacyano complexes the following examples illustrate the "rule":

$K_4[Re(CN)_7]$ d^4 + 14 → 18 electrons

(all nine orbitals doubly occupied)

$K_4[V(CN)_7]$ d^2 + 14 → 16 electrons

(but two of the nine orbitals are singly occupied - high spin)

$K_4[Mo(CN)_7]$ d^3 + 14 → 17 electrons (one of the nine orbitals is singly occupied).

$K_5[Mo(CN)_7]$ d^4 + 14 → 18 electrons

Similarly, for octacyano complexes, the following examples may be cited:

$K_3[Mo(CN)_8]$ d^1 + 16 → 17 electrons

$K_4[Nb(CN)_8]$ d^1 + 16 → 17 electrons

$K_5[Nb(CN)_8]$ d^2 + 16 → 18 electrons

As these examples illustrate, all the known octa- and hepta-cyano complexes are 17 or 18-electron systems (the alleged $K_4[Ti(CN)_7]$[18a] could be a 15-electron system, but the evidence for its existence is very weak), and few, if any, 19 or 20-electron cyano complexes are known. As a consequence, we expect electronic configurations of d^0-d^2 for octa-cyano and d^0-d^4 for hepta-cyano species. It is only for

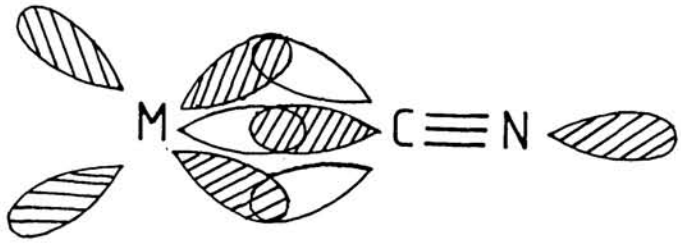
the early transition metals (e.g., groups IV-VII) that such configurations are likely, and hence it is in this area that our work has been concentrated.

The interest in the chemistry of the transition metal cyano complexes is increasing and recently has been the subject of two reviews.[21,22] The reasons for the geometries adopted in seven and eight-coordination are not very well understood and so more structure determinations are of interest. Also, the fact that interconversion between different polyhedra of the same coordination number quite often occurs when the anion is in different environments (e.g., solid state or solution; variation of number, type and size of cation, etc.), brings to the chemistry of cyanide complexes a great deal of excitement in its investigation.

1. Cyanide Ion - CN^-.

The cyanide ion, CN^-, normally functions as a monodentate ligand with carbon as the donor atom rather than nitrogen. The reason for this is probably that nitrogen is more electronegative so that its lone pair is less available for σ-bonding.

The cyanide ion is isoelectronic with CO, NO^+ and N_2 and the ground state is $(\sigma 1s)^2(\sigma^*1s)^2(\sigma 2s)^2(\sigma^*2s)^2(\sigma 2p_x)^2(\pi 2p_y)^2(\pi 2p_z)^2$ [22] with the two atoms triply bonded (one σ and two π bonds). In transition metal complexes cyanide acts as a σ donor and a π acceptor.



The cyanide ligand lies near the top of the spectrochemical series and is thus likely to produce low-spin complexes.

2. Coordination Number.

Cyano complexes of all coordination numbers from eight to two inclusive are known.[23,24,25] The ability of CN^- to stabilise such a wide range of stereochemistries can be explained by its small size and the adaptability which it can bring to bonding by virtue of a balance of σ-donor and π-acceptor properties.

The higher coordination numbers (octa- and hepta-cyano complexes of the early transition metals) can be interpreted on the basis of the " nine-orbital" rule[19,20] mentioned previously.

For example, for $\underline{d}^1$ species, eight empty orbitals (five n $\underline{d}$, one (n + 1)s, three n p) are available and an octa-cyanide is likely to be formed (e.g., $[Nb(CN)_8]^{4-}$), whereas a $\underline{d}^2$ ion may give either an octa or heptacyanide according to whether a high-spin (e.g., $[V(CN)_7]^{4-}$) or low-spin (e.g., $[Mo(CN)_8]^{4-}$) configuration is preferred. Low-spin species are likely for second- and third-row elements (e.g., $[Re(CN)_7]^{4-}$), because of larger ligand-field splitting.

In the present work, we will be dealing with hepta- and octa-cyano complexes of groups V, VI and VII of transition metals. Table I and Table II shows all known octa- and hepta-cyano complexes and their structures.

3. Stereochemistry of Octacyano Complexes.

The structures of eight-coordinate cyanides have normally been discussed in terms of either: the square antiprismatic (D_{4d}) or the dodecahedron (D_{2d}) and intermediate structures are often found for these complexes (e.g., the anion in $Na_3[W(CN)_8].4H_2O$ has a distorted D_{4d} toward a D_{2d}). Very recently,[17a] a new stereochemical configuration for $[M(CN)_8]^{n-}$ ions, the 4,4-bicapped trigonal prism (C_{2v}) has been found for the anion $[Mo(CN)_8]^{4-}$ of the dihydrated cesium salt.

The energy difference between the D_{2d} and D_{4d} form is very small (29.3 kJ mol^{-1})[38] and fluxional behaviour would not be unexpected in some cases.[39,40] However, there is in the literature still dispute as to which of the two most likely structures (D_{4d} or D_{2d}) octacyano complexes have in solution. In the solid state, X-ray studies may be regarded as unequivocal and arouse little controversy, but for the anion in solution the structural evidence is necessarily less conclusive. For example, it will be seen in Table II that, for the anion $[M(CN)_8]^{4-}$ (M = Mo and W), there is doubt about its structure in solution and we have tried to resolve this in this work.

TABLE I. Known Octacyano Complexes and their Crystallographic Data.

Complex	Metal Electronic Configuration	Anion Symmetry		Symmetry Based on	M-C (A^o) Average	N-C (A^o) Average	Reference
		Solid	Solution				
$K_4[Nb(CN)_8].2H_2O$	d^1	D_{2d}	D_{4d}	X-ray (solid) IR, Raman, EPR (Solution)	2.255(5)	1.16	12, 35
$M_4[Nb(CN)_8].xH_2O$ $M = Cs^+, Na^+, Tl^+$	d^1	D_{2d}	distorted D_{2d}	EPR (solid) IR, Raman (solution)			36
$(R_4N)_4[Nb(CN)_8]$ $R = CH_3, C_2H_5$	d^1	D_{2d}	distorted D_{2d}	EPR (solid) IR, Raman (solution)			36
$\{[C_3H_7].2NH_2\}_4[Nb(CN)_8]$	d^1	D_{2d}	distorted D_{2d}	EPR (solid) IR, Raman (solution)			37
$H_4[W(CN)_8].6H_2O$	d^2	D_{4d}		X-ray (solid)	2.180(10)	1.127(10)	13
$H_4[W(CN)_8].4HCl.12H_2O$	d^2	D_{4d}		X-ray (solid)	2.176(10)	1.150(10)	15
$K_4[W(CN)_8].2H_2O$	d^2	D_{2d}	D_{2d}	IR, Raman (solid and solution)			34
$M_3[W(CN)_8].xH_2O$ $M = Na^+, K^+$	d^1	D_{4d}	D_{2d}	X-ray (solid sodium salt) IR, EPR, Raman (solution)	2.139	1.164	31,32,33

TABLE I (continued)

Complex	Metal Electronic Configuration	Anion Symmetry		Symmetry Based on	M-C (A^o) Average	N-C (A^o) Average	Reference
		Solid	Solution				
$K_4[Mo(CN)_8].2H_2O$	d^2	D_{2d}	D_{2d}	X-ray (solid) IR, Raman, EPR (solution)	2.163(5)	1.156(6)	10, 32
$H_4[Mo(CN)_8].6H_2O$	d^2	D_{4d}		isomorphous with W analogue			13
$H_4[Mo(CN)_8].4HC\ell.12H_2O$	d^2	D_{4d}		X-ray of powder (solid)			13, 15
$Cd_2[Mo(CN)_8].2N_2H_4.4H_2O$	d^0	D_{4d}		X-ray (solid)			16
$Cs_3[Mo(CN)_8].2H_2O$	d^1	C_{2v}		X-ray (solid)	2.17(2)	1.14(2)	17a
$(Bu^nN)_3[Mo(CN)_8]$	d^1	D_{2d}		X-ray (solid)	2.12	1.16	11
$M_3[Mo(CN)_8].xH_2O$	d^1	D_{4d}	D_{4d}	EPR, powder X-ray (solid) IR, Raman, EPR (solution)			31,32,33

TABLE II. Known Heptacyano Complexes and their Crystallographic Data.

Complex	Metal Electronic Configuration	Anion Symmetry		Symmetry based on:	M-C (Å) (average)	N-C (Å) (average)	Reference
		Solid	Solution				
$K_4[Ti(CN)_7].KCN$	d^1	CTP(?)		Electronic spectra			26
$K_4[V(CN)_7].2H_2O$	d^2	PB	PB	X-ray (solid); electronic spectra (solution)	2.15(1)	1.14(1)	4
$K_4[Mo(CN)_7].2H_2O$	d^3	CTP(?)	PB(?)	IR, EPR, electronic spectra (solid); IR, Raman, electronic spectra (solution)			27
$NaK_3[Mo(CN)_7].2H_2O$	d^3	PB	PB	X-ray (solid), IR, Raman (solution)	2.16(1)	1.14(1)	This work
$Cs_4[Mo(CN)_7].2H_2O$	d^3	PB(?)	PB(?)	IR, Raman (solid and soln)			27
$Na_5[Mo(CN)_7].10H_2O$	d^4	PB	PB	X-ray (solid); IR, Raman (solution)	2.15(3)	1.16(4)	7
$K_5[Mo(CN)_7].H_2O$	d^4	PB (distorted)	PB	X-ray (solid); IR, Raman (solution)	2.14(3)	1.16(10)	7
$K_5[Mo(CN)_7]$	d^4	CTP(?)		IR, Raman (solid and soln.)			7

/..... continued.

TABLE II (Continued)

Complex	Metal Electronic Configuration	Anion Symmetry		Symmetry based on:	M-C (Å) (average)	N-C (Å) (average)	Reference
		Solid	Solution				
$K_4[Re(CN)_7].2H_2O$	d^4	PB	PB	X-ray (solid); IR, Raman (solution)	2.08(3)	1.161(5)	28, 6
$K_4[Tc(CN)_7].2H_2O$	d^4	PB	PB	IR, Raman (solid and soln.)			29

- The Square Antiprism:

The square antiprism is shown in Figure 1. All eight ligand sites are identical, it has square top and bottom and eight isosceles triangles for the vertical faces. This possesses D_{4d} symmetry with an S_8 and four C_2 axes, with all eight vertices equivalent.

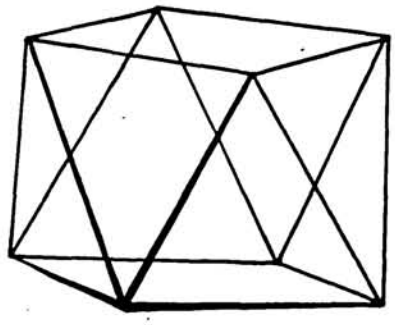


Figure 1. The Square Antiprism (D_{4d}).

This configuration has been found with minor distortions for the anion $[M(CN)_8]^{n-}$ (M = Mo, W ; n = 3 and 4) in certain salts and acids (see Table I).

- The Dodecahedron

The dodecahedron is shown in Figure 2. It is important to note that its vertices are not all equivalent but are divided into two sets [each one formed by four equivalent vertices (A,B)]. It has D_{2d} symmetry with an S_4 and two C_2 axes, all mutually orthogonal.

Slightly distorted dodecahedra have been found for salts of the anion $[M(CN)_8]^{n-}$ [M = Mo, W, Nb ; n = 3 and 4) (See Table I).

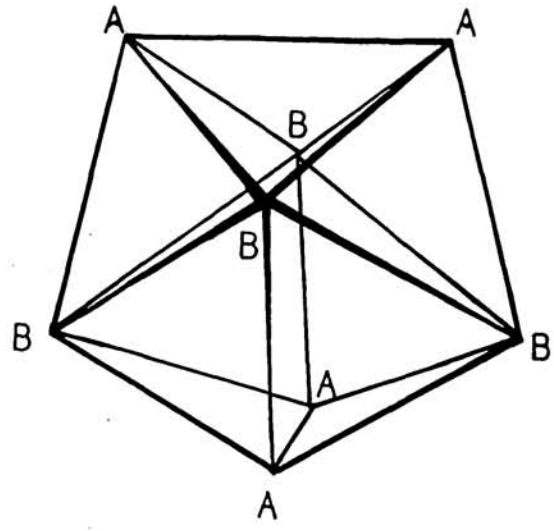


Figure 2. The Dodecahedron (D_{2d})

All the metal carbon distances M-A and M-B have been found to be the same (within the experimental error) for all octacyano complexes hitherto described.

The dodecahedron can be easily converted by relatively small displacements to the square antiprism and to the bicapped trigonal prism as shown in Figure 3.

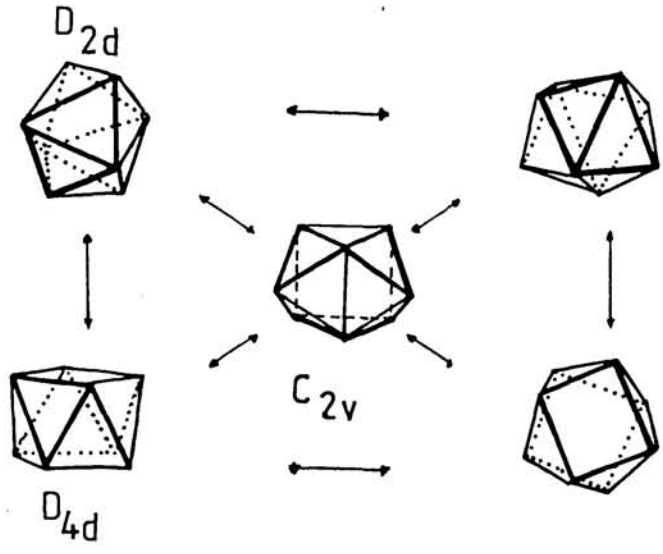


Figure 3. The Relation Between the Polyhedra.

- 4,4-Bicapped trigonal prism.

Very recently, Leipoldt et al.,[17a] reported this new stereochemical configuration for $[M(CN)_8]^{n-}$ ion in the complex $Cs_3[Mo(CN)_8].2H_2O$. The anion in this possesses C_{2v} symmetry. The 4,4-bicapped trigonal prism is shown in Figure 2a.

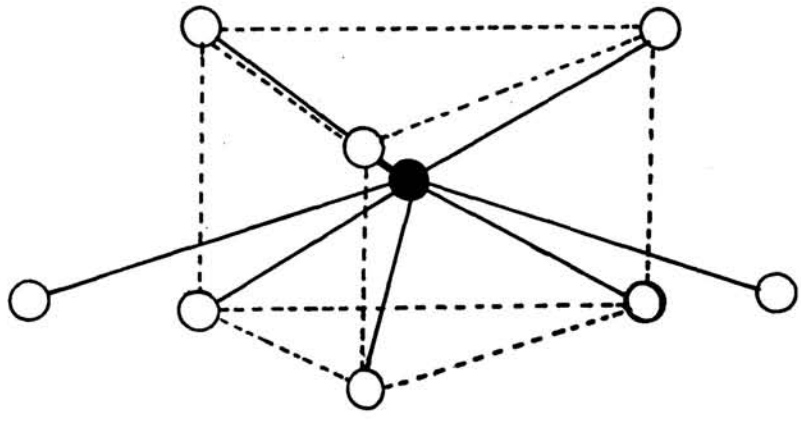


Figure 2a. The 4,4-bicapped trigonal prism (C_{2v}).

4. Stereochemistry of Heptacyano Complexes.

For unsubstituted ML_7 complexes a number of configurations are possible, of which three are the most important: the pentagonal bipyramid (PB; D_{5h}); the monocapped trigonal prism (CTP; C_{2v}) and the capped octahedron (COct; C_{3v}) (Table 3). On the basis of a model[41] in which seven mutually repulsive points can move on a spherical surface the most favourable configuration is PB followed by CTP and finally by COct. However, it seems to be clear that the energy differences between these polyhedra are very small.[1]

TABLE III. Possible Geometries for $[ML_7]^{n-}$ Complexes.

Geometry		Angles			Alternative name
		L_{ax} M L_{eq}	L_{ax} M L_{ax}	L_{eq} M L_{eq}	
Pentagonal Bipyramid	D_{5h}	90^{o}	180^{o}	$72, 144^{o}$	
Capped Trigonal Prism	C_{2v}	Angles not Fixed			Wedge Octahedron
Capped Octahedron	C_{3v}	Angles not Fixed			Capped Trigonal Antiprism

Almost all heptacyano-complexes which have been subjected to X-ray study have been shown to have regular or distorted PB (D_{5h}) coordination. Since the cyanide ligand has none of the steric restraints associated with polydenticity or bulkiness, it seems likely that electronic factors are responsible for the adoption of PB symmetry on the very similar[1] capped trigonal prismatic or capped octahedral configuration.

Crystal field stabilisation has been invoked as a reasonable explanation for the PB geometry in the case of the anion in $K_4[V(CN)_7].2H_2O$[4] with the two electrons occupying the doubly degenerate d_{xz} and d_{yz} orbitals. Another factor operating to stabilise this PB geometry may be the 'ring current'. A combination of the π orbitals on the five equatorial cyanides can form a very stable (and stabilising) bonding orbital, the so-called ring π-orbital. Also, not only will the individual cyanide ligands act as π acceptors and stabilise the d_{xz}, d_{yz} orbitals, but a molecular orbital made up of π^* orbitals in the equatorial ligands should also increase that stabilisation.

- The Pentagonal bipyramid.

The PB is shown in Figure 4 and details of its geometry are listed in Table III.

The axial sites are less crowded than the equatorial position in the ideal model. Thus, in most examples with equivalent atoms in both sites (ML_7 when M = I, Re, and L = fluoride), the M-L_{ax} bond

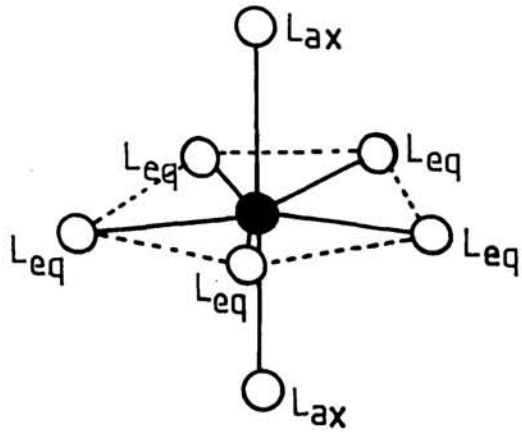


Figure 4. The Pentagonal Bipyramid (D_{5h}).

distances are a little shorter than the M-L_{eq} distances, and axial bond lengths are often equivalent to those found in octahedral complexes.[1] But, for heptacyano complexes the M-L_{ax} and M-L_{eq} distances are about the same ($\sim$ 2.15Å, within experimental error; see Table II) and this could be explained in terms of ligand-electron interaction which will be small and approximately equal for L_{ax} and L_{eq}, since the electrons in the d_{xz} and d_{yz} orbitals point away from the ligands.[1]

- The Capped Trigonal Prism (CTP).

The capped trigonal prism is shown in Figure 5 and details of its geometry are presented in Table III.

The CTP is not often found for $[ML_7]^{n-}$ species particularly those with a predominance of monodentate ligands. The isocyanide complexes of molybdenum and tungsten $[M(CNR)_7]^{n+}$ [M = Mo, W and R = $CNC(CH_3)_3$] are the only examples found in the literature[3,9] which possesses the CTP symmetry.

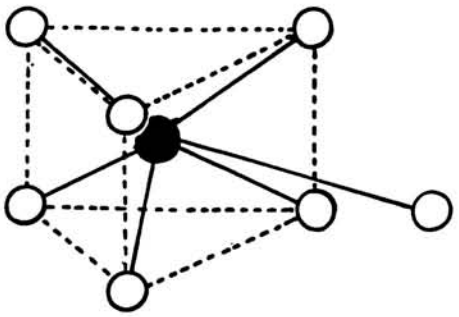


Figure 5. Capped Trigonal Prism (C_{2v}); dotted lines define edges in trigonal prism.

- The Capped Octahedron.

The characteristics of the capped octahedron are illustrated in Figure 6 and listed in Table III.

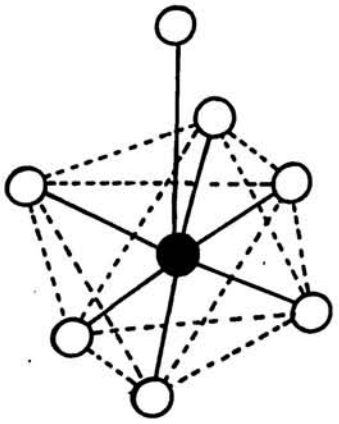


Figure 6. Capped octahedron; dotted lines define edges in octahedron.

In this configuration, the angles between the ligands are not fixed and the only monomer known to possess this structure, the complex $[Mo(CNCH_3)_7](BF_4)_2$, has very recently been reported.[8]

The possible pathways of interconverion between the three geometries are: from PB to CTP, from PB to COct and from CTP to COct, are shown in Figures 7, 8 and 9, respectively.

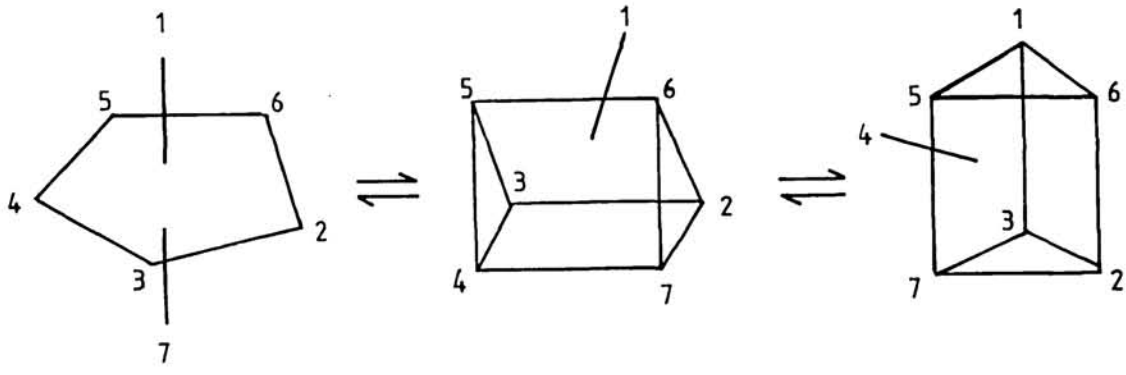


Figure 7. Possible Pathways from PB to CTP.

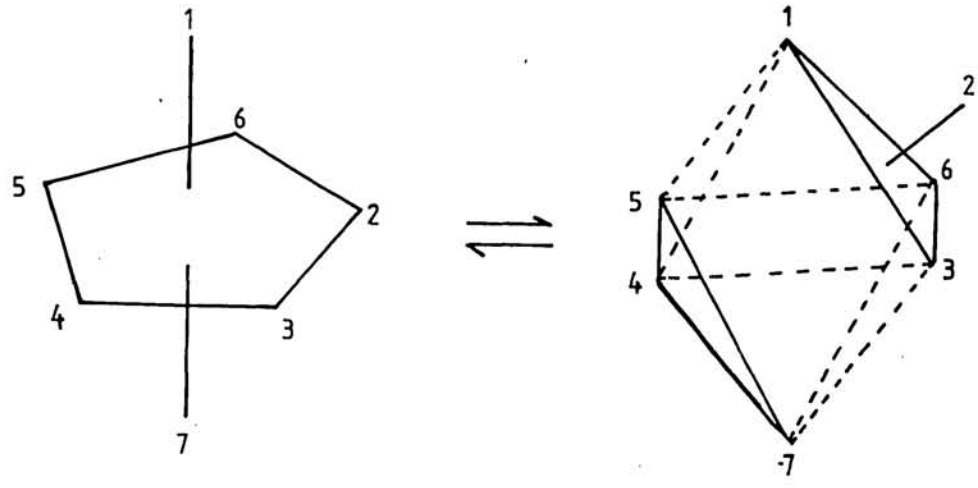


Figure 8. Pathways from PB to COct.

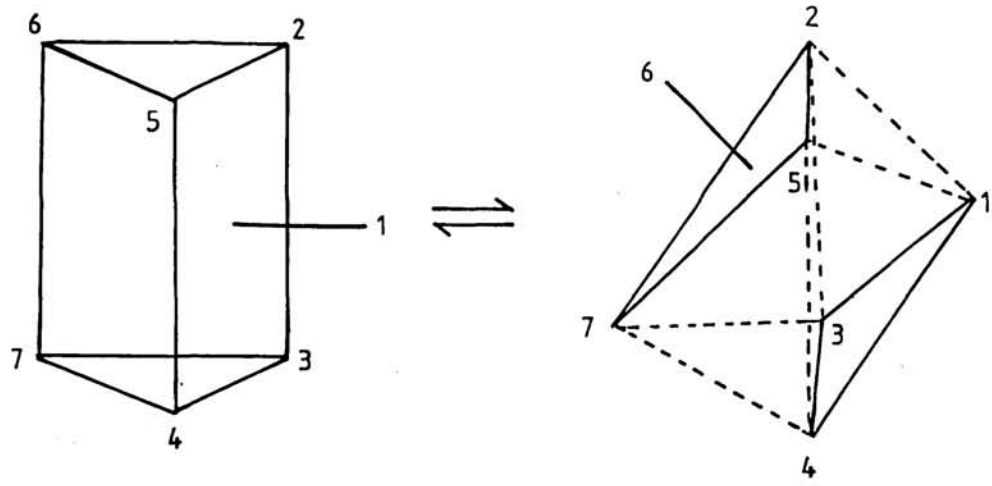


Figure 9. Pathway from CTP to COct

All known heptacyano complexes are listed in Table 2 and it appears, from the X-ray studies which have been carried out, that the PB structure is the most common. Spectroscopic data suggest that this is also true for species in solution.

The only regular CTP characterised by X-ray diffraction are the cations $[Mo(CN^tBu)_7]^{2+}$ [3] and $[W(CN^tBu)_7]^{2+}$.[9] However, in another d^4 molybdenum(II) complex, $K_5[Mo(CN)_7]$, the anion $[Mo(CN)_7]^{5-}$ was shown to be a PB (in the sodium and hydrated potassium salt).[7] The cation $[Mo(CNCH_3)_7]^{2+}$ (which has also been characterised by X-ray studies[8]) possesses a COct geometry. Thus, these heptacoordinate species have different geometries despite the fact that in all of them the metal has a d^4 configuration. The fact that $[Mo(CN^tBu)_7]^{2+}$ is CTP, $[Mo(CNCH_3)_7]^{2+}$ is COct and $[Mo(CN)_7]^{5-}$ is PB can be explained as a consequence of differences in ligand rather than packing effects.[7,8]

The anion $[Mo(CN)_7]^{4-}$ (in the potassium salt) has been claimed to possess a CTP structure in the solid state and a PB in solution,[27] but such conclusions have been based only on IR, Raman and EPR spectroscopy and we sought to confirm this in this work. Such an interconversion can be rationalised as a consequence of small differences in energy between the two polyhedra and the fact that packing effects are absent in the solution facilitating formation of the more energetically favourable form.[1]

5. Physical Methods.

Here we will mention briefly the more important facts concerning each physical method which has been useful in this present work.

a) X-Ray Diffraction.

Single crystal X-ray crystallography is one of the best method that can fully establish the structures of complexes in the solid state. X-ray powder photographs can be useful when associated with other methods, but the isomorphism between two species does not always indicate exactly the same geometry. For example, $K_5[Mo(CN)_7].H_2O$ and $K_4[V(CN)_7].2H_2O$ are isomorphous but the anions do not have identical structures.[7]

b) Magnetic Measurements.

The magnetic properties of a complex can help in determining the electronic configuration of the metal and its stereochemistry.

However, most of known heptacyano complexes are diamagnetic and only $[Ti(CN)_7]^{4-}$, $[V(CN)_7]^{4-}$ and $[Mo(CN)_7]^{4-}$ are paramagnetic species (Table 4). Of the octacyano complexes, only $[Mo(CN)_8]^{3-}$, $[W(CN)_8]^{3-}$ and $[Nb(CN)_8]^{4-}$ are paramagnetic (Table 4).

Figure 10 presents the splitting diagrams for PB and CTP isomers of $[Mo(CN)_7]^{4-}$.[27] These can help to explain why $K_4[Mo(CN)_7]$, for example, has one and not three unpaired electrons.

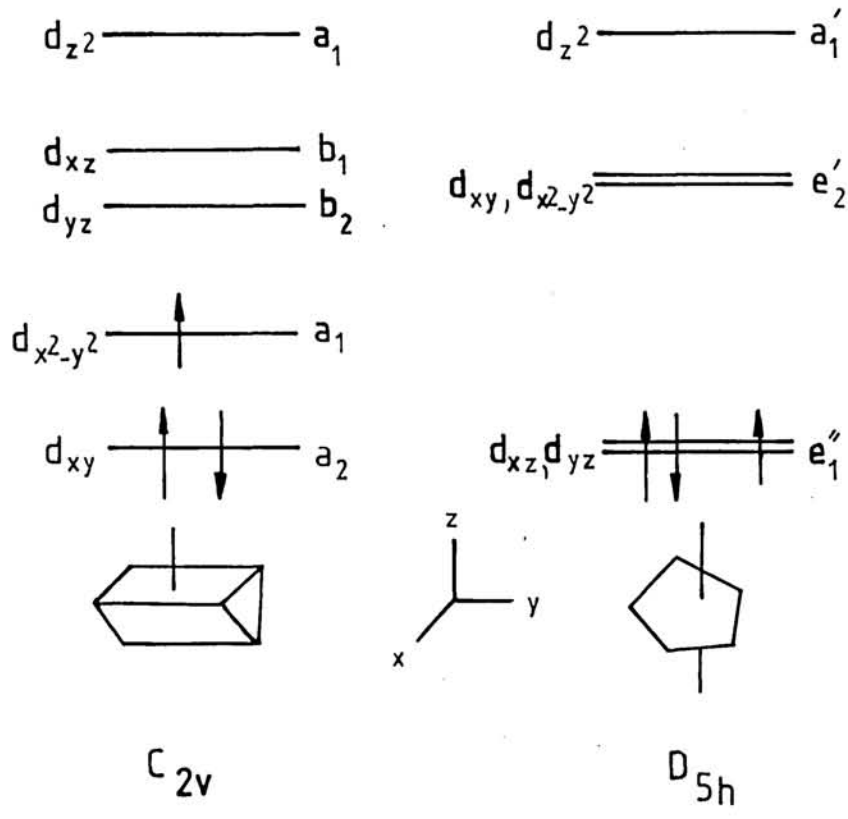


Figure 10. Ligand field energy level diagrams and ground-state electronic configurations for monocapped trigonal prismatic (C_{2v}) and pentagonal-bipyramidal (D_{5h}) isomers of $[Mo(CN)_7]^{4-}$.[27]

TABLE IV. Paramagnetic Hepta- and Octacyano Complexes.

Complex	μ_{eff} (BM)	Temperature K	Metal Configuration	Reference
$K_4[Ti(CN)_7].2H_2O$	not reported		d^1	18a
$K_4[V(CN)_7].2H_2O$	2.80	298	high-spin d^2	42
$K_4[Mo(CN)_7].2H_2O$	1.73	298	low-spin d^3	27
$K_3[Mo(CN)_8].2H_2O$	1.66	298	d^1	23
$K_3[W(CN)_8].2H_2O$	1.61	298	d^1	23
$K_4[Nb(CN)_8].2H_2O$	1.69	293	d^1	44

c) ^{1}H Nuclear Magnetic Resonance (NMR).

If the complex is diamagnetic, and contains one or more hydride ligands, proton NMR is a very useful technique.

Resonances due to hydride ligands normally occur in a high field region of the spectrum, usually in a region containing no interfering absorptions due to solvents or to other ligands.[43] Normally, hydride resonances are relatively easily dectected even at low concentrations, but when the solvent is water the spinning side bands may interfere causing some experimental difficulties. In the present work, since the potassium and sodium complexes are soluble only in water, we attempted to synthesise salts containing large organic cations in order to make them soluble in organic solvents.

^{1}H nmr spectroscopy has been used to study cyano complexes of Co^{III}, Rh^{III} and Ir^{III} containing one hydride as a ligand.[43] The chemical shifts are presented in Table 5.

TABLE V

Chemical Shifts for Transition Metal Hydrides.

Complex	Solvent	Chemical Shift[a] (δ, ppm)	Ref.
$K_3[IrH(CN)_5]$	H_2O	-14.37	43
$K_3[RhH(CN)_5]$	H_2O	-10.61	43
$K_3[CoH(CN)_5]$	H_2O	-12.65	43

[a] upfield from TMS.

d) ^{13}C Nuclear Magnetic Resonance (^{13}C NMR).

It seems natural to assume that ^{13}C nmr spectroscopy should be of great use in cyanide chemistry. The cyanide ion is one of the simplest ligands in which the carbon is directly bonded to the metal. Large chemical shifts are often observed, and if the metal has a nuclear spin, spin coupling is also often measurable.[45] Although little investigation has been carried out on cyano complexes, Muetterties[38,39] was able to suggest the fluxional behaviour of $[M(CN)_8]^{4-}$ (M = Mo and W) anions in solution by the observation of a single sharp resonance as a unique ^{13}C nmr absorption. This result was interpreted as consistent with either (a) D_{4d} symmetry (in which all eight sites are equivalent); (b) D_{2d} symmetry with very small chemical shifts between the two sets of non-equivalent sites; or (c) neither one nor the other, but an averaging of the two (i.e. fluxionality). The last possibility (c) was preferred.[39] Also, some qualitative inspection on the nature of metal-ligand bonding can be obtained by comparing the chemical shifts in cyanide complexes with transition metals.[45]

The ^{13}C nucleous has a spin of $\frac{1}{2}$ and because its natural abundance is very low (1.1%) its signals are inherently weak in the traditional nmr spectrometers. This problem has been solved by the development of the technique of Fourier transformation. The sample is irradiated with pulses of energy, each lasting a few microseconds, separated by intervals of about one second, during which time the nuclei remit their energy (to decay) before the next irradiation.

If two nuclei with different chemical shifts are present, the detector will see the emitted radiation as a " beat pattern". With the help of a computer it is possible to reconstruct the original frequencies. The " beat patterns" can be accumulated by the computer in order to improve the signal-to-noise ratio.

Normally, each ^{13}C resonance would be split into a multiplet by coupling to directly-bonded and near-neighbour hydrogen nuclei. If, however, while observing the ^{13}C spectrum, the sample is also irradiated at the frequency of the proton resonances, the coupling is removed and each ^{13}C resonance collapses to a sharp singlet.

e) Electronic Paramagnetic Resonance (EPR).

EPR can be a very powerful and sensitive technique for the study of paramagnetic species, capable of providing reliable information about the symmetry of the complex and metal electronic distribution.

The theory behind magnetic resonance is common to both electronic paramagnetic resonance (EPR) and nuclear magnetic resonance (NMR). There are differences in the magnitudes and signs of the magnetic interactions involved, which naturally lead to differences in the techniques employed.

While in the NMR experiment, normally only solutions are used, in the EPR experiment, not only solution but the pure solid or a solid solution (in which the paramagnetic material is doped in a

diamagnetic lattice can be used. Data from such experiments can be of great importance in obtaining information about the symmetry of the species in both phases.

EPR spectroscopy normally is handled by a very mathematical approach[46-49] but in the present work only a qualitative analysis of the phenomenon has been used for the interpretation of spectra.

The mathematical expressions that have been useful in this work are:

$$g = \frac{h\nu}{\beta B} \quad \text{(Landé factor)}$$

where

h = Planck constant (6.63×10^{-34} J mol^{-1})

ν = Frequency (MHz)

β = Bohr magneton (9.27×10^{-24} JT^{-1})

B = Applied magnetic field (Tesla)

$$g_{iso} = \frac{1}{3} \left(g_{\parallel} + 2g_{\perp}\right)$$

where

iso = Isotropic

$\parallel$ = Paralell to the applied field

$\perp$ = Perpendicular to the applied field

$$A_{iso} = \frac{1}{3} \left(A_{\parallel} + 2A_{\perp}\right)$$

where

A = Hyperfine coupling constant (measured in Gauss or Tesla G = 10^{-4} T)

In cyanide chemistry very few complexes are paramagnetic, and this restricts the use of EPR as a complementary method in their studies. Extensive work has been done on octa-coordinated species such as $[Nb(CN)_8]^{4-}$ [36,37] and $[M(CN)_8]^{3-}$ (M = Mo and W),[11,32,33,50] but for hepta-coordinated complexes only $K_4[V(CN)_7].2H_2O$[51,52] and $K_4[Mo(CN)_7].2H_2O$[27] have been the subject of EPR studies. In both cases the results presented (concerning EPR data) were not very conclusive and we thought to extend these studies in this present work.

f) Vibrational Spectra.

Since C≡N stretching frequencies are strong and sharp and occur in the relatively clear area of 1900-2200 cm^{-1}, infrared and Raman spectroscopy can be very informative about structure and bonding in cyano complexes of transition metals. The free cyanide ion absorbs at ν_{CN} 2078 cm^{-1}, (ν_{CN} is the C≡N stretching frequency).

The formation of a strong metal-carbon σ bond will tend to tighten the C≡N bond causing ν_{CN} to rise, while metal-carbon π-bonding weakens the C≡N bond by increasing the contribution of (b) (ν_{CN} drops):

$$\underset{\text{(a)}}{M—C\equiv N} \qquad \underset{\text{(b)}}{M{=}C{=}\overset{+}{N}}$$

Thus, ν_{CN} in cyano complexes can be above or below that of free CN^- depending on the relative contribution of metal-ligand σ and π bonding.[25,54]

In the region of the spectrum between 200-500 cm^{-1}, metal-carbon stretches (ν_{MC}) can be found, but their assignment is not always simple, and the degree of splitting is less than for ν_{CN}. The selection rules for octa- and heptacyano complexes are presented in Tables 6 and 7 respectively.

TABLE VI. Selection Rules for Octacyano Complexes, $[M(CN)_8]^{n-}$.

Point Group	D_{4d}	D_{2d}
ν_{CN} : Raman Active	3 (A_1, E_2, E_3)	6 ($2A_1$, $2B_2$, $2E$)
- polarised	1 (A_1)	2 ($2A_1$)
Infrared Active	2 (B_2, E_1)	4 ($2B_2$, $2E$)
Raman and IR coincidences	0	4 ($2B_2$, $2E$)
$\nu_{MC} + \delta_{MCN}$:		
Raman Active	8 ($2A_1$, $3E_2$, $3E_3$)	16 ($4A_1$, $2B_1$, $4B_2$, $6E$)
- polarised	2 ($2A_1$)	4 ($4A_1$)
Infrared Active	5 ($2B_2$, $3E_1$)	10 ($4B_2$, $6E$)
Raman and IR coincidences	0	10 ($4B_2$, $6E$)

TABLE VII. Selection Rules for Heptacyano Complexes, $[M(CN)_7]^{n-}$.

Point Group	D_{5h} (Pentagonal bipyramidal)	C_{3v} (Capped octahedral)	C_{2v} (Capped trigonal prismatic)
(a) CN stretches	5 ($2A_1' + A_2'' + E_1' + E_2'$)	5 ($3A_1 + 2E$)	7 ($3A_1 + A_2 + 2B_1 + B_2$)
Raman Active	3 ($2A_1' + E_2'$)	5 ($3A_1 + 2E$)	7 ($3A_1 + A_2 + 2B_1 + B_2$)
- polarised	2 (A_1')	3 (A_1)	3 (A_1)
Infrared Active	2 ($A_2'' + E_1'$)	5 ($3A_1 + 2E$)	6 ($3A_1 + 2B_1 + B_2$)
Raman and IR coincidences	0	5	6
(b) All vibrations	25 ($4A_1' + A_2' + 4A_2'' + 6E_1' + 3E_1'' + 4E_2' + 2E_2''$)	26 ($10A_1 + 3A_2 + 13E$)	39 ($12A_1 + 7A_2 + 11B_1 + 9B_2$)
Raman Active	11 ($4A_1' + 3E_1'' + 4E_2$)	23 ($10A_1 + 13E$)	39 ($12A_1 + 7A_2 + 11B_1 + 9B_2$)
- polarised	4 (A_1')	10 (A_1)	12 (A_1)
Infrared Active	10 ($4A_2'' + 6E_1'$)	23 ($10A_1 + 13E$)	32 ($12A_1 + 11B_1 + 9B_2$)
Raman and IR coincidences	0	23	32

The most reliable data are provided by spectra of complexes in solution where " free ions" are present; for aqueous solutions, Raman spectroscopy is particularly useful, water having a very weak Raman spectrum. Distortion arising from site symmetry or solid state effects would give rise to a more complicated spectrum.

As mentioned in Section e, most of the conclusions from the vibrational spectra will be drawn from profile comparisons with spectra of compounds of known symmetry.

g) Electronic Spectra.

Amongst heptacyano complexes, the electronic spectra of only four, $K_4[Ti(CN)_7].2H_2O$ (solid state),[26] $K_4[V(CN)_7].2H_2O$ (solution),[4] $K_4[Mo(CN)_7].2H_2O$ (solid and solution)[27] and $K_4[Re(CN)_7].2H_2O$ (solid and solution[53] have been used for the structure determination. However, the method is not at all conclusive because no simple rules exist for distinguishing between the different possible configurations. It may however be useful, on a qualitative basis, for showing a change of configuration for solid to solution by comparison of the reflectance spectrum of the solid with the absorption spectra of the solution.

CHAPTER II

GROUP V

NIOBIUM AND VANADIUM.

A) Niobium

A.1) $K_5[Nb(CN)_8]$

I. LITERATURE INTRODUCTION

The potassium and sodium salts of the octacyanoniobate(III) ion, $[Nb(CN)_8]^{5-}$ were first prepared in this laboratory,[37] and are the first fully established octacyanides of a trivalent transition metal ion. The potassium salt is a deep red, diamagnetic solid (low-spin, d^2) and moderately stable in dry air.

Very little is known about this complex and it has not been prepared in crystalline form before. In this section we report the structure of $K_5[Nb(CN)_8]$ in the solid state and in aqueous solution. We report also the ^{13}C NMR sepctra of $[Nb(CN)_8]^{5-}$ and $[M(CN)_8]^{4-}$ (M = Mo, W) in aqueous solution.

II. RESULTS AND DISCUSSION.

The deep red crystals of $K_5[Nb(CN)_8]$ were obtained by the photolysis of $K_4[Nb(CN)_8].2H_2O$ in aqueous KOH using red laser (krypton-ion 6471Å) radiation. For the first time this complex has been obtained as single crystals. They were studied by X-ray crystallography.†

---

† X-ray studies were carried out by Dr. M.B. Hursthouse, Queen Mary College, Chemistry Department, London.

a) X-Ray Crystal Structure of $K_5[Nb(CN)_8]$.

The crystal is tetragonal, space group $I\bar{4}$ (Z = 2), a = b = 9.220(2), c = 9.144(2)Å. The R factor has reached 0.03.

The structure of the anion in $K_5[Nb(CN)_8]$ is dodecahedral. The two sets of Nb-C distances [2.282(4) and 2.242(4)Å] correspond to the 'A' and 'B' sites (see Figure 2, p. 12) of the dodecahedron. The C≡N distances are dCN(A) = 1.159(6) dCB(B) = 1.152(6). This is the first $[ML_8]^{n-}$ complex studied in which metal-ligand distances are not equal for the two sets (in $K_4[Nb(CN)_8].2H_2O$, for example, all eight Nb-C distances are the same within experimental error, 2.255(5)Å [34]). In the isoelectronic dodecahedral anion of $K_4[Mo(CN)_8].2H_2O$, the average Mo-C bond length is 2.163(7)Å and the C≡N distance is 1.152(9)Å.[10]

The difference observed in Nb-C distances for the 'A' and 'B' sites in $K_5[Nb(CN)_8]$ is consistent with the prediction of Orgel[79] that, in a dodecahedron, the degree of π-bonding to π-acceptor ligands will be greater for 'B' than 'A' sites. Since $[Nb(CN)_8]^{5-}$ is a d^2 species with a large charge to dissipate back to the ligand, we may expect such differences to be reflected in the metal-carbon distances. In $K_4[Nb(CN)_8].2H_2O$, a d^1 species, the difference in degree of π-bonding is likely to be less apparent, and indeed all eight Nb-C distances are equal within experimental error. The structure of the anion $[Nb(CN)_8]^{5-}$ is shown in Figure 2.1. Our data on these has been reported.[80]

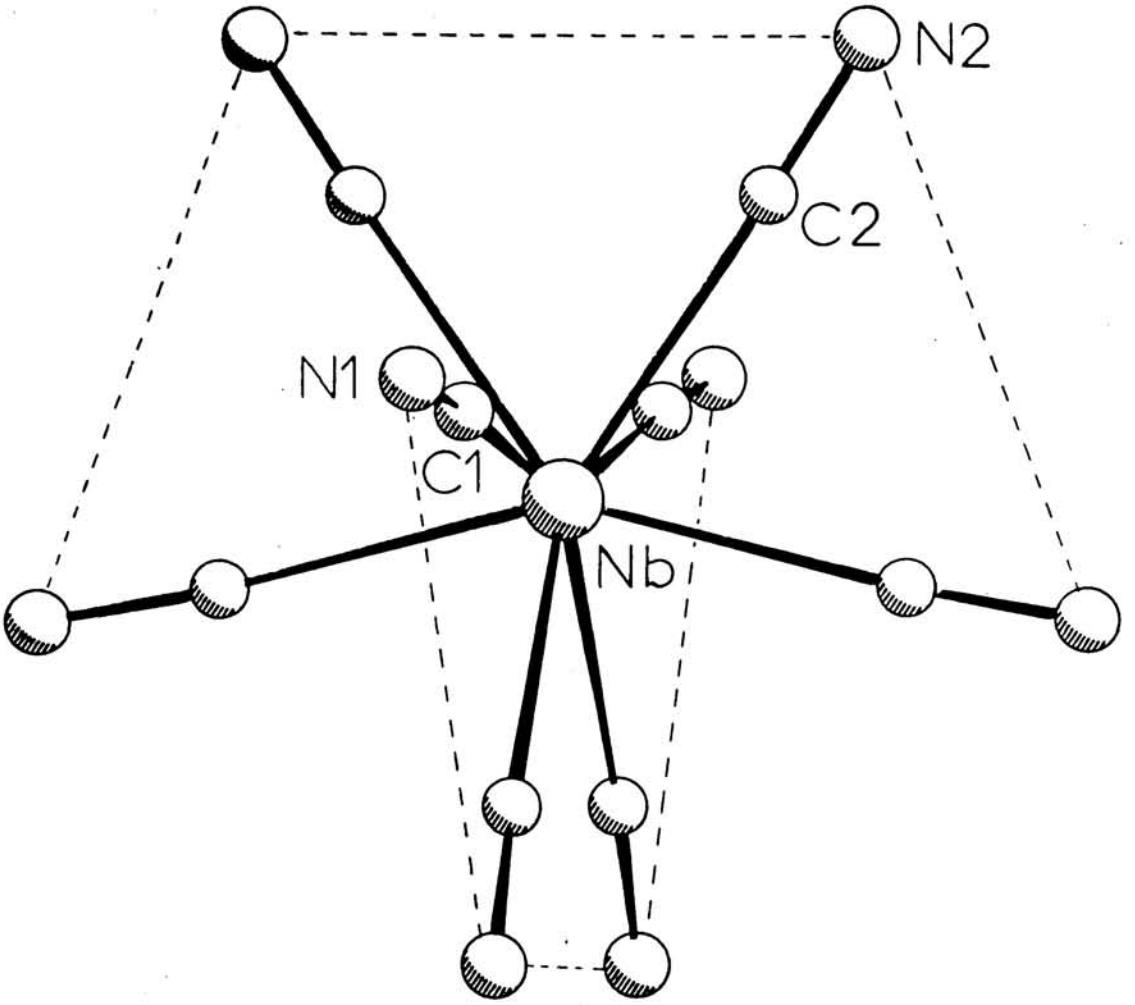


Figure 2.1. The structure of $[Nb(CN)_8]^{5-}$ in $K_5[Nb(CN)_8]$.

b) Vibrational Spectra.

The infrared and Raman spectra of $K_5[Nb(CN)_8]$ in the solid state and of the more soluble sodium salt in aqueous solution are listed in Table 2.1 and illustrated in Figure 2.2.

The spectra of the solid shows six bands in the Raman (2098, 2090, 2067, 2050, 2047, 2042 cm^{-1}) and four bands in the infrared (2092, 2044, 2038, 2020 cm^{-1}). A D_{2d} structure for $[M(CN)_8]^{4-}$ should give rise to six Raman (two polarised) and four infrared CN stretches with four Raman-infrared coincidences, while for D_{4d} a much simpler spectrum of three Raman (one polarised) and two infrared stretches with no coincidences is expected (see Table VI, p. 28). Thus, the spectra of the solid are fully consistent with D_{2d} symmetry. However, in an aqueous solution of the sodium salt the anion $[Nb(CN)_8]^{5-}$ gave only three Raman bands (2105 polarised, 2097 and 2079 cm^{-1}, both depolarised) and two infrared bands (2071 and 2051 cm^{-1}) in the ν_{CN} region. This is in agreement with D_{4d} antiprismatic geometry. The fact that the bands are sufficiently spaced and well resolved constitutes strong evidence that the anion has D_{4d} symmetry in solution. The anion $[Nb(CN)_8]^{5-}$ is only stable in solution in the presence of some excess cyanide-ion and the band observed at 2079 cm^{-1} could be due to this. However, this band was shown to be essentially depolarised while the C≡N stretch of free cyanide is polarised. To confirm the genuineness

Figure 2.2. Raman spectra in the ν_{CN} region of $[Nb(CN)_8]^{5-}$ in solid $K_5[Nb(CN)_8]$ and of the sodium salt in aqueous 0.1 M CN^-.

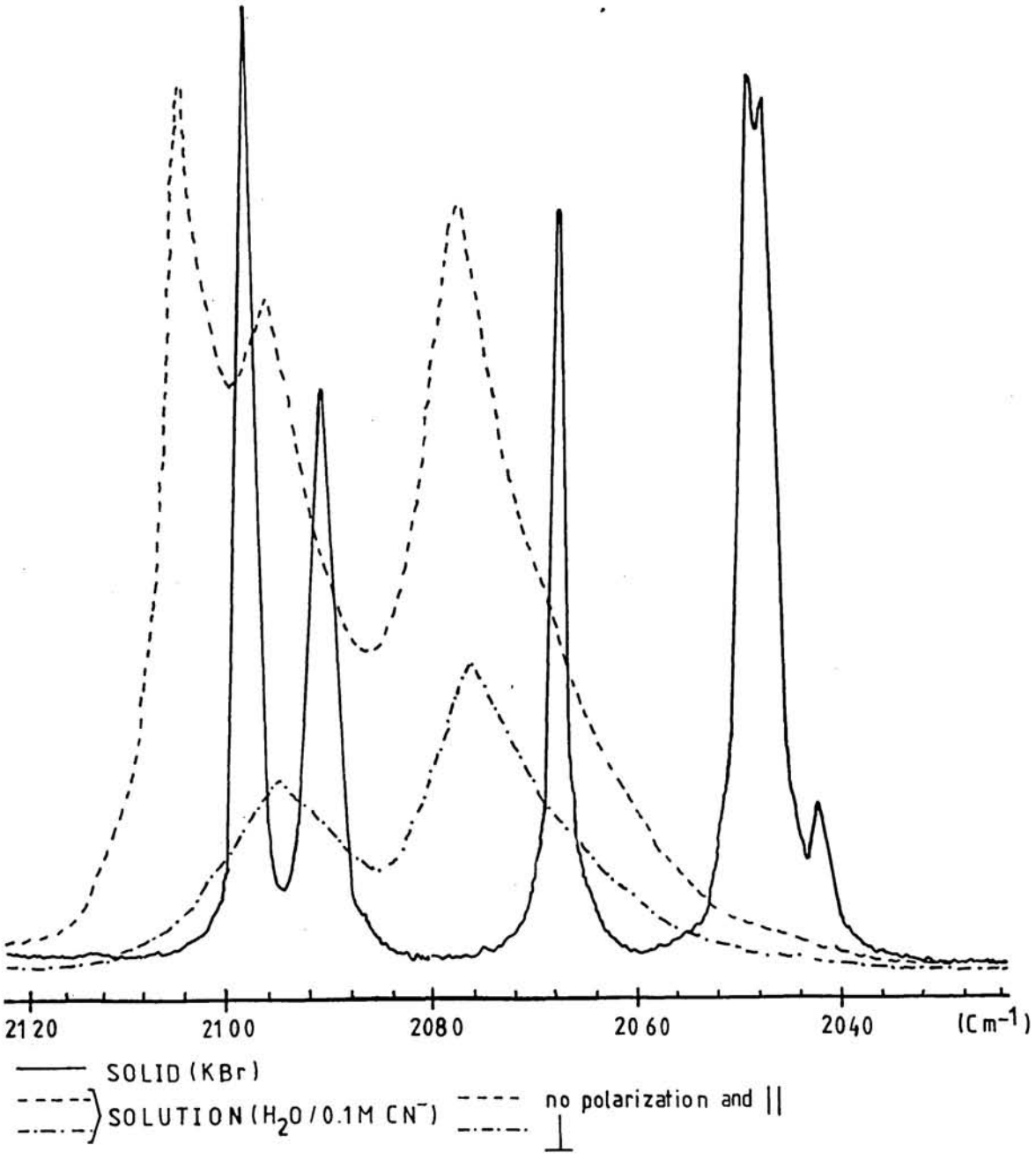


TABLE 2.1. Vibrational Spectral Data for $K_5[Nb(CN)_8]$.

	ν_{CN} (cm^{-1})	ν_{MC}, δ_{MCN} and δ_{CMC} (cm^{-1})
IR (solid)	2092(s)	471(s)
	2044(vs)	442(w)
	2038(sh)	431(m)
	2020(sh)	386(s)
		343(vs)
		317(vw)
		310(vw)
IR (solution)[a]	2071(vs)	
	2050(sh)	
Raman (solid)	2098(10)	466(3)
	2090(6)	435(2) 194(3)
	2067(8)	388(1) 180(8)
	2050(9)	345(4) 135(2)
	2047(9)	318(5) 123(2)
	2042(2)	305(2) 110(3)
Raman (solution)	2105(10) pol	460(3)
	2097(8) depol.	330(7)
	2079(8) depol.	310(7)

[a] Solution of the sodium salt $Na_5[Nb(CN)_8]$ in 0.1 M aqueous NaCN.

of that absorption we allowed the sample to oxidise to $[Nb(CN)_8]^{4-}$ by bubbling oxygen through it . The Raman spectrum of this new solution showed the bands characteristic [37] of $[Nb(CN)_8]^{4-}$ (2127 polarised and 2114 cm^{-1}) and one band at 2080 cm^{-1}, completely polarised, due to free cyanide. This experiment confirmed that the band observed at 2079 cm^{-1} is genuine and arises from cyanide bound to the central atom. Assignments of the observed bands and comparison with those of $[M(CN)_8]^{4-}$ (M = Nb, W, Mo) are considered later (Section A.2, page 44).

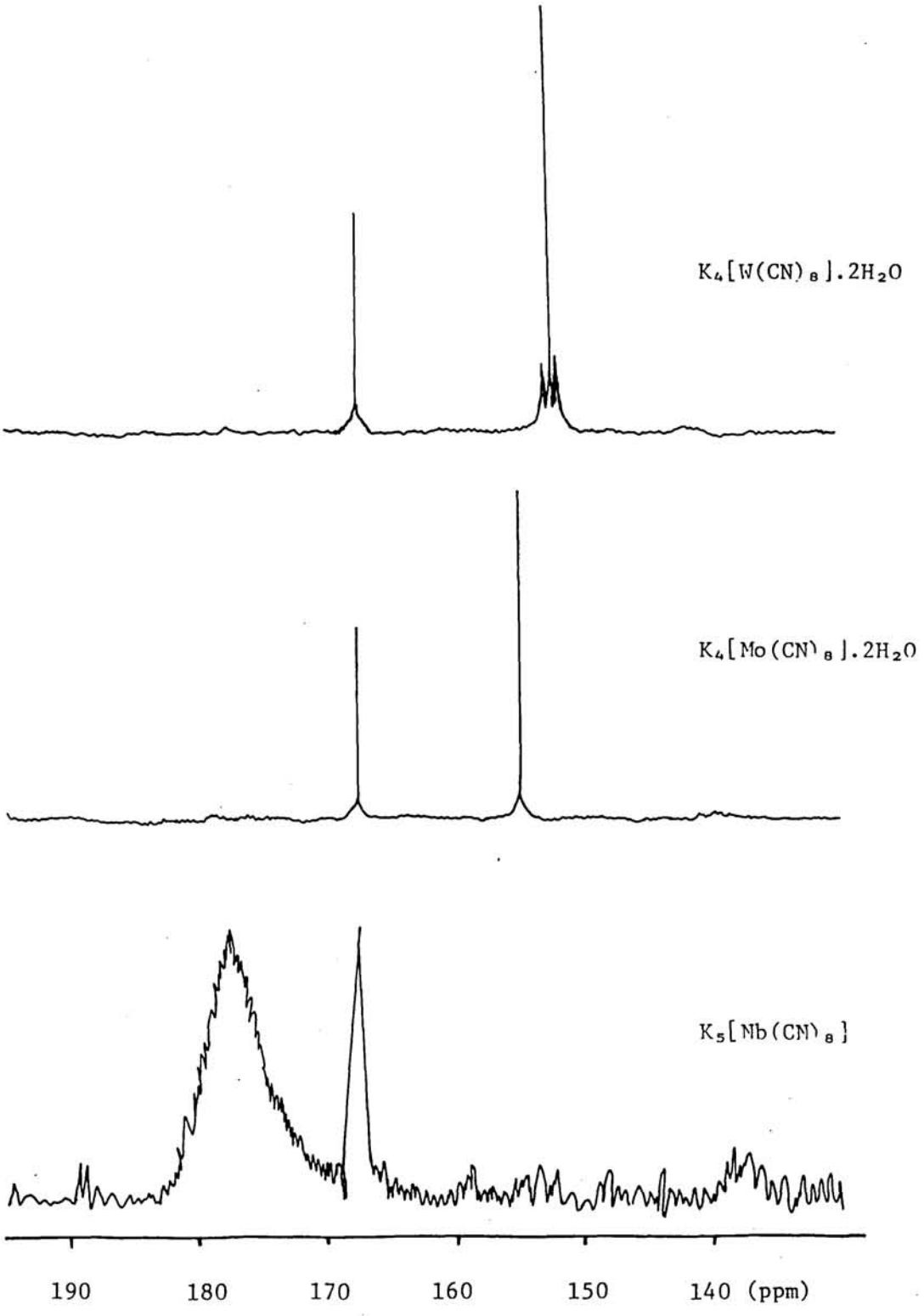
We conclude that the D_{2d} structure of $[Nb(CN)_8]^{5-}$ changes to D_{4d} in aqueous solution. This is also likely to be the case for the anion in $K_4[M(CN)_8].2H_2O$ (M = Nb, Mo, W) (See Section c below).

c) ^{13}C-NMR.

Table 2.2 gives the chemical shifts for diamagnetic cyano complexes in ^2H_2O including the three octacyano complexes, {$[Nb(CN)_8]^{5-}$, $[Mo(CN)_8]^{4-}$, $[W(CN)_8]^{4-}$ }. For comparison we include here data for the heptacyano complexes, $[Mo(CN)_7]^{5-}$, $[W(CN)_7]^{5-}$ and $[Re(CN)_7]^{4-}$; the preparation and structural chemistry of these are discussed later (Chapter III, p. 68 and 111). The Figure 2.3 shows the spectra of the $[M(CN)_8]^{n-}$ species. This is the first report of ^{13}C NMR spectra for octacyano or heptacyano species in aqueous solution.

Muetterties[38] has reported ^{13}C spectra for $K_4[M(CN)_8].2H_2O$ (M = Mo, W) in aqueous solution and $(Pr^n_4N)_4[M(CN)_8]$ (M = Mo, W) in CHF_2Cl-CD_2Cl_2 solution. The slight difference between

Figure 2.3. The ^{13}C NMR Spectra of $K_5[Nb(CN)_8]$ and $K_4[M(CN)_8].2H_2O$ (M = W, Mo) in ^2H_2O solutions in Excess CN^-.



shifts reported for these two species [δ(Mo) = 150.5 and δ(W) = 155.5 ppm[38]) and our results [δ(Mo) = 154.6 and δ(W) = 151.1 ppm], all relative to TMS (on the low field side), are probably due to the different solvents used.

The ^{13}C NMR spectrum of $[Nb(CN)_8]^{5-}$ in ^2H_2O shows a single, broad resonance unaffected either in position or band-width by added free cyanide (see Figure 2.3). The sharpness of the free cyanide peak indicates that the rate of exchange of free CN^- with complexed CN^- is very slow on the NMR time scale. The breadth of the peak is almost certainly due to the fact that ^{93}Nb (100% natural abundance) has a nuclear spin of $S = \frac{9}{2}$.

The resonance line for the free CN^- ligand in ^2H_2O was observed at 167.2 ppm and the chemical shift δ for the $[Nb(CN)_8]^{5-}$ ion in ^2H_2O is 176.2 ppm (both relative to TMS). For the species $[Mo(CN)_8]^{4-}$ and $[W(CN)_8]^{4-}$ sharp lines are observed at δ = 154.6 and δ = 151.1 ppm respectively, and the sharpness of these absorptions suggests fluxionality between the two polyhedra (dodecahedron and antiprism) observed on NMR time scale (in agreement with the conclusions of Muetterties[38,39]).

Too little is known about the factors governing ^{13}C chemical shifts to attempt to interpret the data in Table 2.2. However, we may note that some of the trends found in hexa-, tetra- and di-cyano complexes[45] are also evident in our octa- and heptacyano species. Firstly, there is a shift to higher field (i.e., lower δ value) from second to third row both for $[M(CN)_8]^{4-}$ (M = Mo, W) and $[M(CN)_7]^{5-}$ (M = Mo, W); similar effects are observed for $[M(CN)_6]^{4-}$ (M = Fe, Ru, Os);

TABLE 2.2. Chemical Shifts for Diamagnetic Cyano Complexes in ^2H_2O.

Complex	Structure	δ[a]	Reference
Octacyano			
$[Nb(CN)_8]^{5-}$	antiprismatic	176.2	This work
$[Mo(CN)_8]^{4-}$	antiprismatic	154.6	This work
$[W(CN)_8]^{4-}$	antiprismatic	151.1	This work
Heptacyano			
$[Mo(CN)_7]^{5-}$	pentagonal-bipyramidal	188.4	This work
$[W(CN)_7]^{5-}$	pentagonal-bipyramidal	148.2	This work
$[Re(CN)_7]^{4-}$	pentagonal-bipyramidal	142.2	This work
Hexacyano			
$[Fe(CN)_6]^{4-}$	octahedral	177.2	45
$[Ru(CN)_6]^{4-}$	octahedral	162.3	45
$[Os(CN)_6]^{4-}$	octahedral	142.5	45
$[Co(CN)_6]^{3-}$	octahedral	140.1[b]	45
$[Rh(CN)_6]^{3-}$	octahedral	131.9[c]	45
$[Ir(CN)_6]^{3-}$	octahedral	110.9	45
$[Pd(CN)_6]^{2-}$	octahedral	104.2	45
$[Pt(CN)_6]^{2-}$	octahedral	84.7[d]	45
Tetracyano			
$[Ni(CN)_4]^{2-}$	square planar	136.6	45
$[Pd(CN)_4]^{2-}$	square planar	131.9	45
$[Pt(CN)_4]^{2-}$	square planar	125.7[e]	45
$[Ru(CN)_4]^{-}$	square planar	105.2	45
$[Au(CN)_4]^{-}$	square planar		

TABLE 2.2 (continued)

Complex	Structure	δ^a	Reference
Tetracyano			
$[Cu(CN)_4]^{3-}$	Tetrahedral	161.6	45
$[Zn(CN)_4]^{2-}$		147.0	45
$[Cd(CN)_4]^{2-}$		149.8	45
$[Hg(CN)_4]^{2-}$		153.2	45
Dicyano			
$[Ag(CN)_2]^-$	linear	150.0	45
$[Au(CN)_2]^-$		154.2	45
$[Hg(CN)_2]$		144.6	45

a To low field of Me_4Si in ppm

b Eight-line pattern, $^1J_{C-Co} = 126.0 \pm 0.8$ Hz

c Doublet, $^1J_{C-Rh} = 36.6$ Hz

d Three-line pattern(^{195}Pt, 33.7%), $^1J_{C-Pt} = 808$ Hz

e Three-line pattern, $^1J_{C-Pt} = 1034$ Hz

$[M(CN)_6]^{3-}$ (Co, Rh, Ir); $[M(CN)_6]^{2-}$ and $[M(CN)_4]^{2-}$ (Pd, Pt)[45]; secondly, there is a shift to high field (lower δ) with increasing oxidation state for isoelectronic species, e.g., $[Nb^{III}(CN)_8]^{5-}$ and $[Mo^{IV}(CN)_8]^{4-}$, and $[W^{II}(CN)_7]^{5-}$ and $[Re^{III}(CN)_7]^{4-}$, as in the case with $[M^{II}(CN)_6]^{4-}$ (Fe, Ru, Os) and with $[M^{III}(CN)_6]^{3-}$ (Co, Rh, Ir).[45] As with other cyano species in Table 2.2[45] there is no obvious correlation of δ with either the number of metal d electrons or with the coordination number.

d) Conclusions.

The anion $[Nb(CN)_8]^{5-}$ in $K_5[Nb(CN)_8]$ has been shown to possess dodecahedral (D_{2d}) symmetry in the solid state, and this is the first octacyano complex studied in which metal-carbon distances are not equal for the two sets corresponding to the 'A' and 'B' sites of the dodecahedron. Vibrational data suggest that there is a change of the anion configuration from dodecahedral (D_{2d}) to anti-prismatic (D_{4d}) symmetry in solution.

A.2) $K_4[Nb(CN)_8].2H_2O$, $K_4[Mo(CN)_8].2H_2O$ and $K_4[W(CN)_8].2H_2O$.

In this section we will briefly present our results for the Raman spectra of these three complexes. For convenience, and because of the similarity of the species (all being $[M(CN)_8]^{n-}$) we also consider molybdenum and tungsten in this Chapter (under Group V), and comment on the frequencies observed in the Raman spectrum of $[Nb(CN)_8]^{5-}$.

a) Raman Spectra

We have measured the laser-Raman spectra in the ν_{CN} region of $[Nb(CN)_8]^{4-}$, $[Mo(CN)_8]^{4-}$ and $[W(CN)_8]^{4-}$ in aqueous solution under conditions of high resolution with the help of a computer for collecting data from a number of repetitive scans (ten per spectrum).

The spectra are shown in Figure 2.4 and the data are presented in Table 2.3.

TABLE 2.3. Data for $K_4[M(CN)_8].2H_2O$ in Aqueous Solution (ν_{CN} region).

Complex		ν_{CN} (cm^{-1})	Reference
$K_4[Nb(CN)_8].2H_2O$	R	2127(10) pol, 2118(6) dp.	This work
		2127(10) pol, 2114(6) dp.	37
$K_4[Mo(CN)_8].2H_2O$	R	2135(10)pol, 2118(5)dp, 2110(3)dp	This work
		2134(vs)pol, 2119(ms)pol, 2109(w)	34
$K_4[W(CN)_8].2H_2O$	R	2136(10)pol, 2116(6)dp, 2105(3)dp	This work
		2135(vs)pol, 2118(ms)pol, 2104(w)	34

Figure 2.4. Raman spectra in the ν_{CN} region of $[M(CN)_8]^{4-}$ (M = W, Mo, Nb) in aqueous solution (0.1 M CN^-).

$[W(CN)_8]^{4-}$

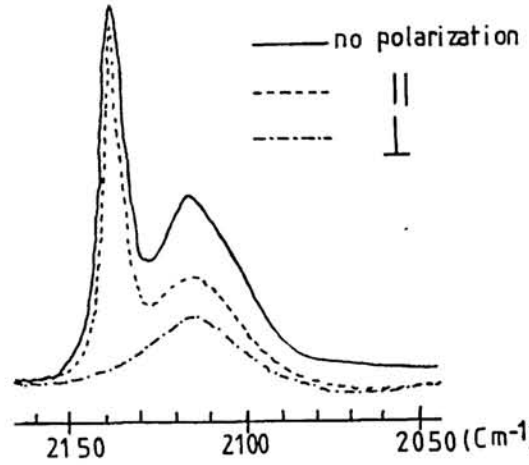
Spinning cell computer control

10 scans. Scan speed 0.2

slits, 1.1 cm^{-1}

s. length 2.0 cm

Time constant 0.3 sec.



$[Mo(CN)_8]^{4-}$

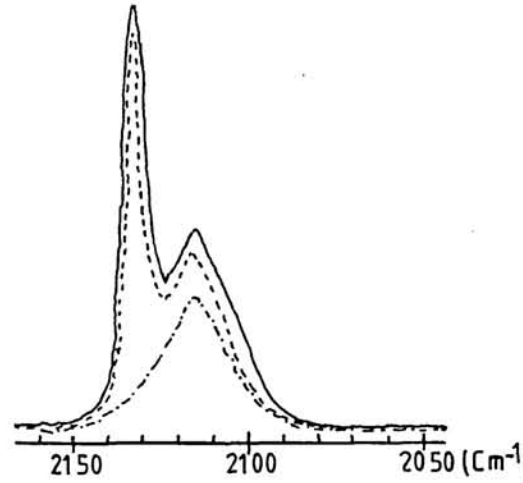
Spinning cell computer control

10 scans. Scan speed 0.2

slits, 1.1 cm^{-1}

s. length 2.0 cm

Time constant 0.3 sec



$[Nb(CN)_8]^{4-}$

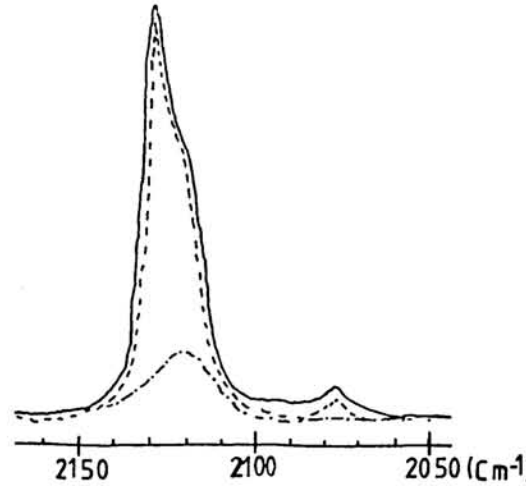
Spinning cell computer control

20 scans. Scan speed 0.2

slits 1.1 cm^{-1}

s. length 2.0 cm

Time constant 0.3 sec.



There have been many reports of the spectra of $[M(CN)_8]^{4-}$ salts (M = Mo, and W) in the solid state[10] and in solution,[74,75,76,77,78] the most recent being that of Long and Vernon.[34] There is a real division in the literature between

(a) those who think {for $K_4[M(CN)_8].2H_2O$ (M = Mo, W)} that there is stereochemical conversion of the anion $[M(CN)_8]^{n-}$ from D_{2d} (solid) to D_{4d} (solution).[74,75,76]

(b) those who think that the D_{2d} geometry is maintained in solution.[34,77,78]

Griffith and Kiernan[37] proposed such a change of configuration for the salt $K_4[Nb(CN)_8].2H_2O$ from D_{2d} (solid) to D_{4d} (solution) on the basis of EPR and vibrational data.

Our Raman data for the complexes $K_4[M(CN)_8].2H_2O$ (M = Nb, Mo, W) in aqueous solution are in agreement with those reported for the niobium salt $[Nb(CN)_8]^{4-}$ but disagree, as far as polarisation is concerned, with those presented by Long and Vernon.[34] (For convenience, Table 2.3 contains our Raman spectra as well as those with which we are comparing our recent studies). In the most comprehensive work, Long and Vernon[34] claim that, for $[Mo(CN)_8]^{4-}$ and $[W(CN)_8]^{4-}$, two of the three bands in the C≡N stretching region are polarised, and their conclusion is that the retention of the anion configuration (D_{2d}) in solution was based only on this evidence.

A careful examination of our Raman spectra, which were carried out under conditions of higher resolution than any previous studies, shows only one polarised band and two depolarised bands. The selection rules (see Table VI, page 28) predict three (A_1, E_2, E_3) absorptions with one polarised to be Raman active for D_{4d} symmetry and six ($2A_1$, $2B_2$, 2E) absorptions with two polarised for D_{2d} symmetry. In this case we suggest the number of bands (three) and the fact that only one is

polarised is more consistent with D_{4d} geometry for the anion $[M(CN)_8]^{4-}$ (M = Mo, W) in solution. For $[Nb(CN)_8]^{4-}$, the observation of only two bands may arise from overlapping of two modes.

It seems reasonable to assign the highest frequency polarised band to the A_1^1 totally symmetric mode, and likewise we may assign polarised bands in the 400-500 cm^{-1} region to the corresponding A_1^1 totally symmetric metal-carbon stretches. These, as the simplest vibrations for D_{4d} polyhedra,[53] provide some guide to the nature of the metal-ligand bond (Table 2.4) (see also Section

TABLE 2.4. C≡N and M-C Stretches (A_1^1 modes) in the Raman Spectra of $[M(CN)_8]^{n-}$ in Aqueous Solution.

	Metal Electronic Configuration	ν_{CN} (cm^{-1})	ν_{MC} (cm^{-1})	Reference
$[Nb(CN)_8]^{4-}$	d^1	2127	414	37
$[W(CN)_8]^{4-}$	d^1	2168	417	37
$[Mo(CN)_8]^{3-}$	d^1	2158	401	37
$[Nb(CN)_8]^{5-}$	d^2	2105	460	This work
$[W(CN)_8]^{4-}$	d^2	2136	471	34
$[Mo(CN)_8]^{4-}$	d^2	2135	470	34

The higher the value of ν_{MC} and the lower those of ν_{CN} the greater the degree of π-bonding in the M-C linkage there is likely to be. This appears to be the case here: ν_{MC} is highest for the d^2 species and ν_{CN} lowest. This is particularly so for $[Nb(CN)_8]^{5-}$ which, although still d^2, has a higher negative charge to dissipate via π-bonding to the ligand (see also X-ray data, section A.1, page 31).

The ^{13}C NMR spectra of $[M(CN)_8]^{4-}$ (M = Mo, W) have already been described (see Section A1-c, p. 38).

b) Conclusions.

We propose, on the basis of Raman data in aqueous solution, that the configuration of the anions in solid $K_4[Nb(CN)_8].2H_2O$, $K_4[Mo(CN)_8].2H_2O$ and $K_4[W(CN)_8].2H_2O$ change from D_{2d} to D_{4d} symmetry in solution. This conclusion is supported in the case of $K_4[Nb(CN)_8].2H_2O$ by EPR data.[37]

B) Vanadium

B.1) $K_4[V(CN)_7].2H_2O$

I. LITERATURE INTRODUCTION.

The salt $K_4[V(CN)_7].2H_2O$ was the first heptacyano complex to be studied by single crystal X-ray analysis[4] and is the best characterised vanadium(III) cyano complex. It was earlier believed to be octahedral, i.e., $K_3[V(CN)_6]$, first reported by Locke and Edwards in 1898.[62] The anion was shown to be pentagonal bipyramidal with equivalent $V-C_{ax}$ and $V-C_{eq}$ distances (2.15(1)Å). The complex is paramagnetic (high spin, d^2, μ = 2.9 BM)[20] and because it is well characterised structurally, we attempted to be more successful in measuring its EPR and consequently establishing a model for hepta-coordinated complexes containing PB geometry.

Vibrational data suggested that the anion $[V(CN)_7]^{4-}$ retains its symmetry (PB, D_{5h}) in aqueous solution[35,51] and its electronic spectrum has been interpreted on the basis of crystal field theory[56] and molecular orbital theory,[57] assuming retention of PB symmetry in solution. Ligand field splitting parameters have been evaluated.[56] The energy ordering of the metal 3d orbital is thought to be[56,57]

$$d_{xz}, d_{yz} < d_{x^2-y^2}, d_{xy} < d_{z^2}$$

In an attempt to measure the EPR spectrum of the compound, Bennett and Nicholls[58] found that $K_4[V(CN)_7].2H_2O$ disproportionates in aqueous cyanide producing $[V(CN)_6]^{4-}$ and $[VO(CN)_5]^{3-}$, both of which

are paramagnetic species.[51] More recently, Sergeeva, et al.[52] were unsuccessful in recording the EPR spectrum of the solution, and reproduced the previous published results.[51,58]

We re-examined the vibrational spectra of the salt in solid and aqueous solution phases, and attempted to measure its EPR spectra in aqueous solution and also in solid solution in the diamagnetic, isomorphous host lattice $K_4[Re(CN)_7].2H_2O$.

II RESULTS AND DISCUSSION

a) Vibrational Spectra

The infrared and Raman spectra of $K_4[V(CN)_7].2H_2O$ in the solid state and in aqueous solution containing excess cyanide ion are reported in Table 2.5. (The complex is unstable in the absence of excess CN^- ion).

TABLE 2.5. Vibrational Data for $K_4[V(CN)_7].2H_2O$.

	ν_{CN} (cm^{-1})	ν_{MC} or ν_{MCN} (cm^{-1})	Reference
IR	2108(m), 2090(s),	475(m), 442(m) 400(sh), 365(m) 335 (m)	This work
IR[a] (solution)	2104(s), 2072(m)		51
R	2110(w), 2104(m) 2100(m)	605(w), 470(m), 375(w), 340(w)	This work
R[a] (solution)	2104(s) pol., 2100(sh) pol.		This work

[a] 6.0 M aqueous KCN.

Our experimental results are in agreement with those previously reported[35,51] and suggest that the D_{5h} symmetry found for the $[V(CN)_7]^{4-}$ anion in solid $K_4[V(CN)_7].2H_2O$ is retained in aqueous solution. Under D_{5h} symmetry the fundamental cyano stretching modes A_2'' and E_1' are infrared active while there are three Raman active modes ($2A_1'$ and E_2', the A_1' modes being polarised) with no Raman-infrared coincidences are expected (see Table VII, p. 29). Thus,it appears that in solution, $[V(CN)_7]^{4-}$ is a regular pentagonal bipyramid since there is little difference between the infrared and Raman spectra of the solid and the aqueous solution. The Raman spectrum of the solution shows two polarised absorptions (as expected for D_{5h} symmetry) in the ν_{CN} region with no infrared-Raman conincidence.

Using similar arguments to those used for our spectra of octacyano complexes (see Table 2.4), and assuming D_{5h} symmetry for $[M(CN)_7]^{n-}$ species in solution, we may again attempt comparison of Raman ν_{CN} and ν_{MC} (A_1' modes) with d^n electron configuration (Table 2.6). As before, we take the strongest polarised Raman band in the CN stretching region as the A_1' totally symmetric C≡N stretch (ν_{CN}) and the strongest band in the 400-450 cm^{-1} region as the totally symmetric A_1' metal-carbon (ν_{MC}) stretch.[53]

As with the octacyano species, the higher the d orbital occupancy the greater the M-C π-bonding leading to higher ν_{MC} and lower ν_{CN} frequencies.

TABLE 2.6. C≡N and M-C Stretches (A_1' modes) in the Raman Spectra of $[M(CN)_7]^{n-}$ in Aqueous Solution.

	Metal Electronic Configuration	ν_{CN}	ν_{MC}	Reference
$[V(CN)_7]^{4-}$	d^2	2104	397	35
$[W(CN)_7]^{5-}$	d^4	2076	475	This work
$[Mo(CN)_7]^{5-}$	d^4	2115	400	This work
$[Mo(CN)_7]^{4-}$	d^3	2106	not observed	This work
$[Re(CN)_7]^{4-}$	d^4	2123	438	35

b) EPR Spectra

We carried out many experiments in order to obtain a good EPR signal for $K_4[V(CN)_7].2H_2O$ (high spin, d^2, PB species, μ = 2.9 BM).[20]

We have tried using the pure solid, the aqueous solution and the solid solution of $K_4[V(CN)_7].2H_2O$ doped in the isomorphous and diamagnetic $K_4[Re(CN)_7].2H_2O$ as host lattice at different temperatures. In all cases, we could only reproduce the literature data.[51,52] The signals observed arose from small amounts of paramagnetic impurities, $[V(CN)_6]^{4-}$ and $[VO(CN)_5]^{3-}$ which can not be avoided during the preparative work and are not in sufficient amounts to interfere with the analytical results.

Although attempts to use $K_4[V(CN)_7].2H_2O$ as an EPR model for a pentagonal bipyramid were unsuccessful, we subsequently did discover such a model in

$NaK_3[Mo(CN)_7].2H_2O$ which we showed by X-ray study to contain pentagonal bipyramidal anion (see Chapter III, Section B.1a, p. 95). The EPR spectrum of this is detectable only at temperatures below 50 K; however, we found that pure $K_4[V(CN)_7].2H_2O$ at 13.8 K shows no corresponding signal. This may be the result of fast spin-lattice interaction between neighbouring ions and no further work has been done with the solid solution (at such low temperarures) in which case this effect should be minimised.

c) Conclusions.

In view of the difficulty of obtaining $[V(CN)_7]^{4-}$ in environments suitable for EPR study, we abandoned the idea of using this ion as a model for EPR spectra of a pentagonal bipyramid. We did however, subsequently find such a model ($NaK_3[Mo(CN)_7].2H_2O$, mentioned briefly above).

We have extended the vibrational data showing that this symmetry is maintained in aqueous solution.

III MISCELLANEOUS

We tried the reaction of $K_4[Nb(CN)_8].2H_2O$ with nitric oxide unsuccessfully. The only product observed was a white precipitate identified as Nb_2O_5, so presumably reduction of NO had occurred, possibly via an intermediate unstable cyanonitrosyl complex of niobium.

E X P E R I M E N T A L

Potassium Octacyanoniobate(III) - $K_5[Nb(CN)_8]$.

The preparation of this complex has been already reported in the literature.[37] However, improvement of the method described has been necessary to obtain the complex as single crystals.

The crystals of $K_5[Nb(CN)_8]$ were made by a five-minute photolysis of $K_4[Nb(CN)_8].2H_2O$ (1 g) in oxygen-free aqueous KOH (pH = 12) (2 ml of solution in a 10 ml Shlenck tube) using the focussed 647.1 nm red line (500 nm) of a krypton ion laser. The dark red crystals were filtered under argon, washed several times with oxygen-free methanol and dried under vacuum (yield, 80%). One specimen was transferred and sealed under argon in a Lindemann capillary for the X-ray work.

Analysis: (Found: C, 19.37% ; N, 22.23% ; K, 39.8% . $C_8N_8K_5Nb$ requires C, 19.46% ; N, 22.70% ; K 39.3%).

Sodium Octacyanoniobate(III) - $Na_5[Nb(CN)_8].nH_2O$

The more soluble sodium salt has been made by the addition of oxygen-free aqueous solution of sodium perchlorate dropwise to a suspension of the potassium salt in oxygen-free aqueous-cyanide (0.1 M NaCN) solution. When the precipitation of white potassium perchlorate was complete the dark red solution was filtered under argon straight into the Raman cell or NMR tube.

Potassium Octacyaniobate(IV) dihydrate - $K_4[Nb(CN)_8].2H_2O$, Potassium Octacyanomolybdate(IV) dihydrate - $K_4[Mo(CN)_8].2H_2O$ and Potassium Octacyanotungstate(IV) dihydrate - $K_4[W(CN)_8].2H_2O$.

These complexes have been prepared by their literature methods. References 37, 60 and 61 respectively.

Analysis:

$K_4[Nb(CN)_8].2H_2O$ - Found: C, 19.7; N, 22.9; H, 0.8%, $C_8H_4K_4N_8NbO_2$ requires C, 19.5; N, 22.7; H, 0.8% .

$K_4[Mo(CN)_8].2H_2O$ - Found: C, 19.5; N, 22.8; H, 0.8%. $C_8H_4K_4N_8MoO_2$ requires C, 19.3; N, 22.6; H, 0.8%.

$K_4[W(CN)_8].2H_2O$ - Found: C, 16.7; N, 19.8; H, 0.8%. $C_8H_4K_4N_8WO_2$ requires C, 16.4; N, 19.2; H, 0.7%.

Potassium Heptacyanovanadate(III) dihydrate - $K_4[V(CN)_7].2H_2O$.

Many methods for preparing $K_4[V(CN)_7].2H_2O$ have been reported[58,62,63] but we found that a modification based on the reported procedure[64] for $K_4[Mo(CN)_7].2H_2O$ gave the best results.

Vanadium trichloride (1.0 g, 6.3×10^{-3} mol) and KCN (4.1 g, 6.3×10^{-2} mol) were placed in a 50 cm^3 three-necked flask (equipped with a magnetic stirrer bar). The air was replaced by argon in a vacuum line, 27 cm^3 of oxygen-free water was added (using a steel needle technique) and the mixture was stirred at room temperature for 22 hours. The resulting violet precipitate was filtered off and the filtrate kept at 0^oC overnight. The deep red crystals formed were filtered off, washed with oxygen-free ethanol and then with oxgyen-free ether. The product was recrystallised in a mixture of oxygen-free 5% aqueous KCN and oxygen-free methanol. A second crop of crystals was obtained by adding ethanol to the mother liquor and following the above procedure. Total yield, 73%.

Analysis: Found; C, 20.63; N, 22.69; H, 0.39%. $C_7H_4K_4N_7VO_2$ requires; C, 19.70; N, 23.04; H, 0.94%.

CHAPTER III

GROUP VI

A) Tungsten

B) Molybdenum

I. LITERATURE INTRODUCTION.

Although salts of $[M(CN)_8]^{n-}$, (M = W, Mo and n = 4, 3)[65,66,67] are well known, very few unsubstituted cyano complexes of the two metals in the oxidation states (II) and (III) are known. The complex $K_4[Mo(CN)_7].2H_2O$ was reported for the first time in 1932[64] and has been the subject of Raman, IR, EPR and electronic spectroscopy studies.[27] The molybdenum(II) complex $K_5[Mo(CN)_7].H_2O$ was first obtained and characterised in this laboratory.[28] Its structure, as the molybdate, has been proved to be $PB(D_{5h})$ by X-ray diffraction[7] in the solid state and the anion $[Mo(CN)_7]^{5-}$ keeps this configuration in solution.[7] In our original work[28] we suggested that $[Mo(CN)_7]^{5-}$ had a CTP structure in aqueous solution, but the data presented below suggest that, as with all heptacyano complexes so far studied, it has a PB structure in solution. The rather ill-defined $K_4[W(CN)_6]$ [68] and $K_3[W(CN)_6]$ [68] are the only low oxidation state unsubstituted complexes of tungsten that have been reported. They were made by reaction of $K_4[W(CN)_8].2H_2O$ with molecular hydrogen at 390°C for eight hours. In the same paper[68] the preparation of the analogous " $K_4[Mo(CN)_6]$" and " $K_3[Mo(CN)_6]$" species were reported; these were made by the same method using $K_4[Mo(CN)_8].2H_2O$ as starting material.

Kiernan[28] proposed the refomulation of "$K_4[Mo(CN)_6]$" as $K_5[Mo(CN)_7]$, on the basis of the similarity of their reported[68] infrared spectra with those of $K_5[Mo(CN)_7]$. He also isolated[83] a green product he believed was the analogue of $K_4[Mo(CN)_7].2H_2O$ by repeating the procedure of reference 68.

In this Chapter we report an investigation on these low oxidation state species. We made them first by following the original preparations and then by modification of these procedures. We now re-formulate these complexes as $K_4[W(CN)_7H].2H_2O$, $K_5[W(CN)_7].H_2O$ and $K_4[Mo(CN)_7H].2H_2O$ rather than as $K_3[W(CN)_6]$, $K_4[W(CN)_6]$ and $K_3[Mo(CN)_6]$,[68] and also give new methods of preparation for them. Their structures are discussed on the basis of vibrational, ^1H and ^{13}C NMR sepctroscopy, and some of their reactions described.

II. AIM.

Our initial aim was the preparation, characterisation and the study of some physical and chemical properties of heptacyano complexes of W(II), W(III), Mo(II) and Mo(III).

III. RESULTS AND DISCUSSION

A. Tungsten.

A.1) $K_4[W(CN)_7H].2H_2O$ and $K_5[W(CN)_7].H_2O$.

The existence of cyano complexes of molybdenum(III) (e.g., $K_4[Mo(CN)_7].2H_2O$[27,64]) and molybdenum(II), (e.g., $K_5[Mo(CN)_7].H_2O$[28]), led us to try to prepare analogous tungsten compounds. As this section

shows, we were unable to make salts of $[W(CN)_7]^{4-}$ but obtained instead the novel hydride species $[W(CN)_7H]^{4-}$, the first eight coordinate cyanide hydride to be made, and we were also successful in making salts of $[W(CN)_7]^{5-}$.

a) Preparation of Complexes.

The only unsubstituted tungsten cyano complexes reported with an oxidation state of less than IV are $K_3[W(CN)_6]$ and $K_4[W(CN)_6]$, made from $K_4[W(CN)_8].2H_2O$ and hydrogen at 390°C;[68] reaction of $K_4[W(CN)_6]$ with nitrosyl chloride is said to give $K_3[W(CN)_6]$.[81] Neither salt was fully characterised.[81]

i) Reaction of $K_4[W(CN)_8].2H_2O$ with H_2.

We repeated the experiment of Kleinberg et al.[68] and obtained a black product, the IR spectrum of which was complex but showed features in the C≡N stretching region similar in profile to those exhibited by a mixture of $K_4[Mo(CN)_7].2H_2O$[27] and $K_5[Mo(CN)_7].H_2O$,[28] suggesting that tungsten heptacyano complexes might indeed be present. Extraction with methanol did not, however, give $K_3[W(CN)_6]$ and $K_4[W(CN)_6]$.

A modification of the above procedure (see Experimental Section) gave pure $K_4[W(CN)_7H].2H_2O$ as dark green crystals. Evidence for this formulation is given below (sections ii-d and e). The infrared spectrum of the crude reaction product before purification also contained bands which we were subsequently (see p. 73) able to show were due to $K_5[W(CN)_7].H_2O$, but we were unable to obtain pure $K_5[W(CN)_7].H_2O$ from the reaction product in this way.

ii) Reaction of $K_3[W_2Cl_9]$ with CN^-.

One of the few accessible tungsten(III) complexes is $K_3[W_2Cl_9]$ and we decided to investigate its reaction with cyanide under anaerobic conditions in the hope of obtaining a tungsten(III) cyano complex. The reaction of $K_3[W_2Cl_9]$ (first made by Olsson in 1914[67]) with KCN in the presence of air gives $K_4[W(CN)_8].2H_2O$.[69] We found that, in the absence of air, a mixture of salts which were subsequently shown to be $K_4[W(CN)_7H].2H_2O$ and $K_5[W(CN)_7].H_2O$ were formed, together with an unidentified complex which perhaps contained W-W bonds. Although we tried various conditions (e.g. varying the temperature, changing the $W:CN^-$ ratio) we were unable to obtain a pure product, probably because of the difficulty of breaking the metal-metal bond known[82] to be present in $K_3[W_2Cl_9]$. We then found that reaction of CN^- with $K_3[W_2Cl_9]$ under u.v. light in the absence of air gave the yellow $K_5[W(CN)_7].H_2O$ (see Experimental Section); presumably such irradiation helped to break the W-W bond.

iii) Other Methods.

Since $Mo_2[OAc]_4$ reacts with CN^- to give $K_5[Mo(CN)_7].H_2O$,[28] it might be expected that other tungsten(II) compounds would do so. The existence of $W_2[OAc]_4$ is not fully established, so we tried reaction of $W_2(mhp)_4$[70] with CN^-. However, either because of the low solubility of the starting material or lack of an appropriate solvent, no reaction product could be obtained.

b) X-Ray Studies.

i) $K_5[W(CN)_7].H_2O$

The salt $K_5[W(CN)_7].H_2O$ is isomorphous with the analogous $K_5[Mo(CN)_7].H_2O$ and it is known from single crystal X-ray studies that the anion in the latter salt has pentagonal bipyramidal symmetry.[7] It therefore seems clear that, in $K_5[W(CN)_7].H_2O$, the anion has PB symmetry also, and this is supported by vibrational spectra (see Section f-i, page 72). Attempts to make crystals suitable for single crystal X-ray study were unsuccessful.

ii) $K_4[W(CN)_7H].2H_2O$.

This salt is not isomorphous with $K_4[Mo(CN)_7].2H_2O$ nor with $K_4[M(CN)_7].2H_2O$ (M = V, Re) and the lack of isomorphism between them is consistent with the different formulae. The structural implications of this are considered later (see vibrational spectra, section f-ii, page 75). The X-ray powder pattern data for $K_5[M(CN)_7].H_2O$ (M = W, Mo) and for $K_4[W(CN)_7H].2H_2O$ are given in Table 3.1 and 3.2 respectively. Attempts to make crystals suitable for single crystal X-ray study were unsuccessful.

c) Magnetic Data.

i) $K_5[W(CN)_7].H_2O$

Potassium heptacyanotungstate(II) is diamagnetic in solid state (μ_{eff} = 0.613 BM at 295 K) and no magnetic susceptibility was found for its aqueous solution using the NMR method.[84,85] This is consistent with expectation for a low spin d^4 heptacyano complex.

TABLE 3.1. X-Ray Powder Pattern Data for $K_5[W(CN)_7].H_2O$ and $K_5[Mo(CN)_7].H_2O$.

$K_5[W(CN)_7].H_2O$		$K_5[Mo(CN)_7].H_2O$	
d	Relative Intensity	d	Relative Intensity
6.60	vw	6.60	vw
6.40	vs	6.40	vs
5.70	vw	5.70	vw
4.50	m	4.50	m
4.12	vw	4.12	vw
3.72	s	3.72	s
3.68	m	3.68	m
3.35	vw	3.35	vw
3.24	m	3.23	m
3.15	w	3.15	w
3.02	vw	3.02	vw
2.96	vw	2.95	vw
2.92	vw	2.92	vw
2.89	vs	2.84	vs
2.83	vw	2.83	vw
2.73	vw	2.72	vw
2.67	vw	2.67	vw
2.63	vw	2.67	vw
2.55	vw	2.55	vw
2.45	m	2.44	m
2.42	m	2.42	m
2.38	m	2.38	m
2.28	m	2.28	m
2.25	w	2.25	w
2.14	vw	2.14	vw
2.04	vw	2.04	vw.
2.02	vw	2.02	vw

TABLE 3.2. X-Ray Powder Pattern Data for $K_4[W(CN)_7H].2H_2O$.

d	Relative Intensity	d	Relative Intensity	d	Relative Intensity
9.4	vw	3.60	w	2.52	vw
8.6	vw	3.50	m	2.46	m
8.4	vw	3.40	m	2.45	m
7.4	m	3.32	s	2.42	m
6.7	m	3.22	vw	2.31	vw
6.5	s	3.17	vw	2.21	vw
6.2	w	3.10	vw	2.28	vw
5.90	m	3.02	vw	2.26	vw
5.25	w	2.97	vs	2.24	vw
4.68	m	2.82	m	2.22	vw
4.55	m	2.80	m	2.17	m
4.40	m	2.78	s	2.15	vw
4.20	vs	2.75	vw	2.10	w
4.00	s	2.68	vw	2.08	vw
3.82	vw	2.58	w	2.06	m
3.72	vw	2.55	w	1.95	vw
				1.91	vw
				1.85	w
				1.84	vw

ii) $K_4[W(CN)_7H].2H_2O$

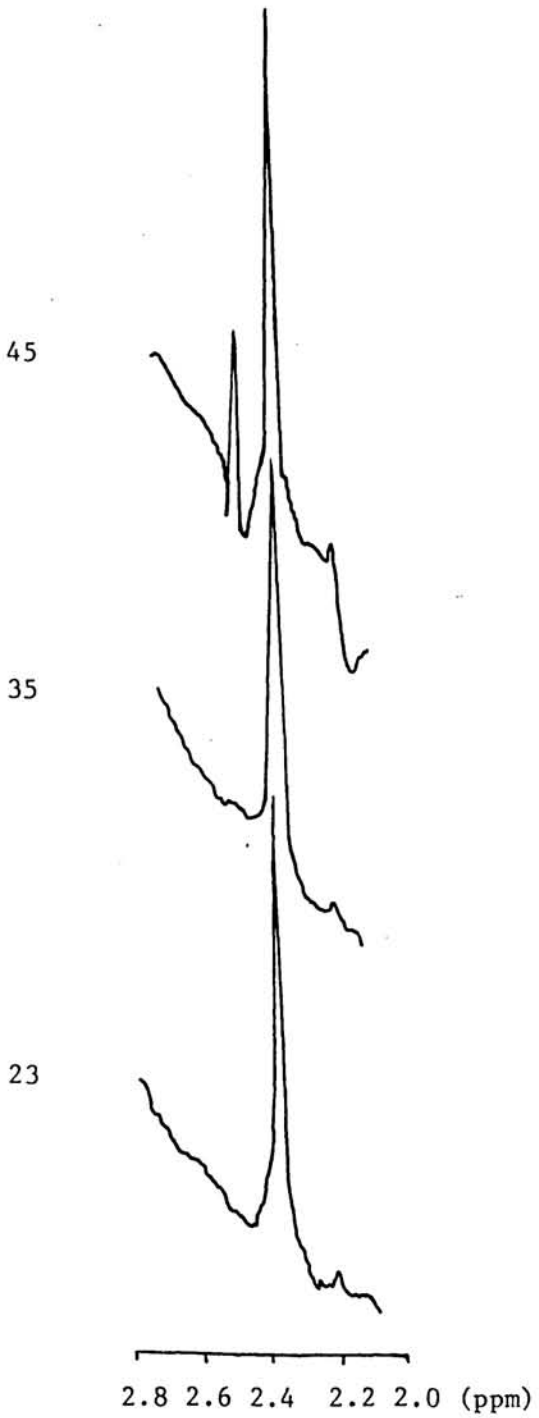
At the beginning of this work, we intended to correlate " $K_3[W(CN)_6]$ "[68] which we surmised might be $K_4[W(CN)_7].2H_2O$, with the known $K_4[Mo(CN)_7].2H_2O$[27] by the similarity their infrared spectra in the ν_{CN} region. The formulation as $K_4[W(CN)_7].2H_2O$ involving tungsten(III) (d^3), suggested by our analytical results (see Experimental Section) would be expected to give a paramagnetic complex. However, the species was found to be essentially diamagnetic in the solid state (μ_{eff} 0.64 BM at 294 K) and in aqueous solution containing excess cyanide. Furthermore, the ^1H NMR spectrum of a 0.05M aqueous solution in the presence of 0.1 M KCN and 3% DSS as external standard shows a shift at δ = 0 ppm relative to DSS, but no splitting due to magnetic susceptibility was observed.

d) ^1H NMR Spectra of $K_4[W(CN)_7H].2H_2O$

The diamagnetism of $K_4[W(CN)_7H].2H_2O$ and its lack of isomorphism with $K_4[M(CN)_7].2H_2O$ (M = Mo, Re, V) are incompatible with its formulation as $K_4[W(CN)_7].2H_2O$, but are consistent with its formulation as a hydride. We sought to confirm this by studying its ^1H NMR spectra.

The ^1H NMR spectrum of the salt in aqueous solution (0.05 M in tungsten and 0.01 M in CN^-) with DSS as internal standard shows the hydride resonance as a sharp singlet at τ = 7.6 (δ = 2.4 ppm), the signal being flanked by two symmetrically placed tungsten satellites ($\underline{J}$ = 34.0 Hz) (^{183}W, 14.4% natural abundance, spin = $\frac{1}{2}$). That this does not arise from water " spinning sidebands" was shown by the presence of the satellite lines, and also the immobility of these

Figure 3.1. ^{1}H NMR Spectra of $[W(CN)_7H]^{4-}$ in excess cyanide aqueous solution at various spinning speeds.



resonances on changing the spin speed. No signal is observed in heavy water (^2H_2O) presumably because of exchange with the proton. The singlet position (δ 2.4 ppm) in this case is in the region observed for other tungsten(IV) complexes containing hydrides, e.g., $WH_2(CO_2CF_3)_2(PMePh_2)_3$ shows a 1:3:3:1 quartet centred at $\tau \sim 7$, (δ: 3).[71] It is, however, very different from other cyanides (see Table V , page 23), in that the hydride shift is at relatively high field, and the reason could well be due to the higher coordination number of the tungsten complex.[71a] The ^1H NMR spectrum of $K_4[W(CN)_7H].2H_2O$ is shown in Figure 3.1.

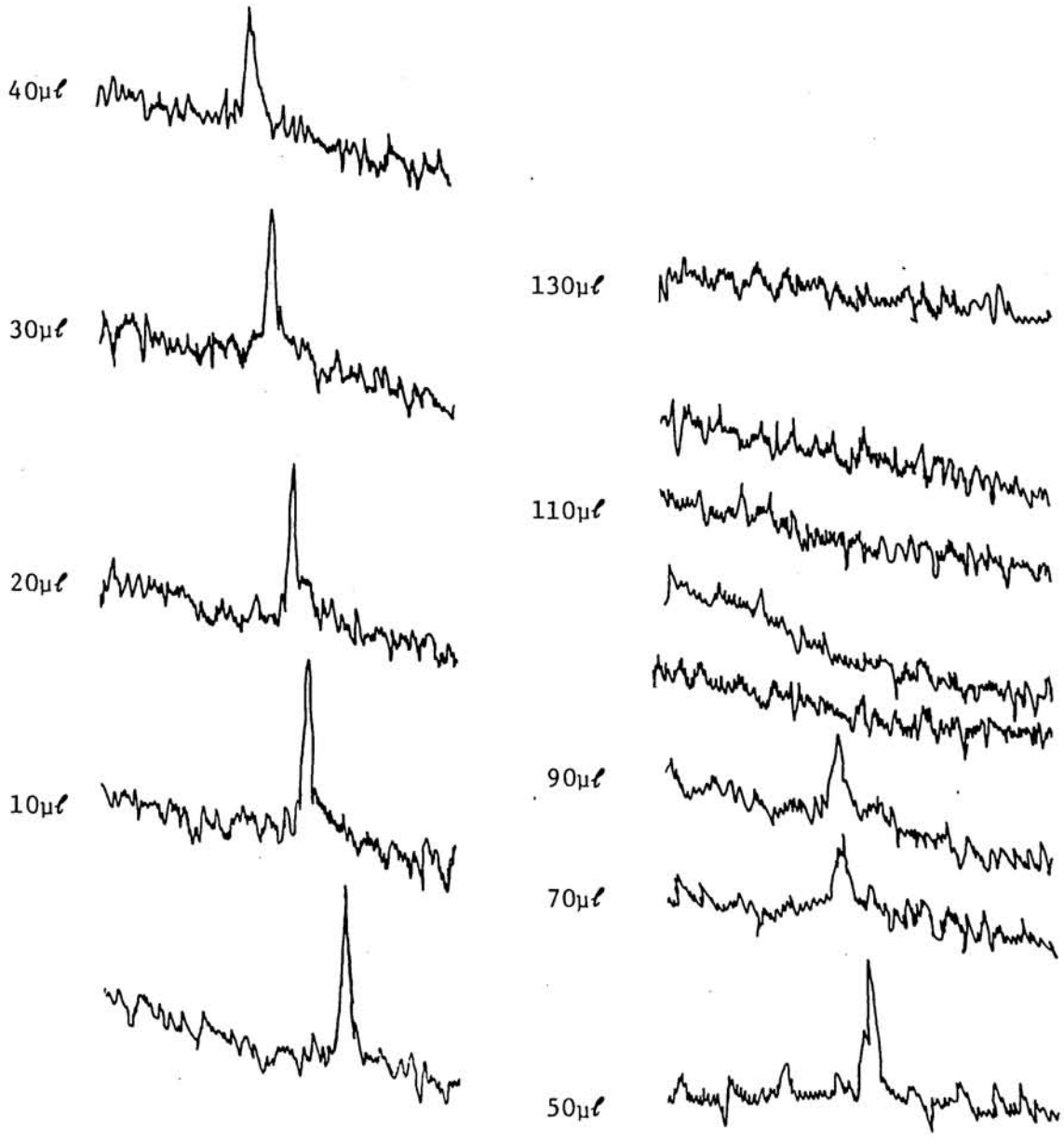
The ^1H NMR spectrum of a weighed quantity of the salt $K_4[W(CN)_7H].2H_2O$ was measured in an aqueous standard solution of tertiary butyl alcohol. A comparison of peak areas between that of the hydride and that of the tertiary methyl protons resonances enabled us to show that the hydride: tungsten ratio is (1.3 ± 0.1) to 1.

On addition of aqueous potassium hydroxide to the green solution, the colour changes to yellow and the hydride peak becomes weaker, finally disappearing when 1.0 M OH^- has been added (Figure 3.2). On careful addition of sufficient 2 M acetic acid, however, the hydride peak is regenerated. Addition of ethanol to the yellow solution containing excess alkali yields pure $K_5[W(CN)_7].H_2O$, suggesting that the equilibrium

$$[W(CN)_7H]^{4-} + OH^- \rightleftharpoons [W(CN)_7]^{5-} + H_2O \qquad (1)$$

exists in these solutions. Further evidence for this equilibrium and more conclusive evidence for the formulation of this complex as a monohydride is given by the ^{13}C NMR spectrum.

Figure 3.2. ^{1}H NMR Spectra of $[W(CN)_7H]^{4-}$ in excess CN^- aqueous solution on addition of KOH 5 M (300 Hz).



e) ^{13}C NMR of $[W(CN)_7H]^{4-}$ and $[W(CN)_7]^{5-}$.

The proton-decoupled ^{13}C NMR spectrum of the dark green salt $K_4[W(CN)_7H].2H_2O$ (0.2 M in 0.01 M aqueous sodium cyanide) with an external ^2H_2O lock and DSS as internal standard, shows three sets of resonances: one due to free $^{13}CN^-$ at δ 167.8 ppm (all shifts on the low-field of tetramethylsilane), and two due to tungsten cyano species, since they show tungsten satellites (see Figure 3.3). These are at δ 153.6 ($J_{^{183}W-^{13}C}$ = 62.9 Hz) and at δ 148.5 ppm ($J_{^{183}W-^{13}C}$ = 57.3 Hz) On removal of proton decoupling the free cyanide peak at δ 167.8 and that at δ 148.5 ppm are unchanged, but the δ 153.6 ppm peak splits into a doublet as do its tungsten satellites as shown in Figure 3.4. This is clearly due to the presence of a monohydride ($J_{^{13}C-H}$ = 11.1 Hz) and we suggest that the species giving rise to this resonance is $[W(CN)_7H]^{4-}$. The resonance at δ 148.5 ppm is unaffected by proton coupling and is therefore, not hydridic; we assign it to $[W(CN)_7]^{5-}$. The sharpness of the resonances, together with the presence of a sharp resonance due to free $^{13}CN^-$ indicates that there is no exchange with free CN^- on our NMR time scale. It also suggests that the structures of the tungsten cyano species are fluxional on the NMR time scale, as in the case of $[M(CN)_8]^{4-}$ (M = Mo, W) discussed in the second chapter of this work. Addition of sodium hydroxide causes the $[W(CN)_7H]^{4-}$ resonance at δ 153.6 ppm to decrease in intensity while that due to $[W(CN)_7]^{5-}$ at δ 148.5 ppm increases (Figure 3.5), again consistent with equilibrium (1) (see Section d, page 66). By use of a long pulse delay to allow for possible different relaxation times of $[W(CN)_7]^{5-}$

Figure 3.3. The decoupled ^{13}C NMR spectrum of (a) $[W(CN)_7H]^{4-}$ and (b) $[W(CN)_7]^{5-}$ in aqueous excess cyanide (c)

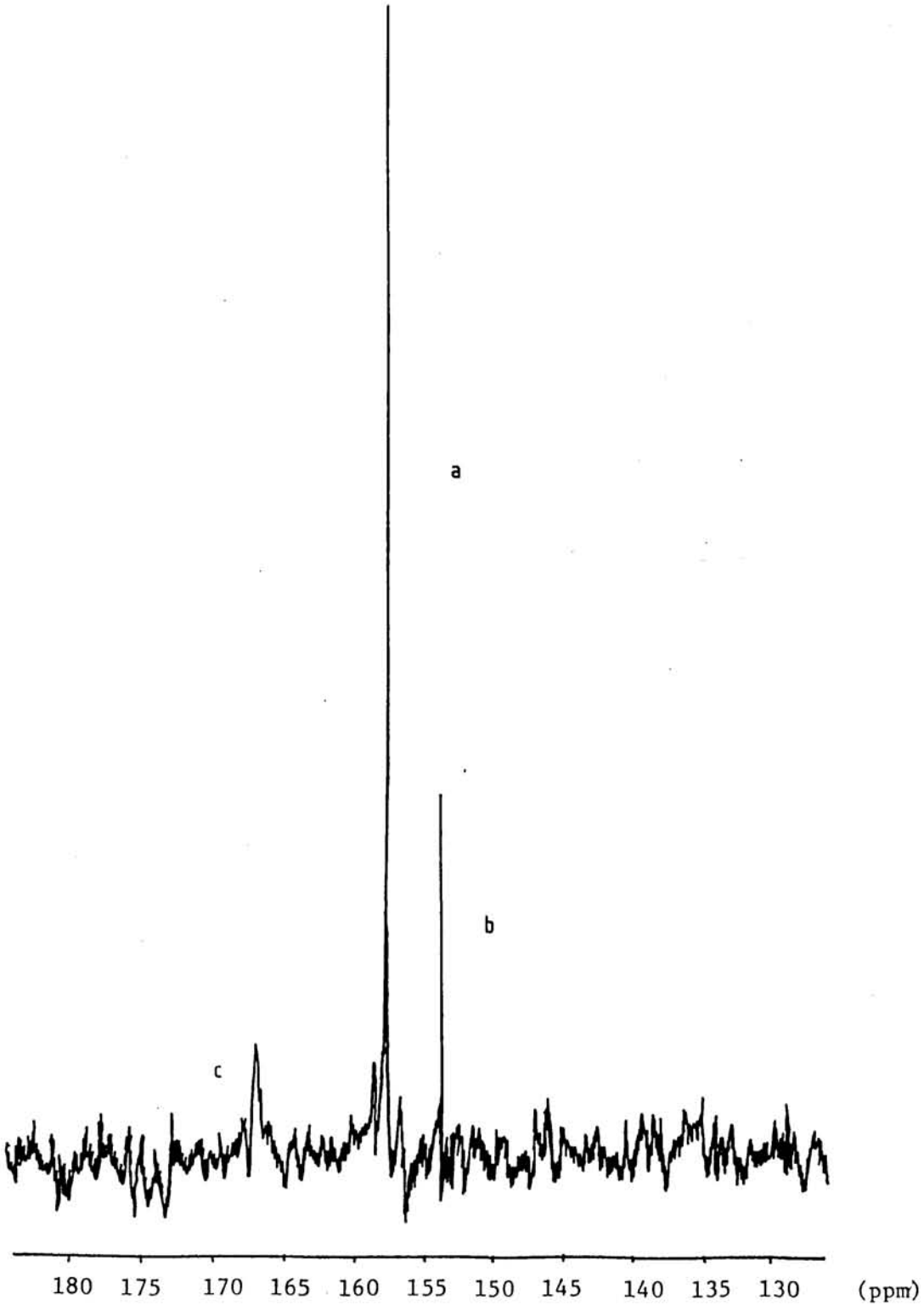


Figure 3.4. The undecoupled ^{13}C NMR spectrum of $[W(CN)_7H]^{4-}$ and $[W(CN)_7]^{5-}$ in excess cyanide aqueous solution.

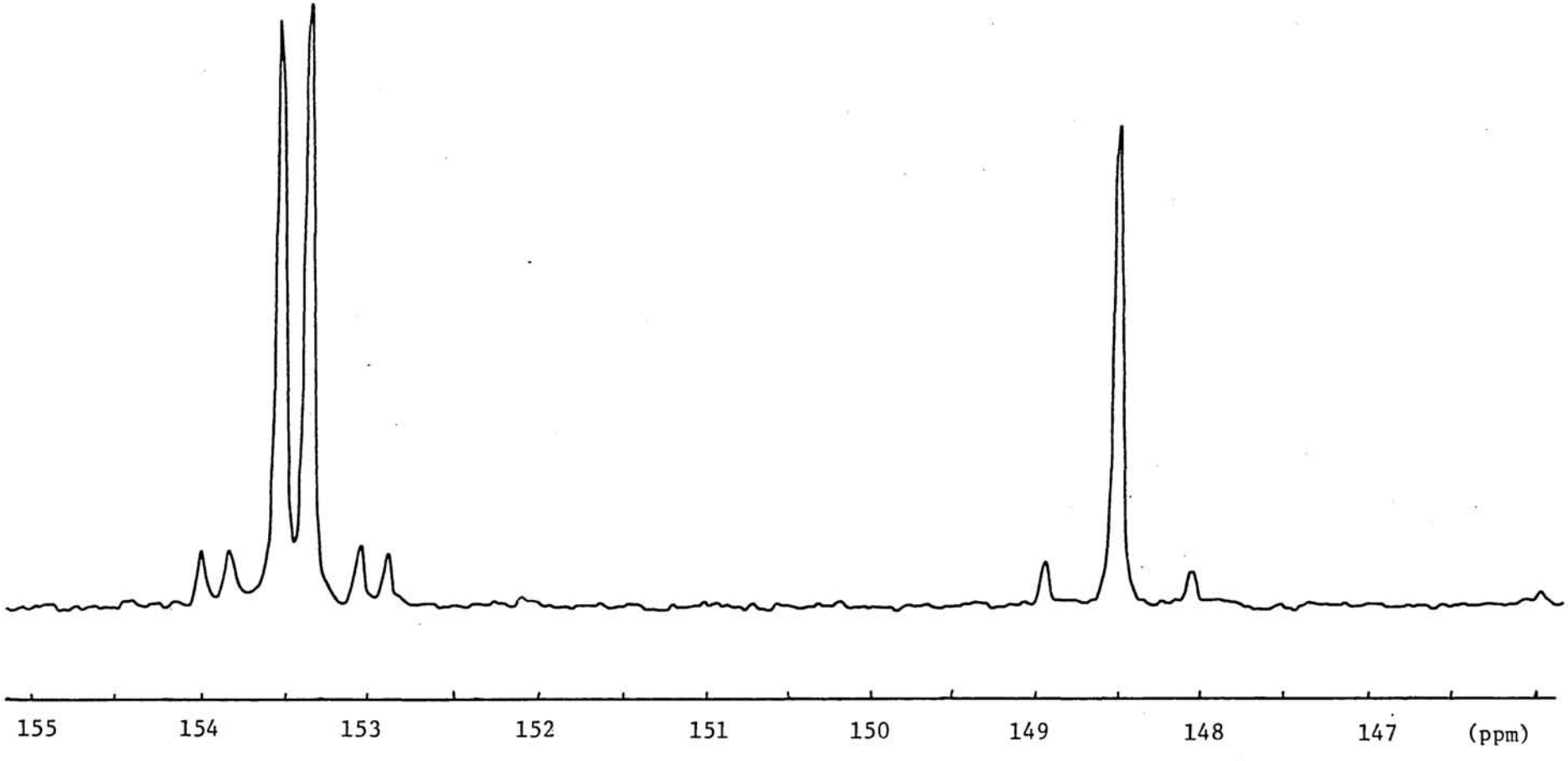
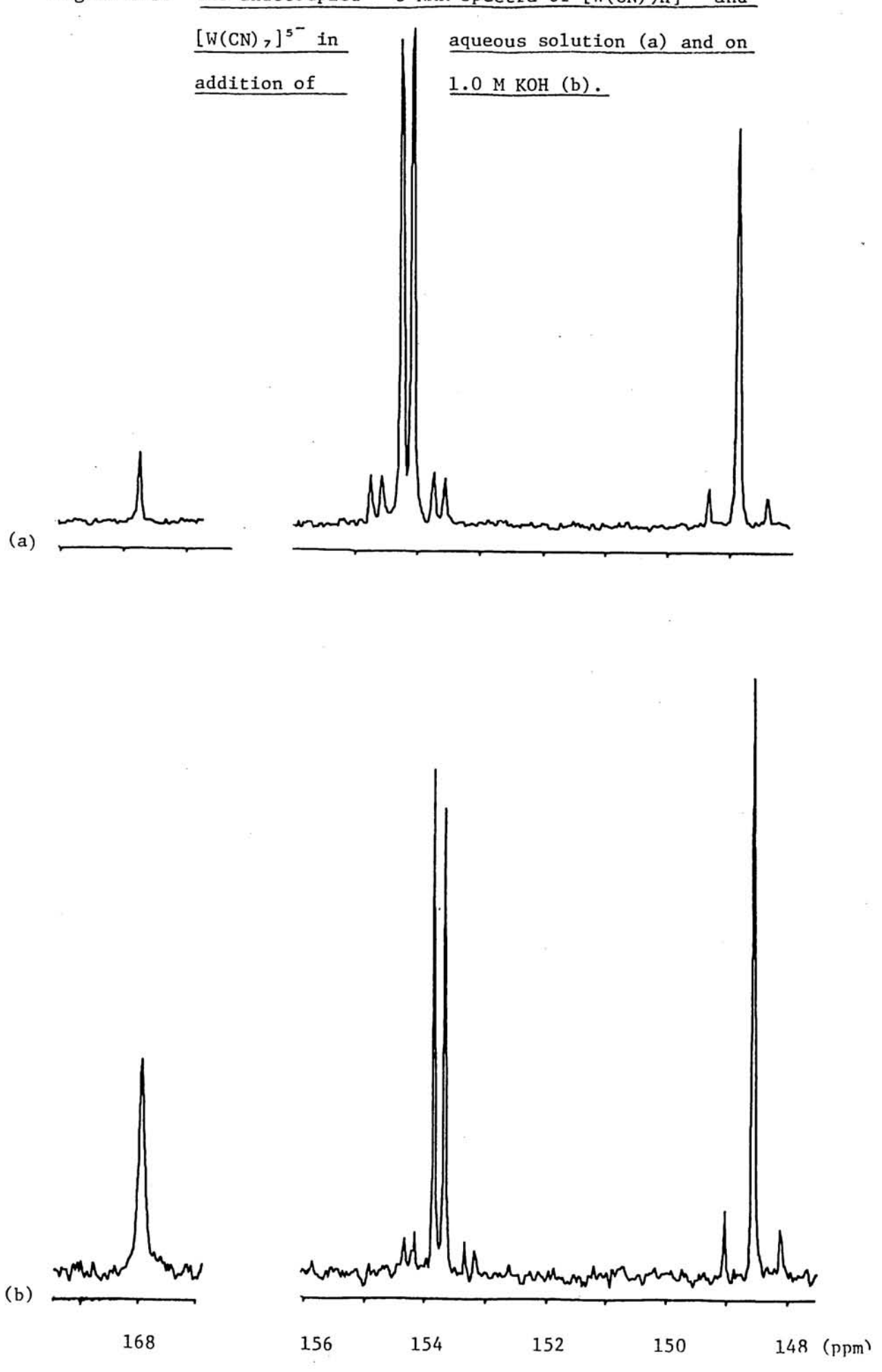


Figure 3.5. The undecoupled ^{13}C NMR spectra of $[W(CN)_7H]^{4-}$ and $[W(CN)_7]^{5-}$ in aqueous solution (a) and on addition of 1.0 M KOH (b).



and $[W(CN)_7H]^{4-}$, a value of

$$K = \frac{[[W(CN)_7]^{5-}]}{[[W(CN)_7H]^{4-}][OH^-]} = 0.4\ M^{-1} \text{ for (1)}$$

was obtained at a total ionic strength of 5.5 M. This gives a value of pKa = 14.4 for $[W(CN)_7H]^{4-}$ (see also Section f below).

f) Vibrational Spectra.

The infrared and Raman spectra of $K_5[W(CN)_7].H_2O$ and $K_4[W(CN)_7H].2H_2O$ in the solid state and in aqueous solution are listed in Table 3.3 and 3.4 respectively. Figure 3.6 shows the spectra of the two species in the solid state. Part (a) of Figure 3.7 corresponds to the Raman spectrum of $[W(CN)_7H]^{4-}$ in aqueous cyanide and part (c) to that of $[W(CN)_7]^{5-}$ in excess hydroxide solution.

i) $K_5[W(CN)_7].H_2O$

In the ν_{CN} region of the infrared spectrum of the solid, seven bands are observed, but in the infrared spectrum of the aqueous solution (containing 0.1 CN^- and 25% hydrazine to avoid decomposition) only two bands are present. The Raman spectrum of solid $K_5[W(CN)_7].H_2O$ also shows seven bands. While in the solution (in excess OH^- ion) three bands at 1970 (depolarised), 2050 and 2076 (both polarised) are observed . As mentioned previously in Section b of this Chapter (page 61), this complex is isomorphous with the analogous pentagonal bipyramidal $K_5[Mo(CN)_7].H_2O$[7] and the profiles of their vibrational spectra are also very similar, suggesting PB symmetry for the anion in the solid state.

Figure 3.6. Vibrational Spectra of $K_4[W(CN)_7H].2H_2O$ and $K_5[W(CN)_7].H_2O$ in the solid state.

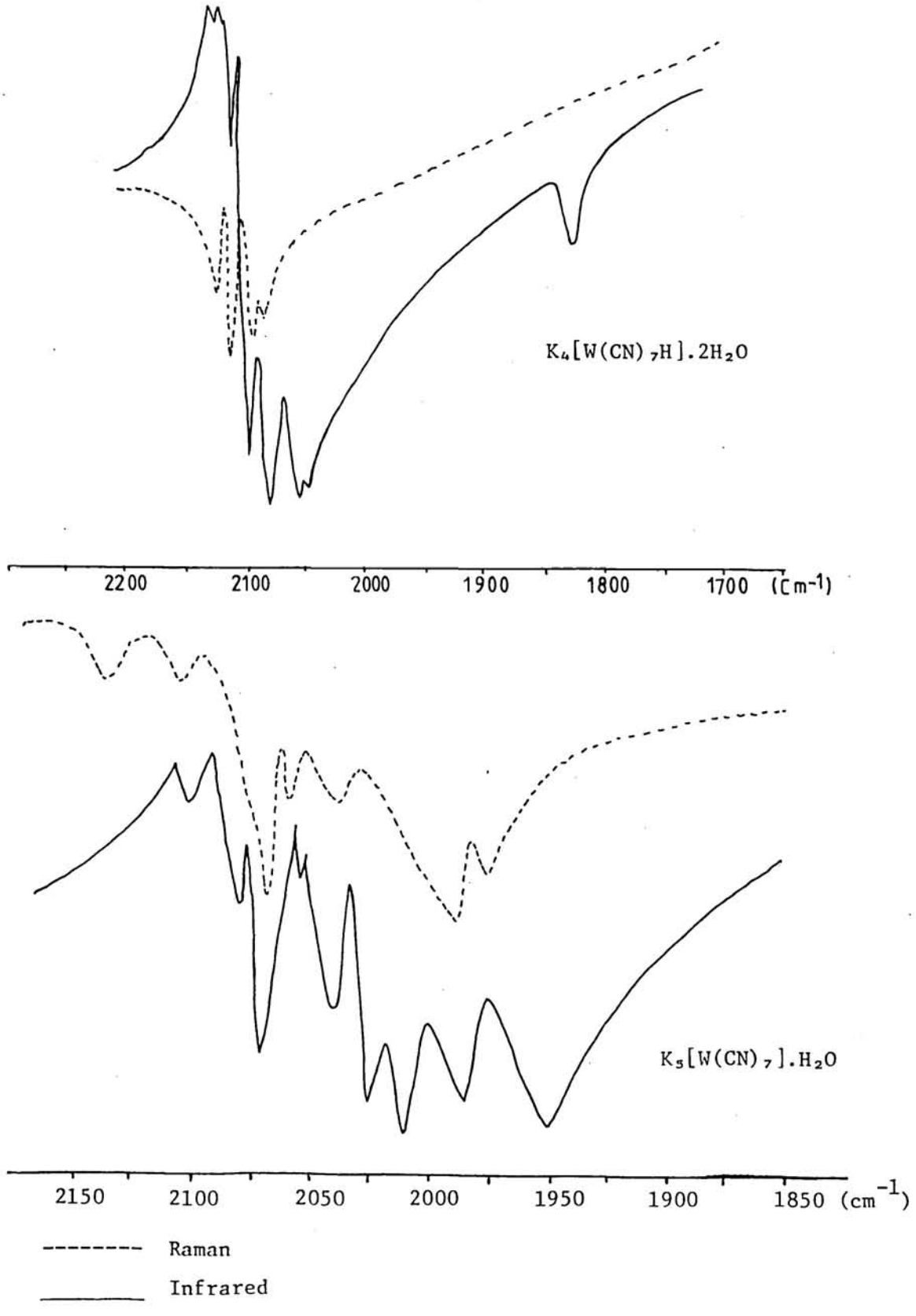


TABLE 3.3. Vibrational Spectra Data for $K_5[W(CN)_7].H_2O$.

	ν_{CN} (cm^{-1})	ν_{M-C} or ν_{MCN} (cm^{-1})
IR (solid)[a]	1950(vs) 1986(s) 2010(vs) 2028(s) 2042(w) 2070(s) 2086(w)	294(s) 315(vs) 335(w) 375(vw) 460(vw) 520(s)
IR (solution)[b]	2078(vs) 2100(s)	
R (solid)[c]	1975(7) 1989(9) 2010(sh) 2036(6) 2058(6) 2072(8) 2100(4)	345(7) 360(6) 390(5) 400(5) 420(6)
R (solution)[d]	1965(5) dp 2050(4) p 2078(6) p	

[a] Nujol mull ; [b] excess cyanide/aqueous solution, 25% N_2H_4;
[c] KBr disc; [d] excess hydroxide/aqueous solution.

For the D_{5h} configuration, two infrared active (A_2'' , E_1') and three Raman-active [$2A_1$ (pol), E_1'] ν_{CN} fundamentals are expected. The complexity of the spectra of solid $K_5[W(CN)_7].H_2O$ is probably due to solid state splitting effects. For the solution however, both Raman and infrared spectra are fully consistent with pentagonal bipyramidal geometry. The similarity of the infrared and Raman spectra of the solid and aqueous solution suggests that there is no change of configuration of the anion $[W(CN)_7]^{5-}$. The two polarised bands found in the Raman spectrum of the solution support the conclusion that D_{5h} symmetry is maintained in solution, as with other heptacyano complexes.

ii) $K_4[W(CN)_7H].2H_2O$

The infrared spectrum of solid $K_4[W(CN)_7H].2H_2O$ in the ν_{CN} region shows six well resolved bands. All of these are unaffected when the salt is recrystaylised from heavy water (^2H_2O), but a band at 1830 cm^{-1} shifts to 1310 cm^{-1} and one at 845 cm^{-1} shifts to 615 cm^{-1}. We assign these to the stretching and deformation vibration of W-H and W-^{2}H bonds respectively. Such bonds are typical of ν_{W-H} and δ_{W-H} vibrations,[71] and for ν_{M-H} and δ_{M-H} in $K_3[Co(CN)_5H]$,[86] $K_3[Rh(CN)_5H]$[87] and $K_3[Ir(CN)_5H]$.[88] The ratio $\nu_{W-H}/\nu_{W-^2H} = 1.39$, is close to the theoretical value (1.414).

The infrared spectrum of solid $K_4[W(CN)_7H].2H_2O$ is very similar in profile to that of $K_4[Mo(CN)_7].2H_2O$[27] in the ν_{CN} region. The anion $[Mo(CN)_7]^{4-}$ may be CTP (C_{2v}) in the solid potassium salt and PB (D_{5h}) in solution[27] (see also Section B,2, page 104). The

TABLE 3.4. Vibrational Spectra Data for $K_4[W(CN)_7H].2H_2O$ and its Deuteriate.

Compound		ν_{CN} (cm^{-1})	ν_{W-H} (cm^{-1})	δ_{W-H} (cm^{-1})	ν_{W-^2H} (cm^{-1})	δ_{W-^2H} (cm^{-1})	ν_{M-C} (cm^{-1})
$K_4[W(CN)_7H].2H_2O$	IR solid[a]	2045(sh) 2050(vs) 2080(vs) 2100(vs) 2112(w) 2126(w)	1830(w)	845(w)			363(s) 390(w) 420(w) 445(w) 490(s)
	IR solution[b]	2020(vw) 2070(vs) 2090(sh)	1830(vw)				
	R solid[c]	2088(s) 2096(6) 2116(7) 2126(5)	1835(w)				

/continued.

TABLE 3.4 (continued)

Compound		ν_{CN} (cm^{-1})	ν_{W-H} (cm^{-1})	δ_{W-H} (cm^{-1})	ν_{W-^2H} (cm^{-1})	δ_{W-^2H} (cm^{-1})	ν_{M-C} (cm^{-1})
$K_4[W(CN)_7].2H_2O$	R solution	2050(2) 2082(6) 2111(7) pol 2128(6) pol	1835(2)				390(w) 450(w) 470(w)?
$K_4[W(CN)_7{}^2H].2H_2O$	IR solid[a]	2050(vs) 2080(vs)			1310(w)	615(vw)	363(s) 400(w) 420(sh) 440(w) 490(s)

[a] Nujol mull; [b] Aqueous solution/excess cyanide; [c] KBr disc.

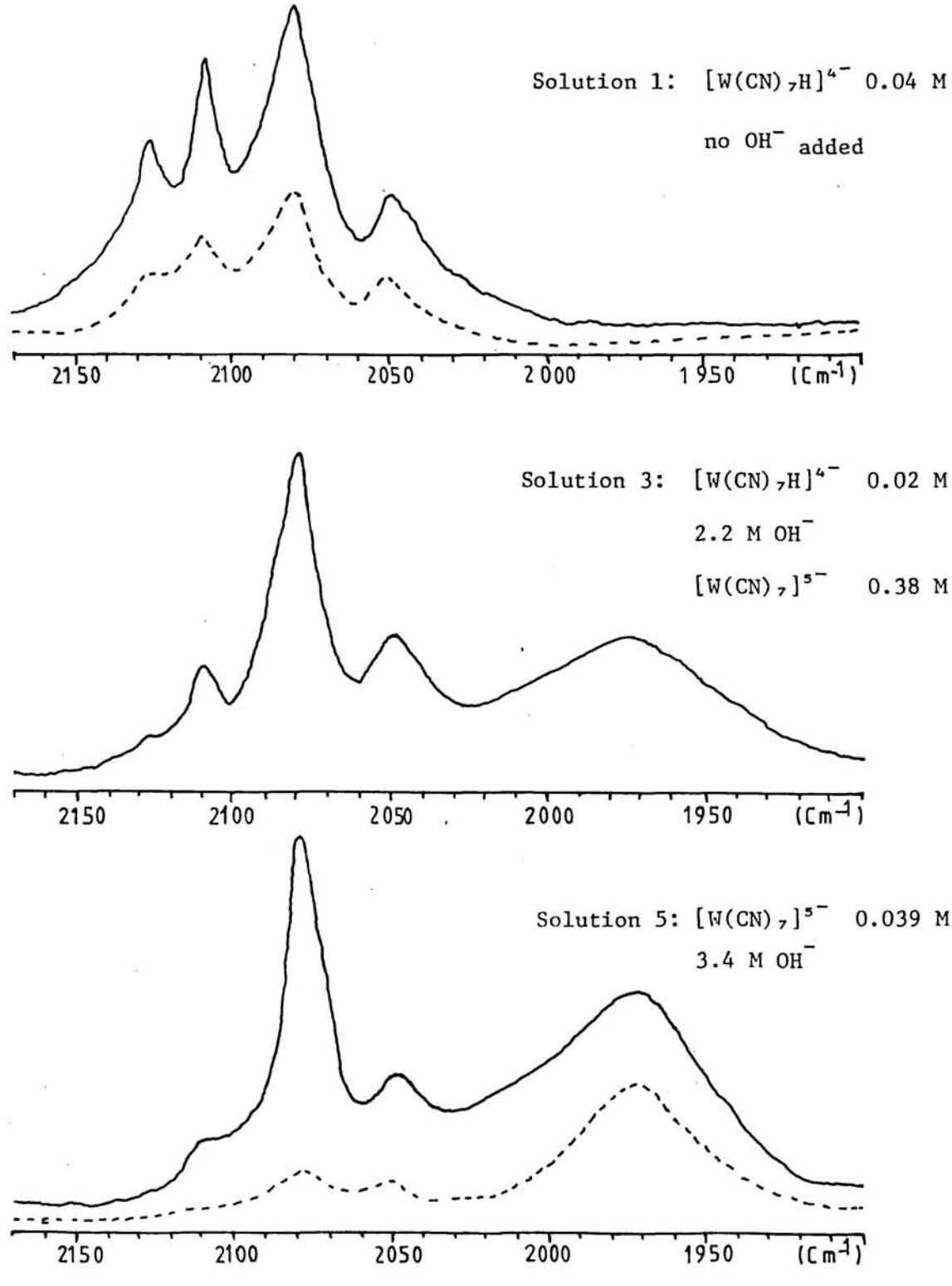
selection rules predict six infrared-active ($3A_1$, A_2, B_2) and seven Raman-active [$3A_1$, A_2, $2B_1$, B_2, with three polarised ($3A_1$)] ν_{CN} fundamentals for C_{2v} symmetry with six infrared-Raman coincidences ($3A_1$, $2B_1$, B_2). The fact that we observe six bands in the infrared and four bands in the Raman spectrum of solid $K_4[W(CN)_7H].2H_2O$ (Figure 3.6) suggests that the hydride ligand could occupy one of the capped positions of a bicapped trigonal prism with C_{2v} symmetry. Although the two complexes, $K_4[Mo(CN)_7].2H_2O$ and $K_4[W(CN)_7H].2H_2O$ are not isomorphous (see Section b, Page 61) and the central atoms have different coordination numbers, the remarkable similarity of their ν_{CN} profiles suggest that the $[M(CN)_7]$ moiety may have the same C_{2v} symmetry. A bicapped trigonal prismatic octacyano complex, $Cs_3[Mo(CN)_8].2H_2O$ has recently been reported,[17a] indicating that such a stereochemistry is feasible for an eight coordinate species.

The Raman spectrum of solid $K_4[W(CN)_7H].2H_2O$ is rather weak because of the deep colour of the salt, and this could be the reason why we see only four of the seven expected absorptions. There is also the possibility of superimposition of bands.

The vibrational spectra of $[W(CN)_7H]^{4-}$ in aqueous solution are similar in profile to those of the solid state. This suggests that the configuration of the anion in the solid state is maintained in solution. The appearance of three polarised bands in the Raman spectrum of the aqueous solution (see Table 3.4) supports this conclusion.

It might be expected that the $M(CN)_7$ moiety is pentagonal bipyramidal (D_{5h}) with the small hydride ligand not significantly dislocating this symmetry. However, more Raman and infrared bands than would be expected for this (see p. 29) are observed, and the

Figure 3.7. Raman spectra of the titration with NaOH of $[W(CN)_7H]^{4-}$ in 0.1 M CN^- aqueous solution at a total ionic strength of 5.5 M.



lack of isomorphism of $K_4[W(CN)_7H].2H_2O$ with $K_4[M(CN)_7].2H_2O$ (M = Re, V) also suggests a structure quite different from PB. Other possibilities are (a) a dodecahedral or (b) an antiprismatic arrangement of the eight ligands in $[W(CN)_7H]^{4-}$; both would have C_s symmetry, but for (a) five polarised and two depolarised Raman CN stretches would be expected and for (b) four polarised and three depolarised Raman stretches.

On addition of base (NaOH) to the green aqueous solution of $[W(CN)_7H]^{4-}$, in 0.01 M NaCN, using Na_2SO_4 as internal standard, the intensity of the Raman band at 2110 cm^{-1} progressively decreases and that at 1970 cm^{-1}, found in the spectrum of pure $[W(CN)_7]^{5-}$, (see i in this Section and Figure 3.7) increases. By using the relative areas of these peaks we obtained a value of K = 0.2 M^{-1} for the equilibrium (1) $[K = \frac{[[W(CN)_7]^{5-}]}{[[W(CN)_7H]^{4-}][OH^-]}]$ (see Table 3.5) at a total ionic strength of $\sim$ 5.5 M. This gives a value of pKa = 14.3 for $[W(CN)_7H]^{4-}$. This result is fairly close to the value of K obtained by using the ^{13}C NMR spectrum of the two species present in the equilibrium (1) (see Section e, page 68). Thus, the acidity of the $[W(CN)_7H]^{4-}$ anion is stronger than that of $[Co(CN)_5H]^{3-}$ (pKa = 20).[89]

g) EPR Spectrum of $K_4[W(CN)_7].2H_2O$

Although $K_4[WH(CN)_7].2H_2O$ has been shown to be diamagnetic, confirmation from EPR spectra was sought, and we also wished to check the possibility of there being very small amounts of $K_4[W(CN)_7].2H_2O$ as impurity. We carried out experiments on the pure solid and a solution in 0.1 M aqueous KCN at 27 and 77 K. A quite strong, sharp and symmetrical signal was observed at the lower temperature with a g = 1.88 for the solid. The tungsten(V) (d^1) complex, $K_3[W(CN)_8]$ shows

TABLE 3.5. Experimental Data for the Equilibrium Constant in $K = \frac{[W(CN)_7H]^{3-}}{[W(CN)_7H]^{4-}[OH^-]}$ in Aqueous 0.01 M CN^-

Experiment	$K_4[W(CN)_7H].2H_2O$		$K_5[W(CN)_7].H_2O$		Na_2SO_4 (standard)		NaOH (M)	NaCℓ (M)	μ (M) $\varepsilon\frac{1}{2}$ miz^2	K (M^{-1})
	Concentration (M)	area of the Raman peak at cm^{-1} 2110 (g)	Concentration (M)	area of the Raman peak at cm^{-1} 1970 (g)	Concentration (M)	area of the Raman peak at cm^{-1} 982 (g)				
1	0.040	0.24	-	-	0.60	0.3756	0	3.3	5.5	-
2	0.019	0.06	0.023	0.3006	0.60	0.2664	1.70	1.6	5.6	2.3×10^{-1}
3	0.023	0.07	0.030	0.3967	0.60	0.2601	2.24	1.0	6.0	1.9×10^{-1}
4	0.016	0.05	0.032	0.4093	0.60	0.2603	2.62	0.5	5.5	2.3×10^{-1}
5	0.009	0.03	0.039	0.4600	0.60	0.1860	3.39	0	5.8	-

a resonance with $g_{\|} = 1.98$ and $g_{\perp} = 1.96$,[37] and so it is unlikely to be the impurity. By comparison with the analogous $K_4[Mo(CN)_7].2H_2O$[27] the signal seemed to be some 75 times weaker (under the same experimental conditions). This observation lead us to think that possibly approximately 1% of a paramagnetic species, presumably $K_4[W(CN)_7].2H_2O$, is present in the solid sample of $K_4[WH(CN)_7].2H_2O$. In solution, a weak, broad signal was observed with $g = 1.83$ and we tentatively assign this band to the same species present in the solid.

Figure 3.8 shows the EPR spectrum for $K_4[W(CN)_7].2H_2O$ as a possible impurity in $K_4[W(CN)_7].2H_2O$.

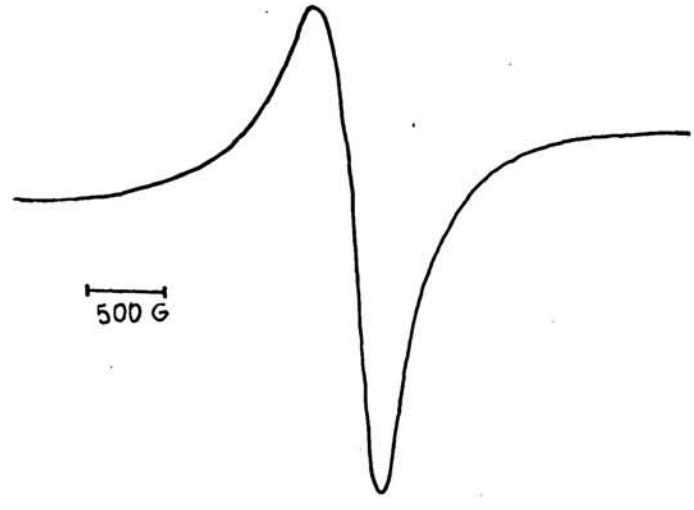


Figure 3.8. EPR spectrum of $K_4[W(CN)_7].2H_2O$ as a possible impurity in $K_4[W(CN)_7H].2H_2O$. Field set 5000 + 5000 G Temp. 27 K; 1-30 dB.

h) Electronic Spectra.

i) $K_5[W(CN)_7].H_2O$

Although a full study has not been made, absorptions at 287 nm (ε = 541.8 ℓ mol^{-1} cm^{-1}), 355 nm (ε = 103.5 ℓ mol^{-1} cm^{-1}) and 410 nm (ε = 35.7 ℓ mol^{-1} cm^{-1}) are observed to occur in the visible region for a solution of $K_5[W(CN)_7].H_2O$ in 0.1 M CN^-.

ii) $K_4[W(CN)_7H].2H_2O$

For an aqueous solution in 0.1 M CN^- absorption at 404 nm (ε = 896 ℓ mol^{-1} cm^{-1}), 355 nm (ε = 2455 ℓ mol^{-1} cm^{-1}) 323 nm (ε = 2570 ℓ mol^{-1} cm^{-1}) and 251.5 nm (ε = 40046 ℓ mol^{-1} cm^{-1}) are observed.

Samotus et al[90.91] reported that the photolysis of $[W(CN)_8]^{4-}$ in aqueous solution under u.v. light produced a species formulated as $[HW(CN)_7(H_2O)]^{2-}$ in equilibrium with $[W(CN)_7(H_2O)]^{3-}$ and $[W(CN)_7OH]^{4-}$; no evidence was given for these formulations. Our spectra of $[W(CN)_7]^{5-}$ and $[W(CN)_7H]^{4-}$ are, however, quite different from those of these species.

i) Polarography.

We studied the reduction of $[W(CN)_7H]^{4-}$ at the dropping mercury electrode in 0.1 M KCN with a saturated calomel electrode; no cathodic waves were observed between 0.0 and -2.0 volts (vs. SCE).

j) Properties.

i) $K_5[W(CN)_7].H_2O$

Potassium heptacyanotungstate(II) is a diamagnetic (low-spin d^4) solid which crystallises as a yellow microcrystalline powder. It is very sensitive to atmospheric oxidation rapidly forming a green surface layer. It is moderately soluble in water giving a yellow solution which is even more air-sensitive. The species $[W(CN)_7]^{5-}$ is stable in presence of excess free cyanide, hydrazine or hydroxide ion under nitrogen. Although the complex forms small crystals they were not suitable for single crystal X-ray diffraction studies.

ii) $K_4[W(CN)_7H].2H_2O$

The potassium salt is diamagnetic (low-spin d^2) solid which crystallises as large dark green flakes. The solid can be exposed to the air for short periods, but slowly decomposes turning to the yellow $K_4[W(CN)_8].2H_2O$. It is very unstable in aqueous solution in the absence of cyanide ion. The concentrated solution is honey coloured, but appears green when very dilute. In the presence of light the complex slowly disproportionates apparently forming $[W(CN)_8]^{4-}$ and $[W(CN)_7]^{5-}$. (The evidence for this is based on the infrared spectrum of the material deposited after addition of methanol to such photolysed solutions).

k) Chemical Reactions of $K_4[W(CN)_7H].2H_2O$.

In general, we investigated the reactions between $[W(CN)_7H]^{4-}$ and substances which are known to react with $[Co(CN)_5H]^{3-}$, the latter being the only cyanide hydride to have been extensively investigated.

i) With Hydroxide Ion (OH^-).

The complex reacts with OH^- in aqueous solution producing $K_5[W(CN)_7].H_2O$. On addition of 0.1 M acetic acid the $[W(CN)_7H]^{4-}$ species can be regenerated, (see p. 64,68) suggesting the reversibility of the reaction,

$$[W(CN)_7H]^{4-} + OH^- \rightleftharpoons [W(CN)_7]^{5-} + H_2O$$

This reaction was characterised by the isolation of pure $K_5[W(CN)_7].H_2O$ by addition of methanol to the yellow reaction mixture, and in solution by ^1H, ^{13}C NMR and Raman spectra (see Sections d, e and f and Experimental Section for details).

ii) With Organic Substrates

Although no hydrogenation reactions seem to have been reported for $[Rh(CN)_5H]^{3-}$ and $[Ir(CN)_5H]^{3-}$, $[Co(CN)_5H]^{3-}$ is an active catalyst for homogeneous hydrogenations,[92] particularly of dienes.[93] However, we find that $[W(CN)_7H]^{4-}$ in aqueous solution with excess cyanide does not react either in the presence or absence of molecular hydrogen with 1-hexene, 2-butyne, 2,3-dimethyl-1,3-butadiene, 1,3-butadiene, 1,3-cyclooctadiene or cyclopentadiene. It does, however, polymerise styrene in good yield and acrylonitrile, methyl methacrylate isoprene in low yield;($[Co(CN)_5H]^{3-}$ will also polymerise some olefins.[94]).

With 1,3-cycloheptadiene and 1,3-cyclohexadiene, cycloheptene and cyclohexene are obtained from $[W(CN)_7H]^{4-}$ in aqueous cyanide in 25 and 50% yields respectively (based on GLC data). Such reactions are effected by $[Co(CN)_5H]^{3-}$, catalytically in the presence of hydrogen[93]; with $[W(CN)_7H]^{4-}$, however, H_2 does not affect the reaction. Blank experiments with all these substrates were carried out, under the same conditions, with $[W(CN)_8]^{4-}$ replacing $[W(CN)_7H]^{4-}$ but no reactions occurred. (The conditions for these reactions are presented in Table 3.6 in the Experimental Section).

iii) With Sulphur Dioxide (SO_2).

With SO_2, solutions of $[W(CN)_7H]^{4-}$ in aqueous cyanide yields the new complex $K_4[W(HSO_3)(CN)_7]$. The infrared spectrum of the orange precipitate shows an absorption in the ν_{CN} region at 2100 cm^{-1} and bands at 1180, 1100, 1053, 1020 and 970 cm^{-1}, assigned to coordinated HSO_3^- vibrations.

Absorptions in this region ($\sim$ 1000-1250 cm^{-1}) of the infrared spectrum have been assigned to HSO_3^- modes in $Ru(NH_3)_4(HSO_3)_2$.[98]

iv) With Nitric Oxide (NO).

Nitric oxide appears to oxidise $[W(CN)_7H]^{4-}$ to $[W(CN)_8]^{4-}$, probably via an intermediate nitrosyl complex.

v) With Oxygen (O_2).

Molecular oxygen gives a transient dark green coloured solution which quickly turns yellow. Raman spectra of this latter solution shows, in addition to bands due to $[W(CN)_8]^{4-}$ and trans-$[WO_2(CN)_4]^{4-}$,

a band at 855 cm^{-1} which could arise from a coordinated peroxo ligand. Both $[Co(CN)_5H]^{3-}$ [95,96] and $[Rh(CN)_5H]^{3-}$ [97] give peroxo complexes with molecular oxygen.

vi) With Nitrogen Dioxide (NO_2).

Reaction of $[W(CN)_7H]^{4-}$ with NO_2 produces a green precipitate with infrared bands at 2160, 1765, 1730, 1280, 1120, 1000 and 820 cm^{-1}. It seems that the complex formed contains NO and NO_2 as ligands, but we could never obtain the pure compound.

vii) Other Reactions of $[W(CN)_7H]^{4-}$.

The complex $K_4[W(CN)_7H].2H_2O$ does not react with: nitric oxide in the presence of hydrazine, H_2S, butadiene, 2,2'-bipyridyl , and the potassium ions can not be easily exchanged by organic cations such as Me_4N^+, Et_4N^+, $(\emptyset_3P)_4N^+$, enH_2^{2+} and the tridecylamminium cation.

ℓ) Conclusions.

i) $K_5[W(CN)_7].H_2O$

The first heptacyano complex of tungsten was prepared. On the basis of vibrational spectra it appears that the anion $[W(CN)_7]^{5-}$ has PB geometry in the solid state and that this is maintained in aqueous solution.

ii) $K_4[W(CN)_7H].2H_2O$

$K_4[W(CN)_7H].2H_2O$ is the first eight coordinate cyanide hydride; it was characterised by ^1H, ^{13}C NMR and vibrational spectroscopy. It reacts with dienes and polymerises acrylonitrile and styrene. The existence of an equilibrium

$$[W(CN)_7H]^{4-} + OH^- \rightleftharpoons [W(CN)_7]^{5-} + H_2O$$

was demonstrated by ^1H, ^{13}C NMR and Raman spectroscopy. A value of pKa = 14.3 was found for $[W(CN)_7H]^{4-}$.

The anion $[W(CN)_7H]^{4-}$ may have bicapped trigonal prismatic structure in the solid potassium salt and this structure is likely to be maintained in solution.

E X P E R I M E N T A L

TUNGSTEN

Potassium Heptacyanotungstate(II) Monohydrate, $K_5[W(CN)_7].H_2O$.

Method 1.

A 50 cm^3 two-necked flask was connected to a manometer and the air replaced by argon. An oxygen-free saturated aqueous solution of KCN (10 cm^3) was transferred to the flask and $K_3[W_2C\ell_9]$ (0.1 g, 1.2×10^{-3} mol) was added. (All operations were carried out under argon).

The suspension was irradiated with ultra-violet light while stirring. After 30 minutes, the temperature of the system had risen to 60°C and the solid dissolved. After 5 hours, the solution had turned dark green, perhaps due to $[W(CN)_7H]^{4-}$. After 8 hours, it became brownish-yellow and a fine yellow precipitate was observed.

The solution was allowed to cool at room temperature when 20 cm^3 of oxygen-free methanol was added, and some more very fine yellow precipitate was formed.

After filtration, the gold-yellow product was washed three times with oxygen-free methanol and then dried under vacuum.

Analysis: Found: C, 14.73% ; N, 16.76% ; H, 0.36% ; K, 33.98%.
$K_5WC_7H_7H_2O$ requires: C, 14.51% ; N, 16.92% ; H, 0.35% ; K, 33.75%.

Method 2.

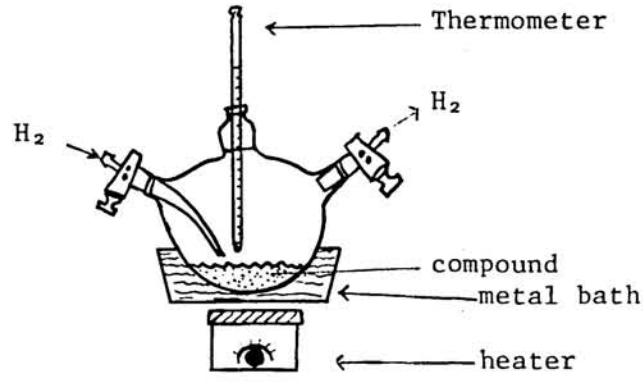
A 50 cm^3 two-necked flask was connected to a vacuum line and the air was replaced by argon. $K_4[W(CN)_7H].2H_2O$ (0.5 g, 8.9×10^{-1} mol) was added and an oxygen—free 0.1 M aqueous KCN solution (5 cm^3) was

transferred to the flask (all operations were carried out under argon). When the solid was completely dissolved this solution was transferred (using the " Suba-seal" technique) to another 50 cm^3 two-necked flask containing NaOH (two pellets, ca. 3.0 g) under argon. The solution turned gold-yellow when all the hydroxide was dissolved. After 15 minutes oxygen-free methanol was added until no more precipitation of yellow microcrystals was observed. The precipitate was filtered and washed three time with oxygen-free methanol and dried under vacuum. Yield: 0.4 g, 80%. Analysis: Found: C, 14.63% ; N, 16.82% ; H, 0.38%. $K_5WC_7N_7H_2O$ requires: C, 14.51% ; N, 16.92% ; H, 0.35%.

Potassium Hydrido Heptacyanotungstate(IV) Dihydrate, $K_4[W(CN)_7H].2H_2O$.

Method 1.

$K_4[W(CN)_8].2H_2O$ (2.0 g, 3.4×10^{-3} mol), and KCN (0.5 g, 7.6×10^{-3} mol) were ground together and placed in a 150 ml three-necked flask equipped with a thermometer, a glass inlet (closed with tap) to carry the hydrogen over the mixture and an exit tap, as shown in the Scheme below.



Air was displaced by argon on a vacuum line and the solid mixture was heated at 150°C for one hour, under argon. The temperature was then increased to 390°C and hydrogen passed over the mixture in place of argon. The heating continued for six hours during which time the solid changed from its original gold-yellow to a black-green colour. The flask was then allowed to cool.

When the solid reached room temperature, oxygen-free water was added (under argon) and the remaining black residue was separated by filtration. To the mother liquor, drops of oxygen-free methanol were added until a brown precipitate was observed. This was also removed by filtration. Repeated precipitation and filtrations were necessary to remove all the brown material before the green $K_4[W(CH)_7H].2H_2O$ had crystallised. The dark green product was washed three times with the oxygen-free methanol and dried under vacuum. Yield 1.4 g, 74%.

Analysis: Found: C, 15.5% ; N, 17.4% ; H, 0.6% ; K, 28.71%. $K_4WC_7N_7H_5O_2$ requires: C, 15.04% ; N, 17.55% ; H, 0.72% ; K, 27.96%. Recrystallisation of $K_4[W(CN)_7H].2H_2O$ in presence of Na^+ produces the salt $NaK_3[W(CN)_7H].2H_2O$.

Analysis: Found: C, 15.10% ; N, 17.45% ; H, 0.82%. $NaK_3WC_7N_7$ requires: C, 15.46% ; N, 18.04% ; H, 0.92%.

Method 2.

$K_5[W(CN)_7].H_2O$ (0.5 g, 8.6×10^{-4} mol) was placed under argon in a Schlenk tube, 5 cm^3, an oxygen-free aqueous solution of KCN (0.01 M) was transferred to the tube. The solid dissolved completely. The yellow solution was kept at 0°C in the dark until the solution became green. Oxygen-free methanol was added and the green flakes then formed. After filtration the solid was washed three times with methanol and dried under vacuum. Yield: 0.3 g, 60%. (NOTE: if yellow $K_5[W(CN)_7].H_2O$

is precipitated together with the green $K_4[W(CN)_7H].2H_2O$, the procedure must be repeated from the beginning).

Analysis: Found: C, 15.35% ; N, 17.42% ; H, 0.65%.

$K_4WC_7N_7H_5O_2$ requires: C, 15.04% ; N, 17.55% ; H, 0.72%.

Reaction with Olefins and Dienes.

General Procedure.

(All steps were carried out under N_2, and oxygen-free solutions were used)

To 1 cm^3 of a 0.05 M $K_4[W(CN)_7H].2H_2O$ aqueous solution containing 0.01 M CN^-, 0.02 M of the organic substrate was added and the mixture shaken vigorously. Depending on whether GLC or NMR were used to identify the products the following procedures were followed:

GLC: The organic substrate and product(s) were extracted with an appropriate volatile organic solvent and dried over molecular sieves before injecting to the chromatograph.

NMR: The reaction mixtures were transferred directly to the NMR tube or the product extracted with purified carbon tetrachloride (see Table 3.6 for details).

In the case for the $[Co(CN)_5H]^{3-}$-butadiene reaction, a procedure similar to that of reference 100 was followed: butadiene was passed into concentrated $K_4[W(CN)_7H]$ solution in aqueous 0.1 M KCN and the Raman spectrum measured from 1000-2200 cm^{-1}. No bands other than those due to $[W(CN)_7H]^{4-}$, CN^- and dissolved butadiene were observed.

TABLE 3.6. Chemical Reactions of $K_4[W(CN)_7H].2H_2O$ in 0.1 M CN^-.

Substrate	Solvent	Time	Temp. (°C)	Product	GLC	NMR	Yield
Acrylonitrile	H_2O	15 min. to 8 days	RT	Polymer	+	+	Low
Methyl methacrylate	^2H_2O	15 min. to 5 days	RT	Polymer		+	Low
2-Butyne	^2H_2O	15 min. to 2 hours	RT	no reaction		+	
Isoprene	^2H_2O	15 min. to 5 hours	RT	Polymer	+	+	Very low
Styrene	H_2O	15 min. to 5 days	RT	Polymer	+	+	Catalytic
2,3-dimethyl-1,3-butadiene	^2H_2O	15 min. to 5 days	RT	no reaction	+	+	
1,3-butadiene	H_2O	30 min. to 5 days	RT	no reaction			
1,3-cyclooctadiene	H_2O	15 min. to 5 days	RT	no reaction	+	+	
1,3-cycloheptadiene	H_2O	15 min. to 5 days	RT	Cycloheptene	+	+	25%
1,3-cyclohexadiene	H_2O	15 min. to 5 days	RT	Cyclohexene	+	+	50%
Cyclopentadiene	H_2O	15 min. to 5 days	RT	no reaction	+	+	

Potassium Hydrosulphito Heptacyanotungstate(IV), $K_4[W(HSO_3)(CN)_7]$.

$K_4[W(CN)_7H].2H_2O$ (0.5 g, 8.9×10^{-4} mol) was transferred to a Shlenck tube and the air replaced by argon. 5 cm^3 of deoxygenated aqueous 0.01 M KCN solution was added and, when the solid was completely dissolved, sulphur dioxide was bubbled into the solution for 30 minutes. The solvent was then removed under vacuum and an orange precipiate formed. Yield: 0.46 g, 85%.

Analysis: Found: C, 14.09% ; N, 16.72% ; S, 5.29%. $K_4WHSO_3C_7H_7$ requires: C, 13.92% ; N, 16.24 ; S, 5.30%.

Measurement of K for $[W(CN)_7H]^{4-}$.

(a) By Raman Spectroscopy. This was accomplished by measuring the Raman spectra of five solutions of $[W(CN)_7H]^{4-}$ in 0.01 M CN^- with different concentrations of OH^- ; Na_2SO_4 was used as an internal reference for intensity measurements (ν_1 at SO_4^{2-} at 982 cm^{-1}, which allows for variation in the overall intensity of the Raman spectra due to changing colour). The ionic strength was maintained at $\mu = 5.5 \pm 0.3$ by adding appropriate amounts of NaCℓ. The relative concentrations of $[W(CN)_7H]^{4-}$ and $[W(CN)_7]^{5-}$ were obtained by measurement of the areas under the 2110 cm^{-1} and 1970 cm^{-1} peaks respectively. Measurements were carried out in a spinning cell. Data are summarised in Table 3.5

(b) By ^{13}C NMR. Approximate values for K were obtained by measurement of the integrals for ^{13}C peaks due to $[W(CN)_7H]^{4-}$ and $[W(CN)_7]^{5-}$ respectively in two solutions in 0.01 M CN^- to which $[OH^-]$ at 1.0 and 3.0 M concentrations had been added. A pulse delay of 16 seconds was used to allow for possible different relaxation times of the two complexes. The total ionic strength of the solution was maintained at 5.5 M.

B. MOLYBDENUM

I. AIM:

The aim was to prepare and to obtain single crystals of salts of $[Mo(CN)_7]^{4-}$ for X-ray crystallographic studies; to carry out a more complete study of their EPR spectra; and to establish whether the $[Mo(CN)_7]^{4-}$ anion in the potassium salt changes configuration from the solid state to solution.

II. LITERATURE INTRODUCTION.

The salts $K_4[Mo(CN)_7].2H_2O$,[64] $K_5[Mo(CN)_7]$,[28] $K_5[Mo(CN)_7].H_2O$,[7] and $Na_5[Mo(CN)_7].10H_2O$[7] have been reported, and the anions of the latter two have been shown to have pentagonal bipyramidal (D_{5h}) structures in the solid state.[7] Salts of $[Mo(CN)_7]^{4-}$ are of interest because EPR and limited vibrational spectroscopic data suggested that the anion in $K_4[Mo(CN)_7].2H_2O$ might have a capped trigonal prismatic (C_{2v}) structure in solution.[27] We therefore prepared this salt, examined its EPR spectrum down to 13 K, measured its vibrational spectra in the solid state and aqueous solution, and performed the same measurements on the new salt $NaK_3[Mo(CN)_7].2H_2O$ and also on $K_5[Mo(CN)_7].H_2O$ and $Na_4[Mo(CN)_7H].2H_2O$. We have published the results of some of this work.[30]

III. RESULTS AND DISCUSSION

B.1) $NaK_3[Mo(CN)_7]2H_2O$.

Dark green crystals of $NaK_3[Mo(CN)_7].2H_2O$ were first obtained by slow oxidation of $Na_5[Mo(CN)_7].10H_2O$ in an aqueous solution containing sodium cyanide, potassium borohydride and methanol. We later made the compound from $K_3[MoCl_6]$ and NaCN. This compound has hitherto been reported

in the literature, and for the first time a molybdenum(III) heptacyanide has been obtained as single crystals. They were studied by single crystal X-ray crystallography.†

a) Single Crystal X-ray Structure .

The single crystal X-ray determination of the structure of the anion in $NaK_3[Mo(CN)_7].2H_2O$ showed it to be a pentagonal bipyramid with only minor deviations from D_{5h} symmetry. The R factor has reached 0.033. The space group is $P2_1/m$. The axial and equatorial Mo-C distances are equal within experimental error, as is the case with the corresponding parameters in $K_4[M(CN)_7].2H_2O$ [M = V [4], Re [6]]. The mean Mo-C distance of 2.160 Å is comparable with that (2.140 Å) observed[7] in $Na_5[Mo(CN)_7].10H_2O$. The structure is shown in Figure 3.3 and the X-ray powder data are given in Table 3.7. This salt is not isomorphous with any of the analogous heptacyano complexes of V(III), Mo(III) Mo(II), W(IV), W(II) and Re(III), probably because of the mixed cation.

b) Magnetic Properties

The salt $NaK_3[Mo(CN)_7].2H_2O$ is paramagnetic (low-spin d^3) in solid state and in solution.

μ_{eff} (solid) = 1.78 B.M. at 298 K

μ_{eff} (solution) = 1.84 $\pm$ 0.05 B.M. at 298 K.

c) EPR Spectra

The EPR spectra and absorption data for $NaK_3[Mo(CN)_7].2H_2O$ in the solid state and aqueous cyanide solution are given in Figure 3.10 and Table 3.8 respectively.

---

† Single crystal X-ray work carried out by K.M.A. Malik and Dr. M.B. Hursthouse, Queen Mary College, London.

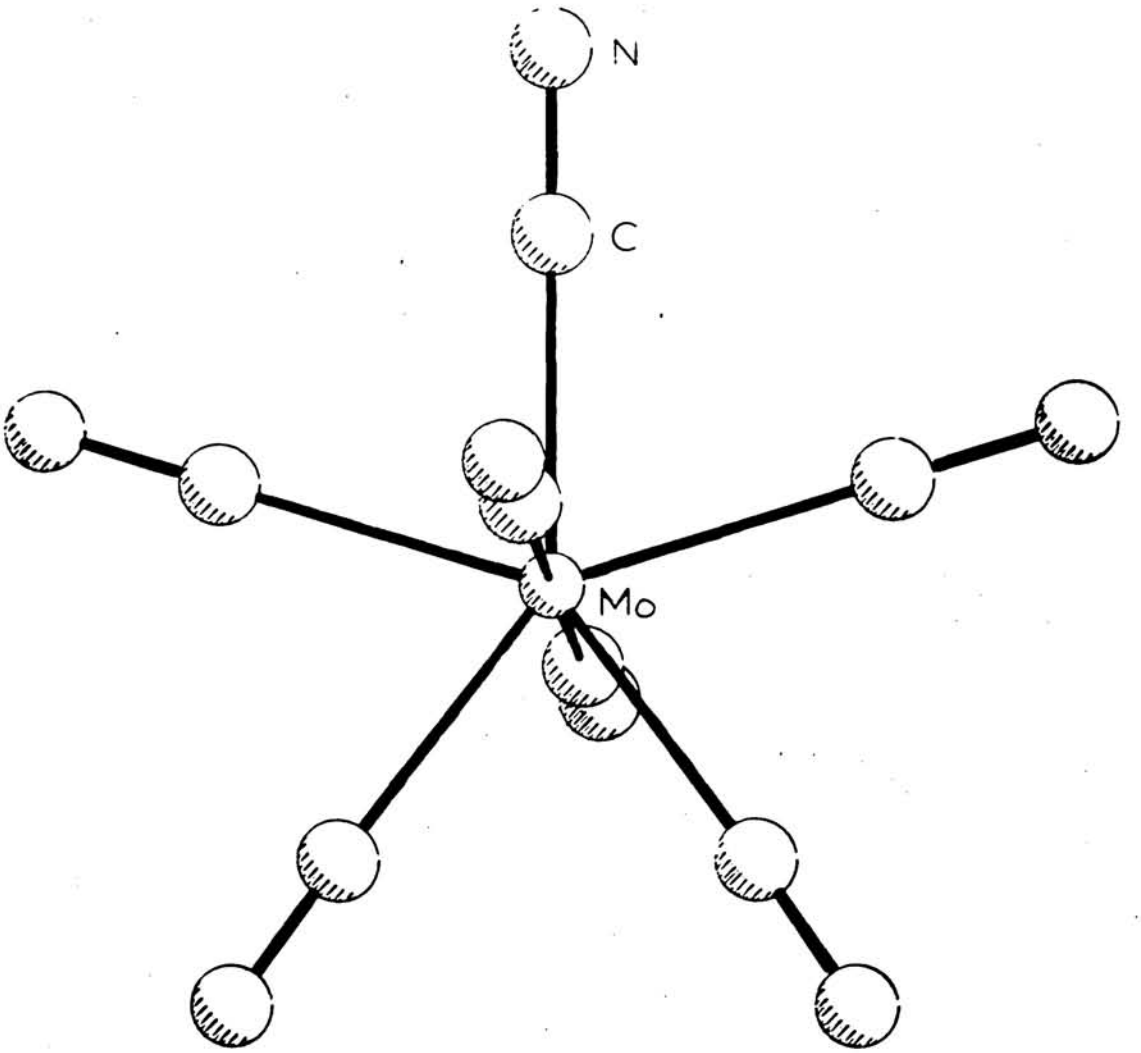


Figure 3.9. X-Ray Crystal Structure of $[Mo(CN)_7]^{4-}$ in $NaK_3[Mo(CN)_7].2H_2O$.

TABLE 3.7. X-Ray Powder Pattern for $NaK_3[Mo(CN)_7].2H_2O$.

d	Relative Intensity	d	Relative Intensity	d	Relative Intensity
8.0	vw	3.54	w	2.35	m
7.5	w	3.45	s	2.24	w
7.4	m	3.38	vw	2.20	vw
6.7	s	3.30	w	2.14	w
6.3	s	3.08	w	2.08	vw
6.0	vw	3.00	vw	2.03	vw
5.8	m	2.92	vs	2.000	vw
5.3	vw	2.86	vs	2.968	vw
4.75	vw	2.72	m	2.965	vw
4.60	vw	2.70	m	1.950	vw
4.41	vs	2.68	m	1.940	vw
4.08	s	2.63	m	1.930	vw
4.00	w	2.58	m	1.685	vw
3.75	s	2.56	w	1.850	vw
3.68	w	2.50	m	1.844	vw
3.60	vw	2.45	m	1.840	w
				1.800	vw

TABLE 3.8. EPR Data for $NaK_3[Mo(CN)_7].2H_2O$.

Compound	Phase	T K	$g_{\|}$	$g_{\perp}$
$NaK_3[Mo(CN)_7].2H_2O$	Solid	16.8	3.89	1.17
		2.4	3.89	1.17
	Solution	13	2.09	1.98
	(0.1 M KCN)	27	2.09	1.98

In the spectrum of an undiluted sample of the powdered material a broad and anisotropic signal was observed at $g_{\|} = 3.98$ and $g_{\perp} = 1.17$ between 2.4 and 24 K (Figure 3.10). The signal became progressively weaker with increasing temperature and was not observed at 50 K. Such behaviour is to be expected for a low-spin d^3 complex of D_{5h} symmetry.[27] As mentioned elsewhere[27] the ligand field energy level diagram for a D_{5h} isomer of $[Mo(CN)_7]^{4-}$ shows the doubly degenerate E ground state (See Figure 10, page 21), which will give rise to fast spin-lattice relaxation time and consequently leads to a broad signal.

At 13 and 27 K, a sharp signal was observed for a 0.1 M aqueous solution (containing 0.1 M KCN) of $NaK_3[Mo(CN)_7].2H_2O$ with a $g_{\|} = 2.09$ and $g_{\perp} = 1.98$. The shape and the g values correspond exactly with those for pure $K_4[Mo(CN)_7].2H_2O$ in the solid state, and it seems likely that some pure potassium salt precipitated out of the solution when frozen down. The presence of KCN (used to avoid photodecomposition) could be responsible for this because of the common ion effect. No signal characteristic of a D_{5h} species could, however, be seen in the EPR spectra

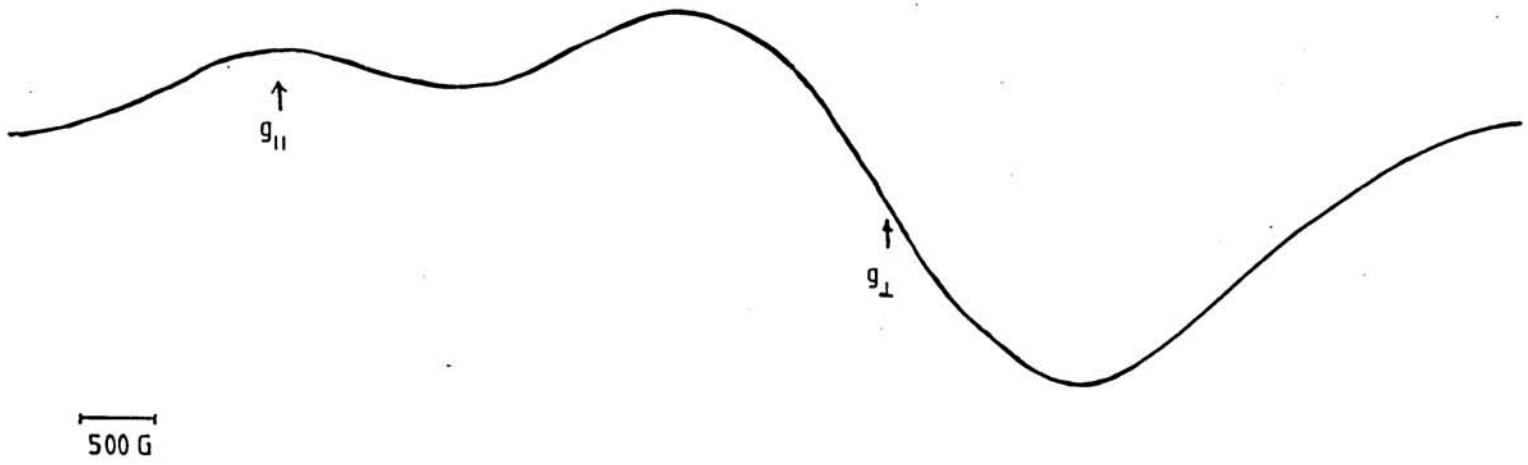


Figure 3.10. EPR sepctrum of solid $NaK_3[Mo(CN)_7].2H_2O$. Field set 5000 ± 5000 G - Temp. 16.8 K - 40 dB.

of aqueous solutions containing NaCN instead of KCN down to 13 K; it is possible that the line is too broad to be detected under these circumstances.

d) Vibrational Spectra.

The vibrational spectral data for $NaK_3[Mo(CN)_7].2H_2O$ in the solid state and in aqueous solution are listed in Table 3.9, and illustrated in Figure 3.11.

In the ν_{CN} region of the spectra of solid $NaK_3[Mo(CN)_7].2H_2O$ four bands in the infrared spectrum and five bands in the Raman spectrum were observed (see Table 3.9). The profiles of both are very similar. In both cases, two are very strong and the others very weak. We have shown by X-ray diffraction (see Section a , page 97) that the anion $[Mo(CN)_7]^{4-}$ in the mixed salt is pentagonal bipyramidal.[30] The greater number of bands observed in both cases, then that expected for D_{5h} symmetry (see Table VII, p. 29) may arise from solid splitting effects. However, the vibrational data for the species $[Mo(CN)_7]^{4-}$ in solution are fully consistent with PB symmetry. The observation of two polarised bands in the Raman spectrum of the solution support the conclusion that the D_{5h} configuration is maintained in solution.

e) Properties.

The salt $NaK_3[Mo(CN)_7].2H_2O$ crystallises as dark green, well formed prismatic needles, and is sensitive to atmospheric oxidation. Its aqueous solution is green and even more sensitive than is the solid to oxidation and photodecomposition. Its decomposition in solution can be minimised by using excess cyanide.

Figure 3.11 Vibrational spectra of solid $NaK_3[Mo(CN)_7].2H_2O$.

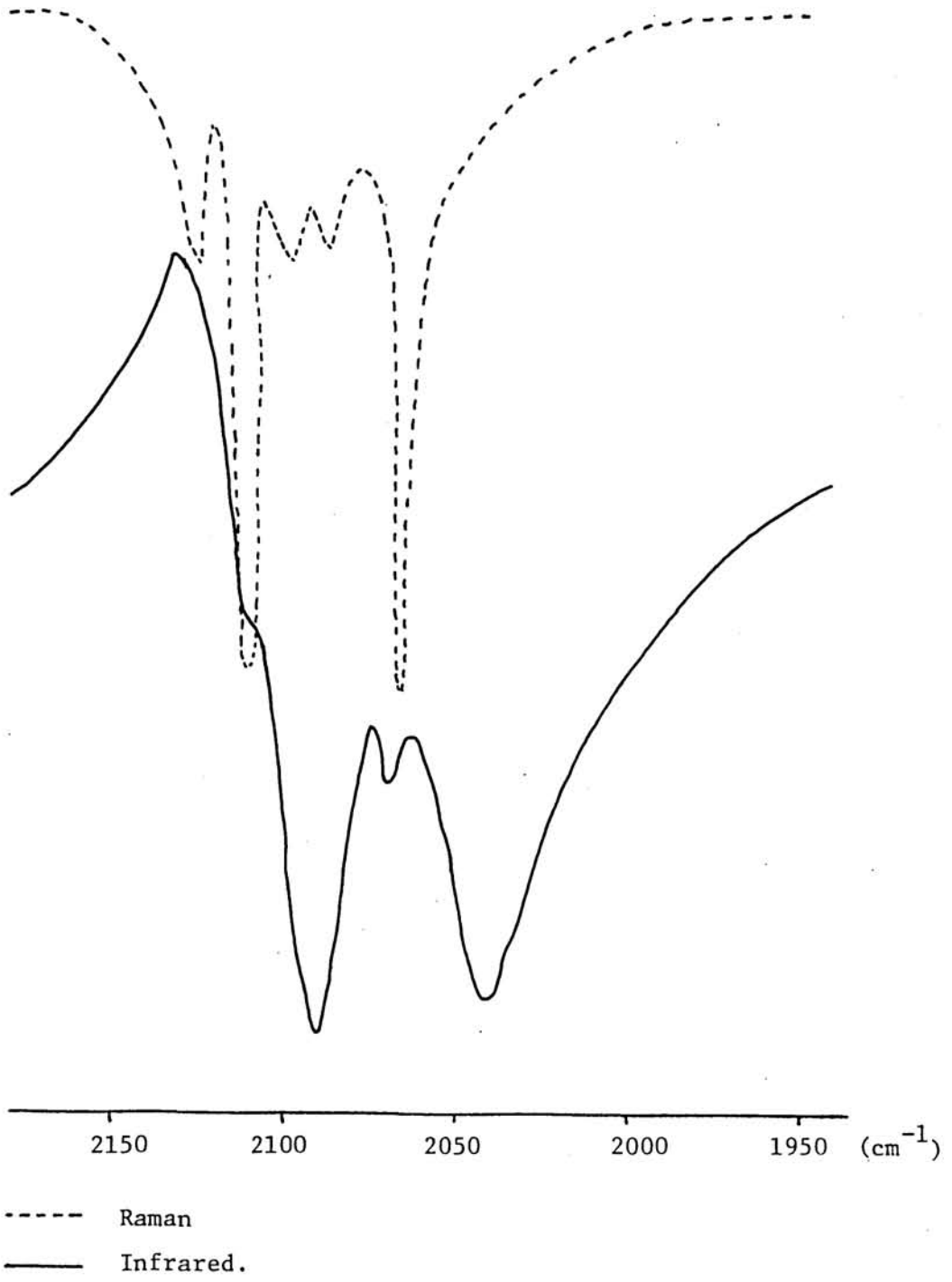


TABLE 3.9. Vibrational Spectra Data of $NaK_3[Mo(CN)_7].2H_2O$ in the Solid State and in Aqueous 0.1 M CN^-.

	ν_{CN} (cm^{-1})	δ_{CN} (cm^{-1})	ν_{MC} or ν_{MCN} (cm^{-1})
IR (solid)	2043(vs) 2070(m) 2090(vs) 2110(sh)	not observed	360(vs) 460(m) 550(s)
IR (solution)	2040(m) 2079(m)		
R (solid)	2065(10) 2089(9) 2100(5) 2110(10) 2124(5)		
R (solution)	2063(8) 2100(5) (polarised) 2115(8) (polarised)		

f) Conclusions

Single crystal X-ray diffraction studies showed that the anion in $NaK_3[Mo(CN)_7].2H_2O$ is pentagonal bipyramidal. The EPR spectrum of the solid sample was obtained, and can be used as a model for other d^3 PB complexes. Vibrational data suggests that the D_{5h} configuration is maintained in aqueous solution.

B.2) $K_4[Mo(CN)_7].2H_2O$

a) X-ray

The X-ray powder pattern of $K_4[Mo(CN)_7].2H_2O$ is given in Table 3.10, and it is important to emphasise that the potassium salt is not isomorphous with the analogous $K_4[V(CN)_7].2H_2O$ (known to have a pentagonal bipyramidal anion[6]). It is also not isomorphous with $K_4[W(CN)_7H].2H_2O$ (see Table 3.2). Suitable single crystals of $K_4[Mo(CN)_7].2H_2O$ could not be obtained for X-ray diffraction studies.

b) Magnetic Properties

Potassium heptacyanomolybdate(III) is paramagnetic (low-spin d^3) with μ_{eff} = 1.73 B.M. at 298 K.[27] We confirmed this result and found for the solid, μ_{eff} = 1.80 at 297 K while a 0.05 F aqueous solution exhibited a magnetic moment of 1.84 $\pm$ 0.05 B.M. (using the NMR method).[84,85] All of these results indicate a spin-doublet ground state for the d^3 complex and suggest that the complex does not have a dimeric or polymeric formulation, with metal-metal bonds or cyano bridges.

c) EPR Spectra

The EPR spectrum of solid $K_4[Mo(CN)_7].2H_2O$ was first reported in 1973[27] and an EPR signal was observed for the undiluted powder sample at $g_{\parallel}$ = 2.103 and $g_{\perp}$ = 1.973 below 150 K.[27]

TABLE 3.10. X-Ray Powder Pattern Data for $K_4[Mo(CN)_7].2H_2O$.

d	Relative Intensity	d	Relative Intensity	d	Relative Intensity
8.2	vw	3.30	m	1.950	m
8.0	vw	3.00	vs	1.930	m
6.4	m	2.82	s	1.842	m
6.3	m	2.79	s	1.838	m
4.80	w	2.66	vw	1.760	w
4.40	w	2.57	vw	1.730	w
4.22	s	2.44	vs	1.720	w
4.18	s	2.20	s	1.682	w
3.95	s	2.10	m	1.658	vw
3.85	vw	2.07	m	1.510	vw
3.45	m	2.05	s	1.500	vw
				1.470	vw

We repeated the experiment at liquid nitrogen (77 K) and liquid helium temperatures (14, 24 K) and we confirmed the results of the earlier publication. Figure 3.12 and Table 3.11 give the spectrum and the EPR data for the solid $K_4[Mo(CN)_7].2H_2O$ respectively.

TABLE 3.11. EPR Data for $K_4[Mo(CN)_7].2H_2O$.

Compound	Phase	T K	$g_{\parallel}$	$g_{\perp}$	< g >
$K_4[Mo(CN)_7].2H_2O$	Pure solid	14	2.11	1.98	2.02
		24	2.11	1.98	2.02
		77	2.11	1.98	2.02
		120			2.01

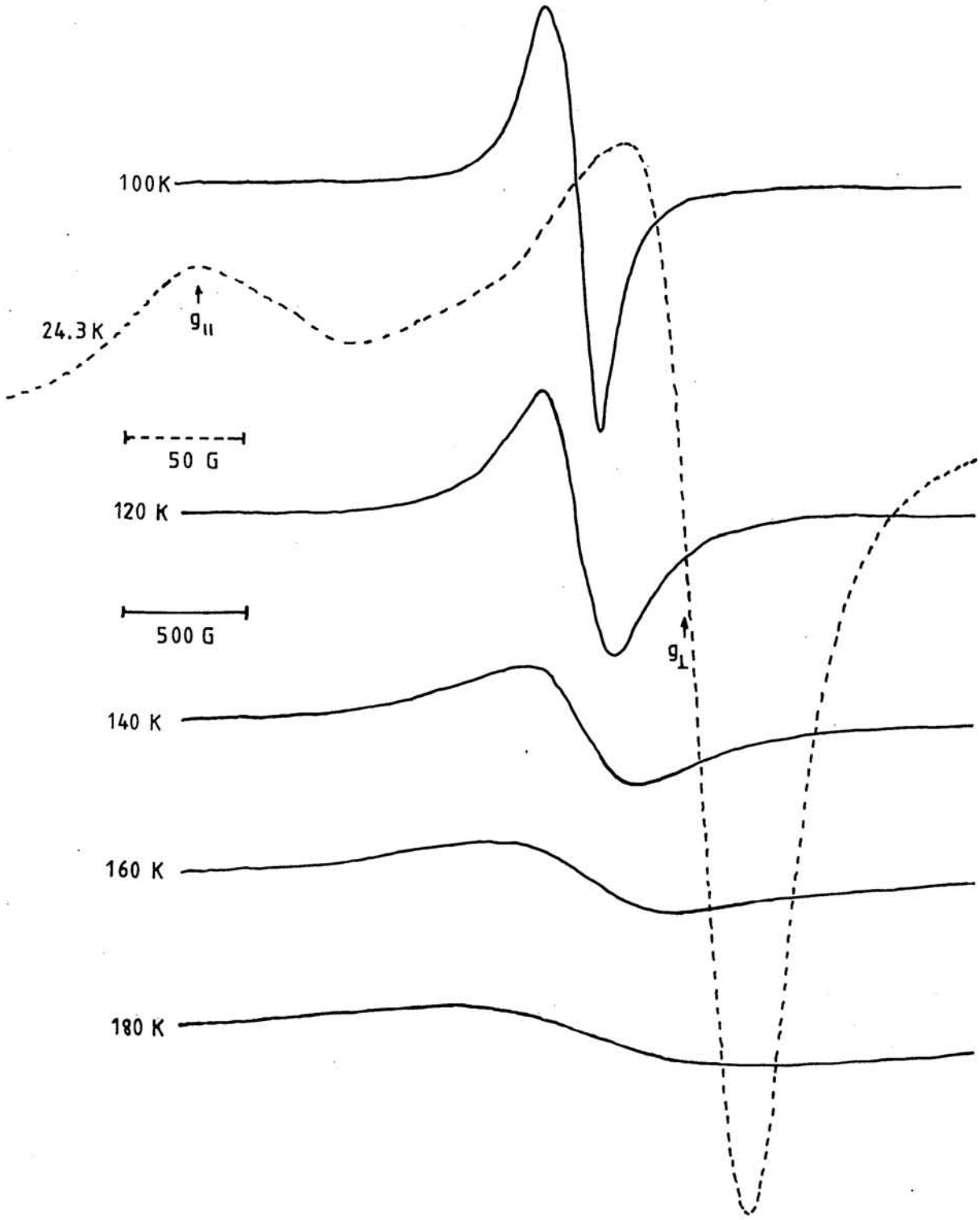
The EPR spectrum of $K_4[Mo(CN)_7].2H_2O$ as an undiluted solid at 14 K shows sharp signals similar to those observed by Gray, et al.,[27] in good agreement with the values calculated by them for the $^2A_1\ (a_2)^2\ (a_1)^1$ ground state ($g_x = 1.983$, $g_y = 1.981$, $g_z = 2.107$) for C_{2v} geometry of the anion.[27] The same spectrum is seen at 77 K but collapses to a single isotropic line (g = 2.01) at 120 K and disappears above 200 K.

For pentagonal bipyramidal symmetry, only a broad signal would be expected, as is indeed the case for $NaK_3[Mo(CN)_7].2H_2O$ (see Section B.1, c, page 96), since its anion is now known to have PB symmetry.

d) Vibrational Spectra.

The Raman and infrared spectra data for $K_4[Mo(CN)_7].2H_2O$ in the solid state and in aqueous cyanide solution are presented in Table 3.12. Our results are in quite good agreement with that of Gray, et al.,[27] but are more extensive.

Figure 3.12. EPR spectra of $K_4[Mo(CN)_7].2H_2O$ in the solid state at various temperatures.



In the solid sample of $K_4[Mo(CN)_7].2H_2O$ four absorptions in the ν_{CN} stretching region were observed in both the infrared and Raman. In both cases, two are strong and the other two are very weak.

The preliminary conclusion that the anion in the solid state has C_{2v} geometry based on EPR studies is now better established. The selection rules predict six IR-active ($3A_1$, $2B_1$, B_2) and seven Raman-active ($3A_1$, A_2, $2B_1$, B_2) ν_{CN} fundamentals for C_{2v} symmetry with six infrared-Raman coincidences ($3A_1$, $2B_1$, B_2). In fact, we observed four Raman bands and four infrared bands with three coincidences for the solid, but for the anion in solution, the vibrational data fit well for D_{5h} symmetry with two infrared (A_2'' , E_1') and three Raman [$2A_1$, E_2'; two polarised (A_1)] absorptions with no infrared Raman coincidences. The profiles in the CN-stretching region are very similar to those observed for $[V(CN)_7]^{4-}$ [35] and $[Re(CN)_7]^{4-}$ [35] which also have PB symmetry.

We may tentatively assign the 2100 and 2115 cm^{-1} bands in the Raman to the A_1 modes since they are polarised, and that at 2063 cm^{-1} to the E_1' mode; by analogy with Raman data for $[Re(CN)_7]^{4-}$ [35]:the 2080 cm^{-1} infrared band is probably the A_2'' mode and that at 2040 cm^{-1} the E_1' mode. The Raman absorption at 2080 cm^{-1} in solution is likely to be due to free cyanide and it disappears if, instead of cyanide, the solution is stabilised with hydroxide ion. The absence of Raman-infrared coincidences is consistent with D_{5h} symmetry.

e) Reactions.

The reaction of $K_4[Mo(CN)_7].2H_2O$ with nitric oxide gave $K_4[Mo(CN)_8].2H_2O$ as the major product. The complex is not oxidised when hydrazine is present in the solution and neither does it form isolable nitrosyl complexes.

TABLE 3.12. Vibrational Data for $K_4[Mo(CN)_7].2H_2O$.

	ν_{CN} (cm^{-1})	δ_{CN} (cm^{-1})	ν_{MC} or ν_{MCN} (cm^{-1})
IR (solid)	2030(sh) 2064(vs) 2100(m) 2110(sh)	840(w)	294(sh), 340(m), 360(m), 390(m), 430(w), 460(w), 498(w)
IR (solution)	2040(m) 2080(m)		
R (solid)	2060(w) 2080(vs) 2097(vs) 2115(w)		270(w) 365(w) 465(w)
R (solution)	2063(w) 2080(s) (due to free cyanide) 2100(sh) p 2115(s) p (A_1)		

solution prepared with aqueous 0.1 M KCN.

f) Conclusions

Although single crystals of $K_4[Mo(CN)_7].2H_2O$ were not obtained for the determination of its structure in the solid state, EPR studies confirmed that the anion in the potassium salt have CTP geometry. Vibrational spectroscopic studies suggest that the anion $[Mo(CN)_7]^{4-}$ changes its configuration to PB in solution. The observation of two polarised bands in the Raman of the solution supports this conclusion.

B.3) $K_5[Mo(CN)_7].H_2O$ and $Na_4[Mo(CN)_7H].nH_2O$.

The salt $K_5[Mo(CN)_7].H_2O$ was first made in this laboratory.[28] Drew, Mitchell and Pygall[7] established (by X-ray diffraction) the structure of the anion $[Mo(CN)_7]^{5-}$ as pentagonal bipyramidal in the hydrated sodium and potassium salts.[7] It has been suggested that the anion $[Mo(CN)_7]^{5-}$ changes its configuration from PB in the solid to CTP in solution.[28,7]

We repeated the preparation of $K_5[Mo(CN)_7].2H_2O$ and extended earlier vibrational data. We now present evidence that the PB geometry is maintained in solution. We also obtained the first hydrido heptacyano complex of molybdenum $Na_4[Mo(CN)_7H].nH_2O$, and preliminary work suggests that the species $[Mo(CN)_7H]^{4-}$ is in equilibrium with $[Mo(CN)_7]^{5-}$ in excess cyanide aqueous solution.

a) Synthetic Methods.

$Na_5[Mo(CN)_7].H_2O$ was made by the literature procedure of reacting CN^- with $Mo_2(OAc)_4$.[28] The new compound, $Na_4[Mo(CN)_7H].nH_2O$ was made by careful addition of dilute acetic acid to $[Mo(CN)_7]^{5-}$ under nitrogen. However, only one preparation was successful in producing this latter salt, and clearly more work is necessary to establish its stoichiometry fully.

b) X-Ray of $K_5[Mo(CN)_7].H_2O$.

Potassium heptacyanomolybdate(II) hydrate is isomorphous with $K_5[W(CN)_7].H_2O$ and its X-ray powder pattern is given in Table 3.1, page 62 , together with that of the latter salt. Single crystal X-ray diffraction studies[7] shows that the anion $[Mo(CN)_7]^{5-}$ in the hydrated sodium and potassium salts have PB geometry.

c) Magnetic Properties of $K_5[Mo(CN)_7].H_2O$.

This salt is diamagnetic (low-spin d^4) in the solid state (μ_{eff} = 0.24 BM at 298 K). No paramagnetic susceptibility was observed (using the NMR methods[84,85]) in the aqueous solution in 0.05 M CN^-.

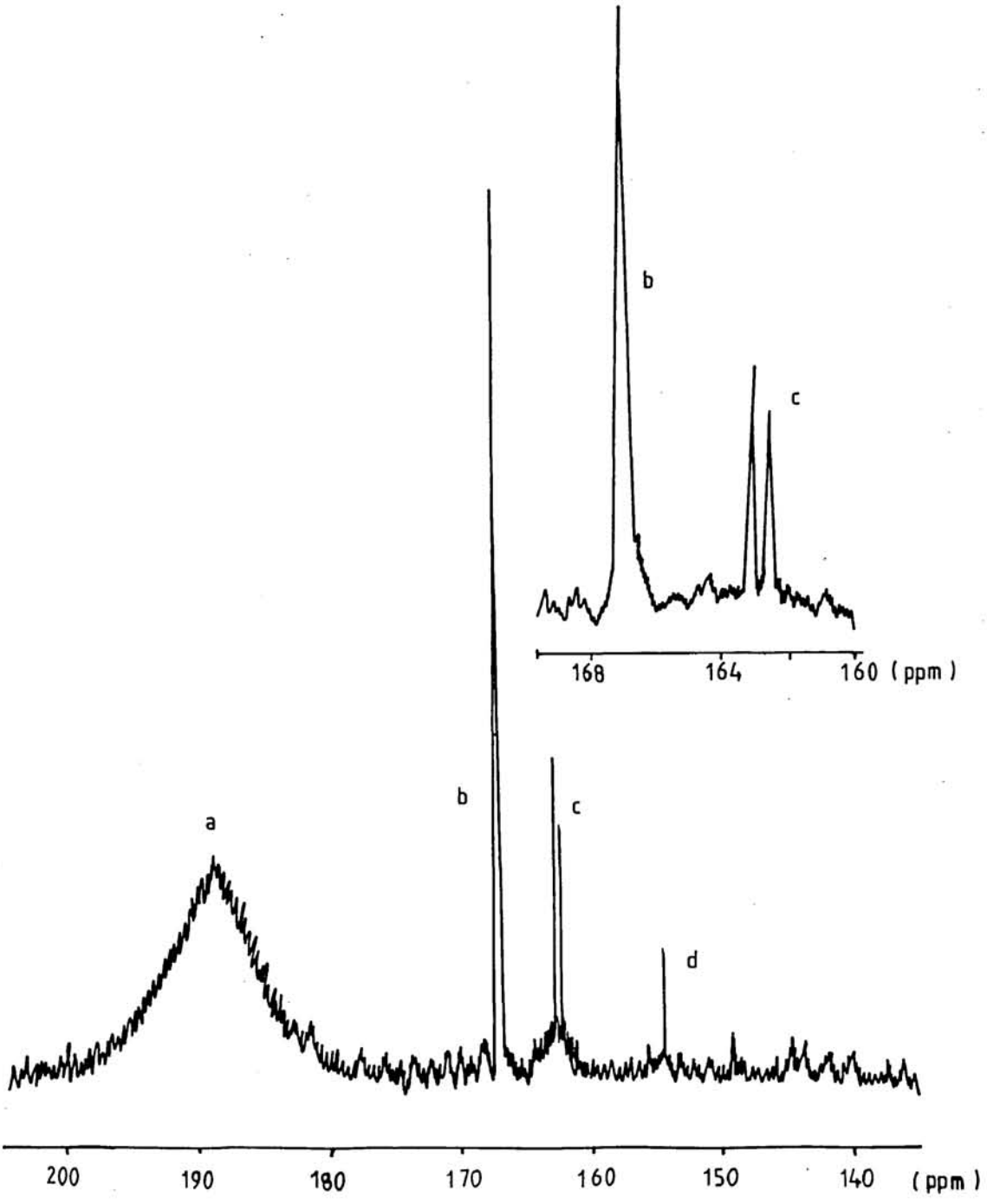
d) ^1H NMR of $[Mo(CN)_7H]^{4-}$.

In the proton NMR spectrum of $[Mo(CN)_7H]^{4-}$ in excess cyanide aqueous solution and DSS as internal standard a singlet at δ = 2.0 ppm was observed. We assign this to a hydride resonance by comparison with the analogous $[W(CN)_7H]^{4-}$ species (see Section A.1 (d), page 64).

e) ^{13}C NMR of $[Mo(CN)_7]^{5-}$ and $[Mo(CN)_7H]^{4-}$.

The undecoupled ^{13}C NMR spectrum of $[Mo(CN)_7]^{5-}$ (0.01 M) in 0.1 M CN^- aqueous solution shows four absorptions at (a) δ 188.4 ppm, (b) δ 167.4 ppm, (c) δ 162.8 ppm and (d) δ 154.6 ppm (all down field to DSS) (a) is broad but (b), (c) and (d) are sharp, (Figure 3.13); the resonances at δ 167.4 ppm and δ 154.6 ppm correspond to free $^{13}CN^-$ and $[Mo(CN)_8]^{4-}$ (present as an impurity) (see page 39) respectively.

Figure 3.13. The undecoupled ^{13}C NMR spectrum of (a) $[Mo(CN)_7]^{5-}$; (c) $[Mo(CN)_7H]^{4-}$; (d) $[Mo(CN)_8]^{4-}$ in aqueous excess CN^- (b) solution.



The broad peak at δ 188.4 ppm is likely to be due to $[Mo(CN)_7]^{5-}$. The doublet centred at δ 162.8 ppm is likely to be due to a monohydride species which, we suggest, is by analogy with its tungsten anlogue $[Mo(CN)_7H]^{4-}$. The value of the coupling constant ($\underline{J}_{^{13}C-H}$ = 11.1 Hz) in the latter is the same as that found for the analogous tungsten hydrido complex (see Section A.1 (e), page 68).

The sharpness of the lines corresponding to free $^{13}CN^-$ and $[Mo(CN)_7H]^{4-}$ indicates that there is no exchange between coordinated and free cyanide, and that $[Mo(CN)_7]^{5-}$ and $[Mo(CN)_7H]^{4-}$ are probably fluxional on the NMR time scale. The broadening of the signal assigned to $[Mo(CN)_7]^{5-}$ could be due to the presence of a very small amount of $[Mo^{III}(CN)_7]^{4-}$ (present as decomposition product). The two species in solution have PB geometry and the only difference between them is the oxidation state of molybdenum(II) and (III) respectively. It is possible, therefore, that electron transfer occurs between these species which could cause such broadening. We were unable to obtain evidence for the existance of $[W(CN)_7]^{4-}$, and such broadening of $[W(CN)_7H]^{4-}$ resonance does not occur (see page 68).

Addition of 0.05 M sodium hydroxide causes the disappearance of the $[Mo(CN)_7H]^{4-}$ absorption at δ 162.8 ppm. This is evidence for the equilibrium

$$[Mo(CN)_7H]^{4-} + OH^- \rightleftharpoons [Mo(CN)_7]^{5-} + H_2O \qquad (2)$$

as found for the analogous tungsten system. Although further work needs to be carried out in order to calculate the equilibrium constant of (2) it appears that $[Mo(CN)_7H]^{4-}$ is a stronger acid than $[W(CN)_7H]^{4-}$, because very little OH^- is needed to reduce the hydride peak to zero intensity.

f) Vibrational Spectra.

i) $K_5[Mo(CN)_7].H_2O$

Vibrational spectra data for potassium heptacyanomolybdate(II) hydrate in the solid state and in aqueous excess cyanide solution are listed in Table 3.13. The anion $[Mo(CN)_7]^{5-}$ has distorted PB geometry with C_s symmetry in the monohydrated potassium salt[7] and seven fundamental stretcing vibrations are expected to be Raman and infrared active. This is indeed observed in the Raman spectrum of the solid. In the infrared, nine absorptions are observed; the complexity of the spectrum is probably due to solid state effects. However, both infrared and Raman spectra for the solution are fully consistent with D_{5h} symmetry for the anion in alkaline solution. The observation of two polarised bands in the Raman and the similarity of profiles of the solid and solution, infrared and Raman spectra suggests that PB geometry is maintained in solution. Kiernan[28] tentatively proposed C_{2v} symmetry for $K_5[Mo(CN)_7]$ in the solid state and in aqueous solution on the basis of vibrational spectroscopy. We re-measured and extended these data and we now conclude, with the knowledge of the X-ray crystal structure of the solid [7] and better Raman instrumentation, that the PB structure of the anion $[Mo(CN)_7]^{5-}$ is retained in solution. This supports the suggestion[83a] that $K_5[Mo(CN)_7].H_2O$ is likely to be identical to the " $K_4[Mo(CN)_6]$" reported by Kleinberg, et al.[68]

TABLE 3.13. Vibtational Data for $K_5[Mo(CN)_7].H_2O$.

	ν_{CN} (cm^{-1})	δ_{CN} (cm^{-1})	ν_{MC} or ν_{MCN} (cm^{-1})	Reference
IR (solid)	2105(vw) 2088(w) 2070(vs) 2050(s) 2040(vs) 2030(s) 2010(s) 1990(m) 1960(vs)	870(vw)	570(w) 526(s) 487(w) 468(w) 407(m) 387(w) 365(w) 348(w)	This work
IR (solution)	2000(sh) 1950(vs)			28
R (solid)	2105(2) 2077(5) 2062(5) 2045(3) 2018(3) 2003(3) 1990(8)		388(5) 365(4) 345(4) 330(4)	This work
R (solution)	2110(6) polarised 2070(8) poalrised 1980(6)		330(4)	This work

ii) $Na_4[Mo(CN)_7H].2H_2O$.

The vibrational spectra of solid sodium hydrido heptacyanomolybdate(IV) dihydrate are shown and the data are listed in Figure 3.14 and Table 3.14 respectively.

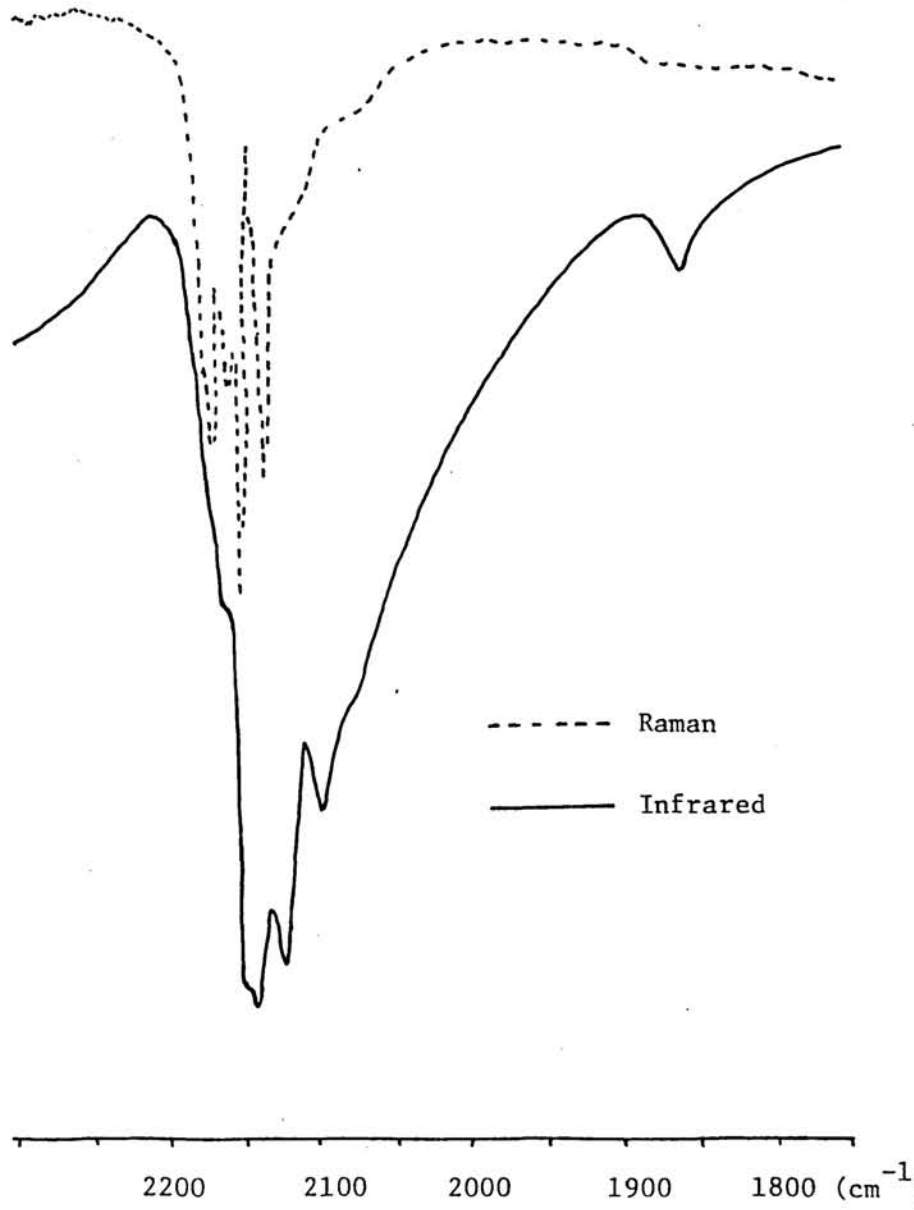
TABLE 3.14

Vibrational Data for $Na_4[Mo(CN)_7H].2H_2O$ in the Solid State.

	ν_{CN} (cm^{-1})	ν_{Mo-H} (cm^{-1})	ν_{MC} or ν_{MCN} (cm^{-1})
IR	2110(sh), 2100(sh) 2090(vs), 2070(vs) 2048(s), 2030(sh)	1810(w)	515(w), 460(w) 390(m), 360(s)
R	2118(7) 2106(6) 2100(9) 2082(7)		

The vibrational spectra of solid $Na_4[Mo(CN)_7H].2H_2O$ are very simliar in profile to those of $K_4[W(CN)_7H].2H_2O$ (see Section A.1, f, page 75)

Figure 3.14. Vibrational spectra of solid $Na_4[Mo(CN)_7H].nH_2O$.



g) Properties.

i) $K_5[Mo(CN)_7].H_2O$

The complex is a diamagnetic (low-spin d^4) yellow solid, which crystallises as well-formed small needles. It is sensitive to atmospheric oxidation, rapidly forming a green surface layer. It is soluble in water to give a yellow solution which is even more sensitive to air than the solid. Single crystals of $NaK_3[Mo(CN)_7].2H_2O$ have been obtained from such partially oxidised solutions in the presence of sodium and potassium ions (see Section B.1a, page 96).

ii) $Na_4[Mo(CN)_7H].2H_2O$

Sodium hydrido heptacyanomolybdate(IV) dihydrate crystallises as dark green mycrocrystals. It is moderately sensitive to air and when dissolved in water forms green solutions more sensitive to atmospheric oxidation. In solution the complex is stable in presence of free CN^-.

h) Reactions.

$Na_5[Mo(CN)_7].H_2O$ reacts with H^+ forming $Na_4[Mo(CN)_7H].2H_2O$. By increasing the pH of the solution the latter converts to the former, indicating reversibility of the reaction:

$$[Mo(CN)_7]^{5-} + H_2O \rightleftharpoons [Mo(CN)_7H]^{4-} + OH^-$$

i) Conclusions

i) $K_5[Mo(CN)_7].H_2O$

The anion in $K_5[Mo(CN)_7].H_2O$ has PB geometry in the solid state, and we propose that this structure is maintained in solution on the basis of vibrational data.

Preliminary studies indicate that the equilibrium

$$[Mo(CN)_7H]^{4-} + OH^- \rightleftharpoons [Mo(CN)_7]^{5-} + H_2O$$

is present in the aqueous solution of $[Mo(CN)_7]^{5-}$ in excess cyanide.

ii) $Na_4[Mo(CN)_7H].nH_2O$

This complex is obtained when $[Mo(CN)_7]^{5-}$ reacts with dilute acetic acid. The presence of a hydride ligand is indicated by infrared and ^1H, ^{13}C NMR spectroscopy. From the similarity of profiles of its vibrational spectra with those of the analogous $K_4[W(CN)_7H].2H_2O$ we suggest that the structure of the anion $[Mo(CN)_7H]^{4-}$ in the solid sodium salt is bicapped trigonal prismatic.

EXPERIMENTAL

Sodium Tripotassium Heptacyanomolybdate(III) Dihydrate, $NaK_3[Mo(CN)_7].2H_2O$.

This was obtained by a modification of the literature method for $K_4[Mo(CN)_7].2H_2O$.[64]

To a 100 cm^3 three-necked flask, equipped with a magnetic stirrer bar, were introduced $K_3[MoC\ell_6]$ (2.0 g, 4.7×10^{-3} mol), NaCN (4.0 g, 8.1×10^{-2} mol) and the air replaced by argon. Oxygen-free water (20 cm^3) was then added (under argon) and the final solution was stirred for 18 hours, during which time the solution was clear. Oxygen-free ethanol (30 cm^3) was then added and the solution was allowed to cool to 0^oC. The dark crystals formed were filtered, washed three times with oxygen-free ethanol and then dried under vacuum. Yield, 1.0 g (47%).

Analysis: Found: C, 18.56% ; N, 21.57% ; H, 0.83%. $NaK_3MoC_7N_7H_4O_2$ requires: C, 18.19% ; N, 21.56% ; H, 0.88%.

Potassium Heptacyanomolybdate(III) Dihydrate, $K_4[Mo(CN)_7].2H_2O$.

This procedure is a modification of that described by Gray, et al.[27] $K_3[MoC\ell_6]$ (0.7 g, 1.6×10^{-3} mol) and KCN (1.2 g, 1.8×10^{-2} mol) were introduced to a 50 cm^3 two-necked flask. The air was replaced by argon in a vacuum line. Oxygen-free water (7 cm^3) was transferred to the flask and the mixture stirred for 24 hours. The red brown solution gradually assumed an opaque, black and colloidal appearance and, after 24 hours, had become transparent and yellow-brown in colour. Oxygen-free ethanol (3 cm^3) was added and a dark green precipitate was formed. After filtration the solid was washed three times with 80% ethanol, then three times with pure ethanol and dried under vacuum. Yield 0.7 g, 91%.

Analysis: Found: C, 18.24% ; N, 20.85% ; H, 0.63%. $K_4MoC_7N_7H_4O_2$ requires: C, 17.86% ; N, 20.93% ; H, 0.85%.

Potassium Heptacyanomolybdate(II) Hydrate, $K_5[Mo(CN)_7].H_2O$.

This procedure is a modification of that described in reference 28. To a stirred saturated aqueous solution of potassium cyanide (5 cm^3) under argon, was added finely divided tetrakisacetato dimolybdenum(II) (0.5 g, 1.2×10^{-3} mol) in small portions. The solution immediately became dark brown before lightening again and depositing yellow crystals. After filtration, oxygen-free water (5 cm^3) was added and the mixture heated to 60°C in order to dissolve the solid. Oxygen-free methanol (10 cm^3) was added and the product precipitated as yellow crystals. This procedure was repeated twice and finally the solid was washed three times with oxygen-free methanol. The solid was then dried under vacuum. Yield 0.9 g, 82%.

Analysis: Found: C, 17.41% ; N, 19.99% ; H, 0.41%. $K_5MoC_7N_7H_2O$ requires: C, 17.74% ; N, 20.69% ; H, 0.42%.

Sodium Hydrido Heptacyanomolybdate(IV) Dihydrate, $Na_4[Mo(CN)_7H].nH_2O$.

A 50 cm^3 two-necked flask was connected to a vacuum line and the air replaced by argon. $Na_5[Mo(CN)_7].H_2O$ (0.5 g, 1.0×10^{-3} mol) was transferred to the flask and dissolved with deoxygenated 0.1 M NaCN aqueous solution (ca. 5 cm^3) (both operations were carried out under argon). Oxygen-free acetic acid (0.1 M) solution was added dropwise to the yellow solution until it turned dark green. Oxygen-

free methanol was added (5 cm^3) and a dark green precipitate was formed. After filtration the solid was washed five times with oxygen-free methanol and dried under vacuum. (The compound was characterised by infrared, Raman and ^1H, ^{13}C NMR. However, good analyses were not obtained due to $Na_4[Mo(CN)_7].2H_2O$ present as impurity`. Found: C, 20.02% ; H, 0.98% ; N, 23.52%).

A very low yield of a material which may be $K_4[Mo(CN)_7H].2H_2O$ was made by passing H_2 over $K_4[Mo(CN)_8].2H_2O$ at 390°C for 6 hours. In the infrared spectra of the crude product bands corresponding to $K_5[Mo(CN)_7].H_2O$ were observed. Repetitive recrystallisations of this, produced the hydrido complex as in the preparation of the analogous $K_4[W(CN)_7H].2H_2O$ (see page 90).

Potassium Heptacyanorhenate(III) Dihydrate, $K_4[Re(CN)_7].2H_2O$.

The complex $K_4[Re(CN)_7].2H_2O$ was obtained by the literature method[28] in 90% yield. The starting material, $K_2[ReCl_6]$ was made by the literature method[99] also, in 61% yield.

Analysis: Found: C, 15.2% ; N, 17.7% ; H, 0.7%. $K_4ReC_7N_7H_4O_2$ requires: C, 15.0% ; N, 17.5% ; H, 0.7%.

This salt was used as a diamagnetic lattice for EPR studies on $K_4[V(CN)_7].2H_2O$ (see page 52).

GENERAL TECHNIQUES AND INSTRUMENTATION.

All reagents used were of A.R. or G.P.R. quality.

Air sensitive solutions were handled in vessels fitted with rubber seals, transferance being effected by steel tubing. Solids were handled in glove-bags filled with argon.

Infrared spectra were run on Perkin-Elmer 683 and 325 instruments; mulls in liquid paraffin, between caesium iodide plates (4000-200 cm^{-1}) were used for solids and calcium fluoride for aqueous solution. Raman spectra were measured on a Spex Ramalog 5 (14018) double monochromator instrument, with a DPC-2 detector, using exciting radiation from a Coherent Radiation model 52 Kr^{+} laser. Solids were run in spinning KBr discs under nitrogen. For aqueous solution a spinning cell was used. A computer driven multiple scanning device over the range 2000-2210 cm^{-1} was used for the high resolution studies of solutions of $K_4[M(CN)_8]$ (M = Nb, Mo, W) and $K_5[Nb(CN)_8]$. Conditions are given in Section A.2, a, Figure 2.4).

Microanalyses were performed by the Microanalytical Laboratory, Imperial College. Potassium was estimated by flame photometry. Several solutions of varying concentrations were compared with solutions of known concentrations of KCℓ as standard. Solution electronic absorption spectra 250-850 nm range, 1 cm quartz cells, were recorded on a Perkin-Elmer 551 instrument.

Magnetic susceptibilities of powdered samples were measured, using the Gouy-Rankine method; diamagnetic corrections were applied.[101] The

calibration was checked using $[Ni(en)_3](S_2O_3)$. Magnetic susceptibilities for solutions were measured by the NMR method.[84,85]

X-ray powder diffraction patterns were recorded photographically by Dr. R.S. Osborn of the University of London Intercollegiate X-ray Service, Imperial College, using a Guinier Nonius Mark II camera with Cu(Kα) radiation. Single crystal X-ray diffraction studies were carried out by Dr. M.B. Hursthouse, of the University of London Intercollegiate X-ray Service, Queen Mary College.

Polarographic measurements were made at a dropping mercury electrode on degassed aqueous solutions, using Princeton Research Instruments or Beckman polarographs. ^1H NMR measurements were performed on a Perkin-Elmer R32 NMR spectrometry (90 MHz). G.L.C. separations were made with a Perkin-Elmer Sigma 1B gas chromatoraphic system.

^{13}C NMR measurements were performed using a Bruker WM 250 Fourier Transform NMR spectrometer. Chemical shifts were referenced to DSS in ^2H_2O as an external standard.

EPR spectra were recorded with a Varian E12 instrument at about 9.26 Hz; samples were cooled by immersion in liquid nitrogen or by flow techniques using either chilled nitrogen or helium gas boiled directly from the liquid.

REFERENCES

1. M.G.B. Drew, Prog. Inorg. Chem., 1977, 23, 67.
2. D.L. Kepert, Prog. Inorg. Chem., 1978, 24, 179.
3. D.L. Lewis and S.J. Lippard, J. Amer. Chem. Soc., 1975, 97, 2697.
4. R.A. Levenson and R.L.R. Towns, Inorg. Chem., 1974, 13, 105.
5. C. Castellani Bisi, M. Gorio, E. Cammilo, A. Coda and V. Tazzoli, Acta Cryst. 1975, A31, 5134.
6. J.M. Manoli, C. Potvin, J.M. Brégeault and W.P. Griffith, J. Chem. Soc., Dalton Trans., 1980, 192.
7. M.G.B. Drew, P.C.H. Mitchell and C.F. Pygall, J. Chem. Soc., Dalton Trans., 1977, 11, 1071.
8. P. Brant, F.A. Cotton, J.C. Sekutowski, T.E. Wood and R.A. Walton, J. Amer. Chem. Soc., 1979, 101, 6588.
9. W.A. LaRue, A.T. Liu, and J.S. Filippo, Jr., Inorg. Chem., 1980, 19, 315.
10. J.L. Hoard, T.A. Hamor and M.D. Glick, J. Amer. Chem. Soc., 1968, 90, 3177.
11. B.J. Corden, J.A. Cunningham and R. Eisenberg, Inorg. Chem., 1970, 9, 356.
12. M. Laing, G. Gafner, W.P. Griffith and P.M. Kiernan, Inorg. Chim. Acta, 1979, 33, L119.
13. S.S. Basson, L.D.C. Bok and J.G. Leipoldt, Acta Cryst., 1970, B26, 1209.
14. N.K. Bel'skii and Yu T. Struchkov, Sov. Phys. Crystallogr. 1965, 10, 15.
15. L.D.C. Bok, J.G. Leipoldt and S.S. Basson, Z. Anorg. Chem., 1972, 392, 303.

16. J. Chojnacki, J. Grochowiski, L. Lebioda, B. Oleksyn and K. Stadnicka, Roczn. Chem., 1979, 43, 273.

17. G. Bombieri, P.T. Moseley and D. Brown, J. Chem. Soc. Dalton Trans., 1975, 2079.

17a. S.S. Basson, J.G. Leipoldt, L.D.C. Bok, J.S.V. Vollenhoven and P.J. Cilliers, Acta Cryst., 1980, B36, 1765.

17b. J.G. Leipoldt, S.S. Basson and L.D.C. Bok, Inorg. Chim. Acta, 1980, 44, L99.

18. C. Castellani Bisi, A. Della Giusta, A. Coda and V. Tazzoli, Cryst. Struct. Commun. 1974, 3, 381.

18a. D. Nicholls and T.A. Ryan, Inorg. Chim. Acta, 1980, 41, 233.

19. H.L. Nigam, R.S. Nyholm and M.H.B. Siddard, J. Chem. Soc., 1960, 1806.

20. R.V. Parish, Coord. Chem. Revs., 1966, 1, 439.

21. W.P. Griffith, Coord. Chem. Revs., 1975, 17, 177.

22. A.G. Sharpe, " The Chemistry of Cyano Complexes of the Transition Metals" . Academic Press, London, 1976.

23. B.M. Chadwick and A.G. Sharpe, Adv. Inorg. Chem. Radiochem., 1966, 8, 83.

24. W.P. Griffith, Comprehensive Inorg. Chem., 1973, 4, 105.

25. W.P. Griffith, Quart. Review, 1962, 16, 188.

26. D. Nicholls, T.A. Ryan and K.R. Seddon, Chem. Commun., 1974, 635.

27. G.R. Rossman, F.D. Tsay and H.B. Gray, Inorg. Chem., 1973, 12, 824.

28. P.M. Kiernan and W.P. Griffith, Inorg. Nucl. Chem. Letters, 1976, 12, 377.

29. H.S. Trop, A.G. Jones and A. Davison, Inorg. Chem., 1980, 19, 1993.

30. M.B. Hursthouse, K.M.A. Malik, A.M. Soares, J.F. Gibson and W.P. Griffith. Inorg. Chim. Acta, 1980, 45, L81.

31. L.D.C. Bok, J.G. Leipoldt and S.S. Basson, Acta Cryst., 1970, B26, 684.

32. B.R. McGarvey, Inorg. Chem., 1966, 5, 476.

33. R.G. Hayes, J. Chem. Phys., 1966, 44, 2210.

34. T.V. Long II and G.A. Vernon, J. Amer. Chem. Soc., 1971, 93:8, 1919.

35. W.P. Griffith, P.M. Kiernan and P.B. O'Hare, J. Mol. Struct. 1978, 46, 307.

36. P.M. Kiernan, Inorg. Chim. Acta, 1976, 20, 89.

37. P.M. Kiernan and W.P. Griffith, J. Chem. Soc. Dalton Trans., 1975, 2489.

38. E.L. Muetterties, Inorg. Chem., 1973, 12, 1963.

39. E.L. Muetterties, Inorg. Chem., 1965, 4, 769.

40. D.G. Blight and D.L. Kepert, Theor. Chim. Acta, 1968, 11, 51.

41. H.B. Thompson and L.S. Bartell, Inorg. Chem., 1968, 7, 488.

42. R. Nast and D. Rehder, Chem. Ber., 1971, 104, 1709.

43. G.M. Whitesides and G. Maglio, J. Amer. Chem. Soc., 1969, 91, 4980.

44. P.M. Kiernan, J.F. Gibson and W.P. Griffith, J. Chem. Soc. Chem. Commun. 1973, 816.

45. J.J. Pesek and W.R. Mason, Inorg. Chem., 1979, 18, 924.

46. M.M. Atherton, " Electron Spin Resonance: Theory and Applications" , Ellis Harwood Ltd., Wiley, Chichester, 1973.

47. H.A. Buckmaster, R. Chatterjee and Y.H. Sing, Phys. Status Solidi A, 1972, 13, 9.

48. E. Semanek and I. Sroubek, " Electron Paramagnetic Resonance" ed. S. Geshwind, Plenum Press, New York, 1972.

49. A. Carrington and A.D. McLaclan, " Introduction to Magnetic Resonance" , John Wiley and Sons, Inc., New York, 1979.

50. R.A. Pribush and R.D. Archer, Inorg. Chem., 1974, 13, 2556.

51. R.A. Levenson, R.J.G. Dominquez, M.A. Willis and F.R. Young III, Inorg. Chem., 1974, 13, 2761.

52. I.N. Marov, V.K. Belyaeva, V.V. Dovgei, and A.N. Sergeeva, Russ. J. Inorg. Chem., 1976, 21, 1784.

53. W.P. Griffith, P.M. Kiernan and J.M. Brégeault, J. Chem. Soc. Dalton Trans., 1978, 1411.

54. L.H. Jones, Inorg. Chem., 1963, 2, 777.

55. This work.

56. R.A. Levenson and R.J.G. Dominquez, Inorg. Chem., 1973, 12, 2342

57. R.A. Levenson, Chem. Phys. Letts., 1973, 22, 293.

58. B.G. Bennett and D. Nicholls, J. Chem. Soc., A, 1971, 1204.

59. W.P. Griffith and G.T. Turner, J. Chem. Soc., A, 1970, 858.

60. J.G. Leipoldt, L.D.C. Bok and P.J. Cilliers, Z. Anorg. Allg. Chem. 1974, 409, 343.

61. J.G. Leipoldt, L.D.C. Bok and P.J. Cilliers, Z. Anorg. Allg. Chem., 1974, 407, 350.

62. J. Locke and G.H. Edwards, J. Amer. Chem. Soc., 1898, 20, 594.

63. A. Müller, P. Werle, E. Diemann and P.J. Aymonimo, Chem. Ber., 1972, 105, 2419.

64. R.C. Young, J. Amer. Chem. Soc., 1932, 54, 1402.

65. A. Chilesotti, Gazz. 1904, 34II, 497.

66. A. Rosenheim and E. Dehm, Chem. Ber., 1914, 47, 392.

67. O. Ollsson, Chem. Ber., 1914, 47, 917.

68. J.S. Yoo, E. Griswold and J. Kleinberg, Inorg. Chem., 1965, 4, 365.

69. E.A. Heintz, Inorg. Synth., 1963, 7, 142.

70. F.A. Cotton, P.E. Fanwick, R.H. Niswander, and J.C. Sekutowski, J. Amer. Chem. Soc., 1978, 100:15, 4725.

71. E. Carmona-Guzman and G. Wilkinson, J. Chem. Soc. Dalton Trans., 1977, 1716.

71a. E.L. Muetterties, ed., " Transition Metal Hydrides" , Marcel Dekker Inc., New York, 1971, p. 78.

72. A. Samotus, A. Kanas and M. Dudek, J. Inorg. Nucl. Chem., 1979, 41, 1129.

73. S.J. Lippard, and B.J. Russ, Inorg. Chem., 1967, 6, 1943.

74. H. Stammreich and O. Sala, Z. Electrochem. 1960, 64, 741; 1961, 65, 149.

75. K.O. Hartman and F.A. Miller, Spectrochim. Acta, Part A, 1968, 24, 669.

76. R.V. Parish, P.G. Simms, M.A. Wells and L.A. Woodward, J. Chem. Soc., A, 1968, 2882.

77. J.R. Perumareddi, A.D. Liehr and A.W. Adamson, J. Amer. Chem. Soc., 1963, 85, 249.

78. R.M. Golding, and A. Carrington, Mol. Phys., 1962, 5, 377.

79. E.L. Orgel, J. Inorg. Nucl. Chem., 1960, 14, 136.

80. M.B. Hursthouse, A.M. Galas, A.M. Soares and W.P. Griffith, Chem. Commun. (Submitted for publication).

81. J.F. Fouler and J. Kleinberg, Inorg. Chem., 1970, 9, 1005.

82. F.A. Cotton and G. Wilkinson, " Advanced Inorganic Chemistry" John Wiley, USA, 1972, p. 961.

83. P.M. Kiernan - Personal Communication.

83a. P.M. Kiernan - Ph.D. Thesis, London, 1975.

84. D.F. Evans, J. Chem. Soc., 1959, 2003.

85. D.F. Evans, G.V. Fazakerley and R.F. Phillips, J. Chem. Soc. (A), 1971, 1931.

86. H.J. Clase, A.J. Cleland, and M.J. Newlands, J. Chem. Soc., Dalton Trans., 1973, 2546.

87. K. Krogman and W. Binder, J. Organomet. Chem., 1968, 11, p. 27.

88. K. Krogman and W. Binder, Angew. Chem. Int. Edn., 1967, 6, 881.

89. H.S. Lim and F.C. Anson, Inorg. Chem., 1971, 10, 103.

90. A. Samotus and B. Sieklucka, J. Inorg. Nucl. Chem., 1978, 40, 315.

91. B. Sieklucka and A. Samotus, J. Inorg. Nucl. Chem., 1980, 42, 1003.

92. J. Kwiatek, Catal. Review , 1967, 1, 37.

93. W. Strohmeier and N. Iglauer, Z. Physik. Chem., 1966, 51, 50.

94. J.L. Lentzner and H.E. De La Mare, J. Polym. Sci.(A), 1971, 9, 1401.

95. J.H. Bayston, R.N. Beale, N.K. King and M.E. Winfield, Austr. J. Chem., 1963, 16, 954.

96. J.H. Bayston and M.E. Winfield, J. Catal., 1964, 3, 123.

97. H.L. Roberts and W.R. Symes, J. Chem. Soc., A, 1968, 1450.

98. J.P. Hall and W.P. Griffith, Inorg. Chim. Acta, in press.

99. G.K. Schweitzer and D.L. Wilhelm, J. Inorg. Nucl. Chem., 1956, 3, 1.

100. H.J. Clase, A.J. Cleland and M.J. Newlands, J. Organomet. Chem., 1975, 93, 231.

101. P.W. Selwood, " Magnetochemistry", Interscience, New York, 1956.